ADVANCED HIGH INTERNAL PHASE WATER-IN-OIL TECHNIQUE FOR THE BENEFICIATION OF WEATHERED ULTRA-FINE COAL DISCARDS

Mashaba Poitah Manche (1081355)

A Masters dissertation submitted to Faculty of Engineering and the Built Environment, University of the Witwatersrand, Johannesburg, South Africa, in fulfilment of the requirements for the degree of Master of Science in Engineering

Supervisor: Prof. Samson. O. BADA

February 2022

DECLARATION

I declare that this dissertation is my own, unaided work. It is being submitted for the degree of Master of Science in Engineering (Metallurgy and Materials) at the University of the Witwatersrand, Johannesburg, South Africa. It has not been submitted before for any degree or examination to any other University.

……………………………
Poitah Manche Mashaba
February 2022

ABSTRACT

Continuous use of mechanised mining and the convectional beneficiation of South Africa's run of mine coal has led to over one billion five hundred million tons of fine discard coal (-1 mm) stored/dumped in South Africa (Department of Energy, 2001). This study was carried out using HIP W/O technique, known as advanced high internal phase water-in-oil emulsion binder. The as-received weathered discards coal comprised of fixed carbon content ranging from 17.79% to 43.29%, with calorific values ranging from 8.48 MJ/kg to 20.94 MJ/kg. The ash content of the coal feeds ranged from 28.63% to 48.71%.

Out of the four prepared HIP W/O emulsion binders, emulsion binder 1 was stable and used to beneficiate all the coal discards. The beneficiation of the coals was conducted at different concentrations (5 kg/ton, 7 kg/ton and 9 kg/ton) for the emulsion binder and kerosene at a constant solid's concentration (25%) and conditioning time of 30 seconds. A clean coal product with an ash content of 11.76%, a mass yield of 15.61%, and calorific value of 28.61 MJ/kg was produced using 5 kg/ton of HIP W/O emulsion from coal 1. In addition, clean coal floats with an ash content of 17.47%, calorific value of 26.42 MJ/kg, and a recovery of 21.59% was also obtained from 5 kg/ton of kerosene using coal 1. The clean coal products were upgraded from coal 1, with a feed ash of 29.34% and calorific value of 20.94 MJ/kg under the second stage of froth flotation. Four highly weathered discard coal feeds (discard coal 2, 3, 4 and 5) were also beneficiated using 5 kg/ton of the emulsion binder. The calorific values (8.48 MJ/kg and 16.29 MJ/kg) for the feed discard coal 2 and 3, respectively, were upgraded to 18.16 and 25.77 MJ/kg, respectively. Moreover, discard coal 4 and 5 produced clean coal products with a heat content of 27.62 MJ/kg and 26.28 MJ/kg. from the feed calorific value of 20.61 MJ/kg and 18.55 MJ/kg, respectively.

The response surface method was applied to the optimisation of low-grade coal 2 and 3. Clean coal products were achieved under the emulsion concentrations (5 kg/ton, 7 kg and 9 kg/ton) and flotation agitation speeds of 1200 revolutions per minute (rpm), 1500 rpm and 1800 rpm. The beneficiation results showed that the calorific value increased with increased agitation speed and decreased emulsion concentration. The feed calorific value of discard coal 2 and 3 was increased from 8.48 MJ/kg and 16.29 MJ/kg to 19.45 MJ/kg and 28.12 MJ/kg, respectively, with 5 kg/ton of emulsion binder and an agitation speed of 1800 rpm. With kerosene and at 5 kg/ton, a clean coal product with 19.05 MJ/kg and 27.20 MJ/kg was achieved.

In this research, the HIP W/O emulsion approach was established as an alternative approach to upgrade weathered discard coal dumped for over three decades and achieved better quality product compared to kerosene. The produced clean coal products can be used directly for combustion and co-combustion solid fuels in power generation. However, the HIP W/O emulsion binder requires only 0.25 kg/ton of organic liquids (kerosene and Span 80). In contrast, 5 kg/ton is required under kerosene to produce clean coal products. The study showed that the HIP W/O process could recover high-grade coal from oxidised fine coal discards with calorific values ranging from 8.48 MJ/kg to 20.94 MJ/kg.

ACKNOWLEDGEMENTS

The warmest appreciation goes to my supervisor Prof S.O BADA for this opportunity and his unconditional guidance and direction throughout this research study. My knowledge of coal beneficiation has broadened due to your constant encouragement and all the resources you have provided. I am grateful for everything, and I can proudly say, I have grown both professionally and personally. To Prof. Falcon Rosemary, thank you for sharing your knowledge of the South African Coal Industry with us. Not to forget Dr J. Abdulsalam, I appreciate your support; you have been patient with me and assisted with the Analysis of Variance results.

I appreciate the financial assistance of the Coaltech Research Association (project number: P2020-1) and the SARChI Clean Coal Technology Grant of the National Research Foundation of South Africa (grant number: 86421). To the DSI/NRF Clean Coal Technology Group of the University of the Witwatersrand, you have done so much for me; the list is endless, so I will forever be grateful for everything. Also, I acknowledge the University of the Witwatersrand for access to research facilities, and I appreciate the assistance and the support that the Richard Ward laboratory technicians have shown throughout the year. To Mintek technicians, I am grateful for the froth flotation demonstrations and the support.

A huge thank you to my parents, brothers and sisters, and friends. I am appreciative of your prayers, support, and encouragement.

May the Lord continue to bless you all!!

DEDICATION

I dedicate this work to my family; my parents and my brothers Moretlwane and Mokgata Mashaba.

Kere go lena bana ba gešo:

"Kodumela Moepa thutse, a go lehumo leo le tswago kgauswi"

TABLE OF CONTENTS

LIST OF FIGURES

LIST OF TABLES

NOMENCLATURE

%: per cent

3D: 3-dimensional

Adj. R^2: adjusted correlation

ADMFB: Air Dense Medium Fluidized Beds

ANOVA: Analysis of Variance

AR: ash reduction

ASTM: American Society for Testing and Materials

CA: cone angle

CR: combustible recovery

CV: Calorific value

DDA: dodecyl amine

DTAB: dodecyltrimethylammonium bromide

DDFB: Dual Density Fluidized Beds

EI: efficiency index

Ep: Ecart Probable

FTIR: Fourier transformation infrared spectrometry

HIP W/O: high internal phase water-in-oil

HIP: high internal phase

kg/ton: kilogram per ton

MJ/kg: megajoule per kilogram

MSFB: Magnetically Stabilized Fluidized Beds

NaCl: sodium chloride

Pa.s: Unit for viscosity

Pred. R^2: Predicted correlation

PSD: particle size distribution

ROM: run of mine

rpm: revolutions per minute

RSM: Response surface methodology

SDS: sodium dodecyl sulfate

Span 80: Sorbitan monooleate (SMO) chemically represented as $C_{24}H_{44}O_6$.

SPD: spigot diameter

VF: vortex finder

VFB: Vibrated Fluidized Beds

VFD: vortex finder diameter

VFL: vortex finder length

Vol%: volume per cent

wt%: weight per cent

XPS: X-ray photoelectron spectroscopy

CHAPTER 1: INTRODUCTION

1.1. Background and motivation

The coal industry loses valuable ultra-fine carbonaceous particles to the slurry ponds because of the friable nature of coal, mechanised mining and the inability to find a suitable technique to beneficiate run of mine (ROM) coal fines (Horsfall et al., 1986; Department of Energy, 2001). In South Africa, about one billion five hundred million tons of discard coal have been generated, and about 60 million tons are generated annually (Department of Energy, 2001). The 2011 South Africa coal road map put the total fines and ultra-fines generated at about 11% of the country's annual tons (Road Map, 2011). Almost 100% of these fines are pumped and stored in slurry ponds or tailing dams. (Bada et al., 2016). As a result of the discharge of these coals, the coal surfaces were exposed to air, thereby altering or oxidizing the coal. Oxygenated groups are formed on the surface of this oxidised coal, which renders the coal hydrophilic, and leads to difficulty in floating oxidised coal with common oily collectors (kerosene or diesel) (Xia et al., 2013; Li et al., 2018; Wang et al., 2018). With the changes in the functional groups of these coals, coupled with the presence of ultra-fines primarily associated with clay minerals, the flotation of this coal would be fruitless with traditional reagents. Peng et al. (2015) demonstrated that ultra-fine particles with high inorganic minerals had high collector adsorption. As a result, the collector becomes insufficient and therefore affects the recovery of carbonaceous particles and the ROM ash reduction potential.

In this investigation, a new technique was used in beneficiating some weathered coals of 20 to 30 years from five different old dumps based on the above-mentioned limitations facing flotation, as well as that of the selective agglomeration technique. Selective agglomeration is a concentration process similar to flotation and separates particles and minerals on the basis of their surface chemistry characteristics. In addition, the process has no limit in terms of particle size to be separated from inorganic minerals. While flotation uses air bubbles to collect the organic/clean products, in coal, agglomeration under agitation uses oil (hydrophobic binder) to wet and agglomerates the carbonaceous particles from a suspension of coal and inorganic (mineral) matters. Both techniques have high efficiency for beneficiating non-weathered ROM coal in terms of product yield and grade. Hence, their drawback has been the high cost of pure oil "hydrocarbon", in which the volume (pure oil) required for successful beneficiation depends on the nature of the coal. Both processes have low separation efficiency for the beneficiation and recovery of carbonaceous oxidised materials from weathered coal (Lu et al., 2019).

Literature has shown that for effective separation, an oil dosage of 10 to 20 weight per cent (wt%) is required to provide the surface layer for coal particles and to fill the spaces within the agglomerates in the traditional agglomeration process (Garcia et al., 1995; Dickinson et al., 2015; Netten et al., 2016). This study used a HIP W/O emulsion technique to recover some of the weathered carbon in the coal discard with low oily collectors, reagents and at a reduced flotation rate.

The process uses a hydrophobic binder (emulsifier), which acts as both a hydrophilic and hydrophobic reagent. The emulsifier consists of a HIP W/O emulsion, which selectively agglomerates individual hydrophobic particles, thus leading to the separation from the hydrophilic particles. The agglomerate rate of this emulsion binder depends on the viscosity of the emulsion. According to Galvin et al. (2001) HIP emulsion, depending on its composition, has a viscosity of about 100 Pa.s., while 100% kerosene possesses a viscosity of 0.0016 Pa.s. A high viscosity solution or binder is expected to adhere to a particle following a collision with greater efficiency than a low viscosity binder. In addition, based on the composition of the emulsion, and its stability, most of the void space between the coal particles are filled with dispersed water droplets rather than oil as in traditional agglomeration. Using advanced agglomeration process, Netten and Galvin (2018) obtained coal products with an ash range from 15 to 17% and combustible recovery of 70 to 80% from 42% ash feed coal. Lu et al. (2019) investigated the suitability of the HIP W/O technique on oxidised fine coal through flotation. The study focuses more on the emulsion dispersion behaviour and its attachment to the coal surface, in addition to the microstructure of the froth. The result showed that the new collector, consisting of 85% internal dispersed water phase, improved the flotation of the oxidised coal.

A few studies have used HIP W/O emulsion technique for agglomeration and flotation (Netten and Galvin, 2018; Lu et al., 2019). Lu et al. (2019), using fine laboratory oxidised coal (− 74 + 38 µm) compared to – 260 µm particle size used by Netten and Galvin (2018), effectively produced clean coal products at a low oil dosage requirement from the HIP W/O emulsion binder (collector). This highlighted the need for further study in which the technique and the emulsion binder can be used to beneficiate weathered coal fines from discard dumps or slurry ponds. In this study, five coal fines of two to three decades with various degrees of oxidation were studied. The performance of HIP W/O emulsion with an internal dispersed water phase of 95% by volume was compared with that of kerosene in terms of the physico-chemical properties of the clean coal recovered from the as-received feeds.

1.2. Research aim and objectives

This study seeks to upgrade South African coal discards from slurry ponds using the novel HIP W/O emulsion technology. The aim of the study was to investigate the capability of an HIP W/O emulsion binder to beneficiate coal fines (− 150 µm). This particle size is noted to be difficult to recover using traditional oily collectors. The success of this approach was established in relation to the following objectives:

I. The five coal discards were characterised to examine the physico-chemical properties (the particle size distribution, inherent moisture, ash, volatile matter, fixed carbon, total carbon, total sulfur, and calorific value) and extent of oxidation of these coals that have been dumped for 20 to 30 years based on the age of slurry ponds on existing mines in South Africa.

II. Evaluate the stability of the emulsion binders produced at various concentrations of sodium chloride (NaCl), kerosene and Span 80 by measuring their conductivity at different times of agitation.

III. Examine the influence of the collectors (emulsion binder and kerosene) concentrations on the mass yield, calorific value and ash content of the coal products obtained.

IV. Investigate the effect of the emulsion binder with respect to different coal feeds during the batch beneficiation test.

V. Investigate and identify the optimum operating conditions using response surface methodology (RSM) to improve the performance of the HIP W/O process in beneficiating the coals.

1.3. Hypothesis

The HIP W/O emulsion binder will recover oxidised and non-oxidised ultra-fine carbonaceous particles from coal slurry ponds. The stability of this emulsion is facilitated by a non-ionic emulsifier, which comprises a neutral hydrophilic head as well as a hydrophobic tail, resulting in the recovery of the clean coal product. The stability is ensured when the hydrophilic head of the Span 80 within the HIP W/O emulsion forms hydrogen bonds with the hydrophilic oxygenated functional groups (O=C–OH, –C=O, –C–OH) of the oxidised and non-oxidised carbonaceous particles.

1.4. Research questions

The main research question of this study is:

To what extent will the advanced HIP W/O emulsion technique be more efficient than traditional methods in recovering coal organic carbonaceous particles from discard coal that have been dumped for decades? It is in this context that the following sub-questions of the study are set out as follows:

I. How does coal oxidation impact the physico-chemical properties of coal particles?
II. How do the different agitation times affect the emulsion stability and conductivity of the emulsion binders prepared under different NaCl, Span 80 and kerosene compositions?
III. How does the HIP W/O emulsion binder compared to kerosene influence the clean coal product yield and grade?
IV. To what extent will the emulsion treat ultra-fine coal particles in discard coal containing different oxygen contents?
V. To what degree can the Design-Expert software be used to optimise discard coal feeds with an ash content of more than 40 percent?

1.5. Layout of the dissertation

The thesis is divided into five chapters:

I. **Section one** presents the research with context and motivation for the study**.** In addition, the aim of the study, five objectives and the research questions are included.
II. **Chapter two** presents literatures related to the beneficiation techniques for ultra-fine particles, with more focus directed to the recovery of ultra-fines from the discard coal using the HIP W/O emulsion technique.
III. **Chapter three** details the experimental approach, which includes the discard coal preparation, coal characterisation and analytical techniques, the HIP W/O emulsion preparation and the beneficiation test procedures, and the modelling using Design-Expert software.
IV. **Chapter four** presents the physico-chemical analysis results and a discussion of the five discard coal feeds. The Fourier transformation infrared spectroscopy (FTIR) results for the as-received coals and the reagents used (HIP W/O emulsion and

kerosene) are included along with the beneficiation, optimisation and modelling results.

V. **Chapter 5** presents conclusions and recommendations related to future work**.**

CHAPTER 2: LITERATURE REVIEW

2.1. Gravity beneficiation processes

Gravity separation is a physical technique grouped into two categories: wet and dry beneficiation processes. Wet beneficiation methods for fine material (ranging from 1 mm to 0.1 mm) include processes such as spirals, water-only-cyclones, shaking tables, batac type jigs and dense medium separation processes. However, shaking tables and jigs also form part of the dry beneficiation processes. They are effective for the beneficiation of carbonaceous particles, which are difficult for wet beneficiation methods because of the high porosity of the feed (Sampaio et al., 2008). Gravity beneficiation processes rely on the differences in the specific gravity of the carbonaceous particles and inorganic mineral matters in the coal (Sampaio et al., 2008; Meshram et al., 2015; Ruhman and Gupta, 2017; Barma, 2018).

2.1.1. Wet beneficiation processes

Spirals and cyclones containing only water are classification techniques that only use water to beneficiate carbonaceous particles. Additionally, they are viewed as pre-treatment or post-treatment techniques for other gravity beneficiation processes (Wills, 2006; Majumder and Barnwal, 2011; Wang et al., 2018). This is due to their ability to treat carbonaceous fine particles of about – 1.5 mm (Wills, 2006; Aslan and Unal, 2011; Chary and Dastidar, 2012; Meshram et al., 2015; Netten et al., 2016). As Wills (2006) indicated, such carbonaceous particles increase the slurry's viscosity and, hence, reduce the sharpness of separation for other gravity beneficiation processes.

The dense medium cyclone, which forms part of the dense medium separation processes, uses both water and medium for beneficiation. Magnetite is the most used dense medium liquid to beneficiate carbonaceous particles from its inorganic mineral matters. However, magnetite is expensive (Mehrotra et al., 1983; Ma et al., 2018). This motivated the study by Chagwedera et al. (2018), who investigated the use of pyrrhotite, silica sand and other wastes as an alternative to magnetite for the beneficiation of carbonaceous particles using a dry Air Dense Medium Fluidized Bed (ADMFB). Regardless of the success of this investigation, where pyrrhotite was established as an alternative medium to magnetite, the application of dry processes remains ineffective for the beneficiation of ultra-fine carbonaceous particles of – 0.5 mm (Aslan and Unal, 2011; Chary and Dastidar, 2012; Meshram et al., 2015).

2.1.1.1. Spiral separators

According to Wills (2006), Ramsaywok et al. (2010) and Ramsaywok and Mathumbu (2017), spirals are gravity flowing film concentrators that use a combination of centrifugal and gravity forces to beneficiate carbonaceous particles from inorganic mineral matters. As a result of these forces and water, carbonaceous particles and the inorganic mineral matters segregate and report to different streams based on their densities (Hornsby et al., 1993; Benusa and Klima, 2008; Zhang, 2008; Benusa and Klima, 2009; Bu et al., 2017). Spirals have three product streams: the concentrate, which comprises carbonaceous particles, the middling and tailing. Unliberated carbonaceous particles and some of the inorganic mineral matters in the coal form part of the middling, while the tailing stream consists of inorganic mineral matters with some unliberated carbonaceous particles (Atasoy and Spottiswood, 1995; Honaker et al., 2007; Mohanty et al., 2014; Nienaber and Auret, 2019). In a study conducted by Ma et al. (2018), a ROM coal of – 1 + 0.125 mm with an ash content of 28.24% from the Huipodi coal preparation plant in Shanxi Province was beneficiated. A clean coal concentrate of 47.76% combustible recovery, 37.39% mass yield and 8.31% ash content was achieved.

2.1.1.2. Water-only-cyclones

Water-only-cyclones, also known as modified hydrocyclones, are used for the classification, desliming and dewatering of coal and other minerals. As shown in Figure 2-1, the difference between the water-only-cyclone and a hydrocyclone is that the vortex finder (VF) in a water-only-cyclone is longer and thicker than that of a hydrocyclone. Another modification made to the water-only-cyclone is the enlargement of its conical section to increase the cone angle (CA) (Hembrom and Suresh, 2018). As indicated by Patil et al. (1997) and Hembrom and Suresh (2018) who beneficiated coal sample from Gajlitand colliery in India, these changes ensure a dense particle bed leading to high separation efficiency. A dense particle bed minimises the loss of carbonaceous particles to the apex (spigot or underflow), thereby improving the recovery of the clean coal particles (Michael et al., 2003; Majumder and Barnwal, 2011; Ozgen, 2013; Maharana and Suresh, 2020).

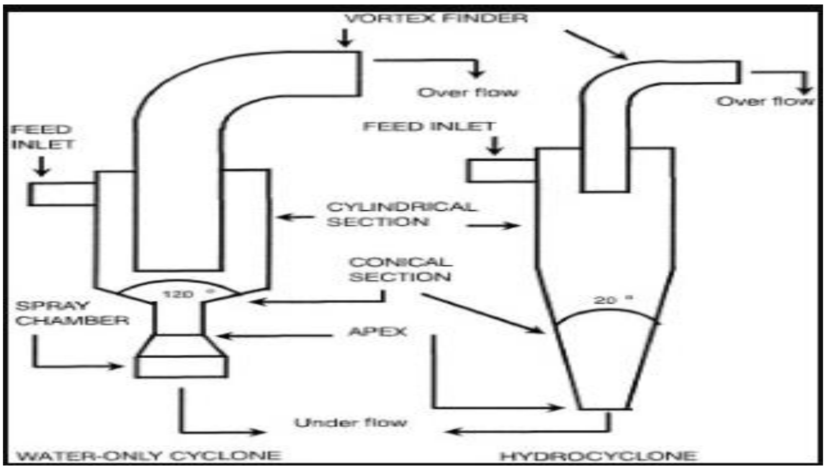

Figure 2-1: Water-only-cyclone and hydrocyclones (Patil et al., 1997)

Majumder and Barnwal (2011) illustrated that water-only-cyclones could reduce the ash content in coal depending on the variation of the cyclone variables. In their study, the vortex finder length (VFL, mm), vortex finder diameter (VFD, mm) and cone angle (CA) were varied to beneficiate ROM coal particles of – 0.5 mm with an ash content of 36.13%. A cyclone with VFD of 37 mm, VFL of 134 mm and CA of 143˚ reduced the coal content to 28.28% and produced a yield of 86.30% (Table 2-1). These results are satisfactory compared to when the variables are minimum with the VFD at 33 mm, VFL at 134 mm and CA at 105˚.

Table 2-1: The effect of VFL, VFD and CA on the yield of carbonaceous particles and the ash reduction in the ROM feed coal (Majumder and Barnwal, 2011)

Experimental number	**Experimental conditions**			**Product carbonaceous particles**	
	VFL, mm	**VFD, mm**	**CA, ˚**	**Yield%**	**Ash%**
1	128	33	105	50.75	21.56
2	134	33	105	54.98	23.23
3	128	37	105	71.86	25.97
4	134	37	105	76.03	27.24
5	128	33	143	59.54	24.45
6	134	33	143	64.39	26.53
7	128	37	143	80.46	28.20
8	134	37	143	86.30	28.28

A similar approach was used by Ozgen (2013) to beneficiate discard coal (− 0.5 + 0.038 mm) from gravity beneficiation plants in Turkey, with an ash content of 75.96%. The effect of the VFD, apex diameter, feed inlet pressure and suspension solid ratio was investigated, and a clean coal concentrate of 29.50% ash was obtained. Another investigation was also reported on the use of a water-only-cyclone. Hembrom and Suresh (2018) studied the effect of VFL, VFD and spigot diameter (SPD, mm) on the beneficiation of ROM coal (− 2.34 + 0.075 mm) and ash content of 37.84%. With the VFL of 150 mm, VFD of 45 mm and spigot of 26 mm, the feed coal was reduced to 30.46% ash, and the yield of carbonaceous particles was 68.62%. However, these results were not appreciable when the VFL was 165 mm with VFD of 40 mm and spigot of 24 mm (Table 2-2).

Table 2-2: The effect of VFL, VFD and CA on the yield of carbonaceous particles and the reduction of the ash in the ROM feed coal (Hembrom and Suresh, 2018)

Experimental number	**Experimental conditions**			**Clean coal**	
	VFL, mm	**VFD, mm**	**SPD, mm**	**Yield% of floats**	**Ash%**
1	150	40	26	43.59	23.10
2	150	40	26	43.15	23.05
3	**150**	**45**	**26**	**68.62**	**30.46**
4	150	35	28	34.08	20.65
5	150	40	26	42.75	22.54
6	150	40	26	42.61	22.10
7	165	35	26	56.52	27.85
8	135	40	24	37.52	21.18
9	135	45	26	34.00	21.15
10	150	45	24	53.18	27.12
11	**165**	**40**	**24**	**67.51**	**29.77**
12	135	35	26	30.64	18.65
13	165	40	28	57.64	27.71
14	150	45	28	41.64	23.57
15	150	35	24	42.43	23.07
16	150	40	26	42.61	22.00
17	135	40	28	29.20	18.54

As indicated in Table 2-2, an increase in VFL at constant VFD increases the product yield because of the reduction of VF clearance, which is defined as the gap between the bottom tip of VF and spigot orifice (Hembrom and Suresh, 2018). According to the authors, some parameters are more significant than others depending on the process specification, and that VFL is the main driving force for yield, while VFL, VFD and SPD are the driving forces for ash content reduction.

2.1.1.3. Shaking tables

Similar to spirals, shaking tables are gravity flowing film concentrators (Manser et al., 1991; Wills, 2006; Çicek, 2008). A shaking table has dressing water, which transports the carbonaceous particles and the inorganic mineral matters (Figure 2-2). As a consequence of water and motion provided by the motor drive, the particles segregate and disperse throughout the table. The low-density carbonaceous particles float above the riffles while the dense inorganic mineral matters sink between the riffles. After separation, the particles report to different streams, including the concentrate discharge stream, heavy mineral discharge stream and the middling stream, which comprises unliberated carbonaceous particles and inorganic mineral matters (Manser et al., 1991; Wills, 2006; Çicek, 2008). The concentrate discharge and the heavy mineral streams consist of carbonaceous particles and inorganic mineral matters, respectively.

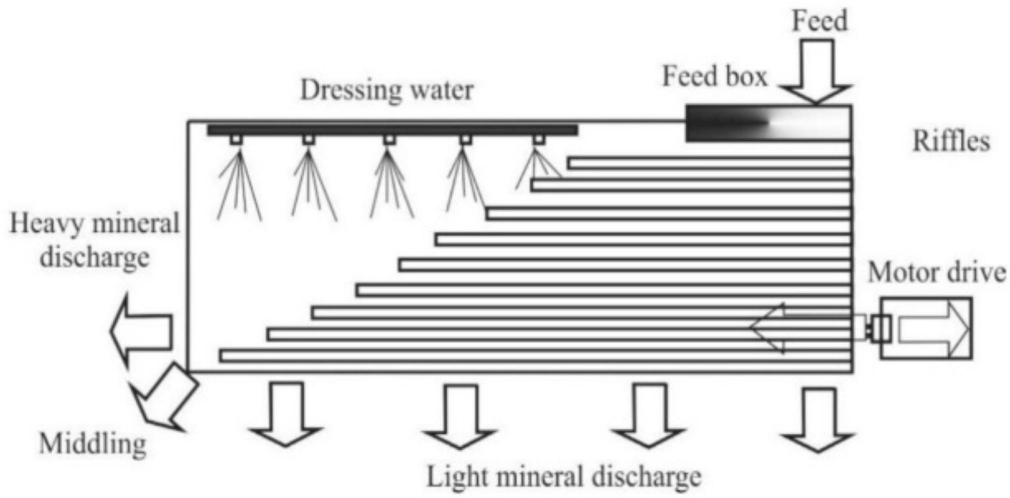

Figure 2-2: Schematic representation of a shaking table (Shariati et al., 2015)

2.1.1.4. Dense medium processes

Dense medium processes are also part of gravity beneficiation processes which are effective for beneficiating coarse coal particles. The process comprises different separators, including dense medium cyclones, Wemco drums, Teska drum, Drewboy separators and many more. These separators are differentiated by their particle size intake and the throughput tonnage requirements. Hayes (2003) and Sivrikaya (2014) demonstrated that drums are mostly used to beneficiate coal particles of – 100 + 25 mm fraction. As indicated by Mehrotra et al. (1983), Michael et al. (2003), and Ma et al. (2018), the dense medium process relies on the principle of float and sink, and it has been demonstrated to use both magnetite and water for the separation of coal organic and its minerals. Dense medium cyclones work in conjunction with desliming screen to deslime the ultra-fine coal particles. This is because the ultra-fines have been demonstrated to contaminate the magnetite by compromising its stability (Ramudzwagi et al., 2020). This section demonstrates other processes available to beneficiate coal, and to meet end user's specifications.

(i). Dense medium cyclones

In South Africa, the medium is initially pumped to the mixing box, where it mixes with the feed coal comprising carbonaceous particles and inorganic mineral matters. Subsequently, the mixed coal feed is pumped to the dense medium cyclone whereby separation occurs with the carbonaceous particles reporting to the overflow while the mineral matter goes to the underflow (Michael et al., 2003; de Korte and Engelbrecht, 2014; Ma et al., 2018). The separator's efficiency in beneficiating coal samples (- 1 + 0.125 mm) from Huipodi Coal Preparation Plant in China with an ash content of 28.24% was carried out by Ma et al. (2018). Clean coal with an ash content of 8.32%, and a mass yield and combustible recovery of 80.84% and 62.98%, respectively, was achieved from a feed coal of 28.24%.

2.1.2. Dry beneficiation processes

As a result of water scarcity and the ineffectiveness of beneficiating porous feed coal particles, dry beneficiation processes have been applied by several authors, including Dwari and Rao (2007), Sampaio et al. (2008), Boylu et al. (2014) and Boylu et al. (2015). The following sections discuss and highlight the dry coal beneficiation techniques and separators available in the market. Given that this study is focused on the beneficiation of coal fines (- 150 µm), the dry beneficiation processes are illustrated to highlight its efficiency and application for coal processing worldwide. In summary, beneficiation processes are connected, the waste of one process can be a feed in another process.

2.1.2.1. Dry air table

The dry air table has been demonstrated to work similarly to the water table (Wills, 2006; Çicek, 2008). As demonstrated by these authors, air tables use air injected at the bottom of the table prior to operation. It has been reported that the combination of air and the vibration (motion) generated by the motor aids the movement of carbonaceous particles and inorganic mineral matters (Dwari and Rao, 2007; Çicek, 2008). Like the water shaking table, the particles segregate because of the motion and consequently report to different streams because of their relative density. An investigation was conducted by Çicek (2008) on the beneficiation of three different coal fractions (- 8 + 5) mm, (- 5 + 3) mm and (- 3 + 1) mm from Soma and Husamlar regions in Turkey. The result show that for the (- 3 + 1) mm size, the feed ash reduced from 42.36% to 21.82% ash and with an Ep (Ecart Probable) value of 0.09 for Soma coal. Whereas for the Husamlar coal (- 3 + 1) mm, a coal product with 17.94% ash was achieved from a feed coal of 29.73% ash. Overall, clean coal products with the lowest ash content were obtained from the lowest particle fractions of (- 3 + 1) mm from both Soma and Husamlar coal.

2.1.2.2. Jigs

Apart from water jigs, air-based jigs are also used to beneficiation coal particles. Water and air jigs use the same principle, given that they both separate because of settling rates (Boylu et al., 2014; Boylu et al., 2015; Sampaio et al., 2020). The differences arise due to the type of medium used. At an initial stage, the mixture of the particles (particle bed) is displaced by the combination of the vibration and the air injected. Subsequently, the settling process occurs, and the less dense carbonaceous particles float while the denser inorganic mineral matters sink to the bottom of the jig (Boylu et al., 2014; Boylu et al., 2015; Sampaio et al., 2020). According to Boylu et al. (2014), the dry approach is effective in the beneficiation of coarse coal particles of > 6 mm. In addition, Wills (2006) also alluded to the fact that jigs can beneficiate coarse feed of (- 10 + 3) mm. However, the investigation conducted by Sampaio et al. (2008) on a run of mine feed coal with an ash content and total sulphur content of 51.8% and 2.42%, respectively, using an air-based jig was not effective. This is demonstrated by the minimum feed ash reduction from 51.8% to 47.95% ash within the clean coal product.

Boylu et al. (2015) used an Allair stratification jig to beneficiate a ROM feed of (– 13 + 4) mm with an ash content of 43%. A clean coal carbonaceous product with 11.7% ash and a yield of 48.8% was achieved. Kumar and Venugopal (2017) furthered the study by investigating the effectiveness of a Denver mineral jig on coal of (- 4.76 + 3) mm using different process variables, including the bed height, water flow and jigging time. Satisfactory results were obtained from the bed height of 45 mm, water flow of 3 L/min and jigging time of 15 minutes. The ash content decreased to 17.02%, with a mass yield of 62.45%. When the flow rate was reduced to 2 L/min with the same bed height of 45 mm and jigging time of 15 minutes, there was no significant reduction in the ash content (17.00%) and mass yield (62.31%).

2.1.2.3. Fluidized beds

Examples of fluidized beds include magnetically stabilized fluidized beds (MSFB), vibrating fluidized beds (VFB), dual density fluidized beds (GFDD) and ADMFB. According to Chikerema and Moys (2012), Mohanta et al. (2013), Zhao et al. (2015) and Sahu et al. (2019), fluidised beds work on the principle of the creation of pseudo-fluid solid gas, which serves as medium for facilitating the distribution of the particle bed. As a result of the movement, the particles become suspended with the following forces: gravity, buoyancy, drag and frictional force acting on the coal particles and the inorganic mineral matters.

The above-mentioned processes have been proven ineffective for beneficiating ultra-fine coal particles of – 150 µm (Luo et al., 2008; Mohanta et al., 2013; Yang et al., 2013). The drawback of this technique is associated with the cost of the media material and the unavailability of the magnetite, which is used mostly in the wet processes and for pyro-metallurgical applications. This motivated the study conducted by Chagwedera et al. (2018), who investigated the use of pyrrhotite, granulated blast-furnace slag, silica sand and coal discards as an alternative of magnetite for the beneficiation of coal particles using ADMFB. The authors concluded that pyrrhotite is the best dense medium material amongst others tested as an alternative (Chagwedera et al., 2018).

(i). Air Dense Medium Fluidized Beds (ADMFB)

Chikerema and Moys (2012) beneficiated coal particles using different size fractions. The study’s objective was to investigate the influence of particle size and particle density on the performance of an ADMFB separator. The authors found that the beneficiation of the coarse coal particles (– 53 + 37) mm and (– 31.5 + 22) mm are better than the less coarse particles (– 22 + 16) mm and (– 16 + 9.5) mm.

Unlike Chikerema and Moys (2012), coal particles of about (– 6 + 3) mm were beneficiated by Zhao et al. (2015), who used different size ranges of magnetite to investigate the pressure drop performance of media sizes on the ADMFB. They concluded that finer magnetite of (– 0.15 + 0.074) mm can effectively beneficiate coal of (– 6 + 3) mm. This is because finer magnetite can expand the lower separation limit of the ADMFB (Zhao et al., 2015).

(ii). Vibrated Fluidized Beds (VFB)

According to Mohanta et al. (2013) and Yang et al. (2013), VFB rely on the vibration motion imparted on the separator, leading to the beneficiation of the coal from its inherent minerals. Vibration frequency or intensity, bubble formation time, superficial air velocity, bed height and fluidising time impact the success of the vibrated fluidized beds.

Luo et al. (2008) used magnetite powder as the bed media for the beneficiation of coal particles of – 6 mm. Separation efficiency with an Ep value of 0.07 and a uniform bed with a maximum comparative error of 1.68% was attained. Yang et al. (2013) furthered the study using coal particles of (– 6 + 3) mm and (– 3 + 1) mm. The effect of the superficial air velocity, bed height, vibration intensity and fluidising time on the segregation performance was investigated. The obtained probable errors for the size fractions (– 6 + 3) mm and (– 3 + 1) were 0.19 and 0.175, respectively. VFB was effective for the beneficiation of fine particles of (– 3 + 1) mm.

2.2. Physico-chemical processes

The physico-chemical beneficiation processes include the froth flotation and agglomeration processes. The separation of particles by these processes is governed by the differences in the coal's surface properties (wettability) and its inorganic mineral content (Netten et al., 2016; Ruhman and Gupta, 2017; Borrow et al., 2018; Netten and Galvin, 2018).

2.2.1. Froth flotation

Froth flotation is a beneficiation technique that relies on air bubbles formed through aeration (Ozer et al., 2017; Barma, 2018; Guan et al., 2018). These bubbles attract and bind the conditioned ultra-fine carbonaceous particles from inorganic mineral matters to form an aggregate called the froth. Froth flotation received tremendous praise over many decades and is still recognised as an effective technique for the beneficiation of carbonaceous particles that cannot be beneficiated using gravity beneficiation processes. However, a factor hindering the technique's success is the exposure of the coal to atmospheric air (coal oxidation), which subsequently impacts the recovery process (Dey et al., 2013; Qu et al., 2015; Liao et al., 2016; Zhang et al., 2020). The other drawbacks associated with the froth flotation of coal, are the size limitation and drying of the products, which require a lot of energy.

It has been demonstrated that the exposure of coal to atmospheric air increases the oxygen content of coal, leading to hydrophilic oxygenated functional groups on the surface of the coal

(Sarikaya and Ozbayoglu, 1990; Sahinoglu and Uslu, 2015; Xu et al., 2017; Li et al., 2018). Consequently, the negative charges provided by the oxygenated functional groups enhance the potential of the air bubbles to repel the coal particles and therefore decrease the rate of attachment. This is the reason why surfactants are added during froth flotation to enhance the hydrophobicity of the coal particles and therefore ensure the spreading of the collectors on the surface of weathered coal discards.

Dey et al. (2013) investigated the efficiency of recovering carbonaceous particles using froth flotation. They studied oxidised non-coking coal particles of – 300 + 74 µm with an ash content of 26.8% from the Talcher area in India. A promoter was used to neutralise the surface charge at the surface of the coal or carbonaceous particles and therefore reduce the acidity provided by the oxygenated functional groups. The attachment of air bubbles reduced the feed ash content to 12%, and a product yield of 49.6% was achieved. Unlike Dey et al. (2013), the effect of both oily and air bubbles on the combustible recovery of oxidised ultra-fine coal of – 74 µm was investigated by Xia et al. (2013). The feed ROM coal from the Taixi coal preparation plant in China had an ash content of 20.11%. A clean carbonaceous coal concentrate with a combustible recovery of 35% and ash content of 18% was achieved under the air bubbles process. However, a higher combustible recovery of 90% with a significantly lower ash content of 16% was obtained from oily bubble flotation, produced using dodecane. Thus, the oily bubble flotation beneficiated the carbonaceous particles from inorganic minerals more effectively than the air bubble flotation (Xia et al., 2013).

In a study conducted by Qu et al. (2015), a combination of surfactant and a collector were used to modify the surface properties of sub-bituminous coal, which comprised of the hydroxyl (C–OH) and carbonyl (O=C–OH) groups. The feed coal (– 500 µm) was collected from the Yujialiang coal preparation plant, Shendong mine area of China. The authors used three surfactants: anionic sodium dodecyl sulfate (SDS), cationic dodecyl amine (DDA) and non-ionic 2-ethyl hexanol. Along with these surfactants, a collector and a frother (2-octanol) were used for the beneficiation test. The collector was prepared by mixing diesel oil and Nalco 9858 in equal proportion. It was found that non-ionic 2-ethyl hexanol enhanced the floatability of carbonaceous particles. The authors investigated the effect of collector dosage on the combustible recovery and the process of selectivity. An increase in collector dosages increased the combustible recoveries and the ash content therefore reducing the grade of the clean coal product (Figure 2-3). However, this was not the case with the non-ionic 2-ethyl hexanol. This might be due to the oxygenated functional groups, C–OH, –C=O and O=C–OH, in the chemical structure of the non-ionic 2-ethyl hexanol (Qu et al., 2015).

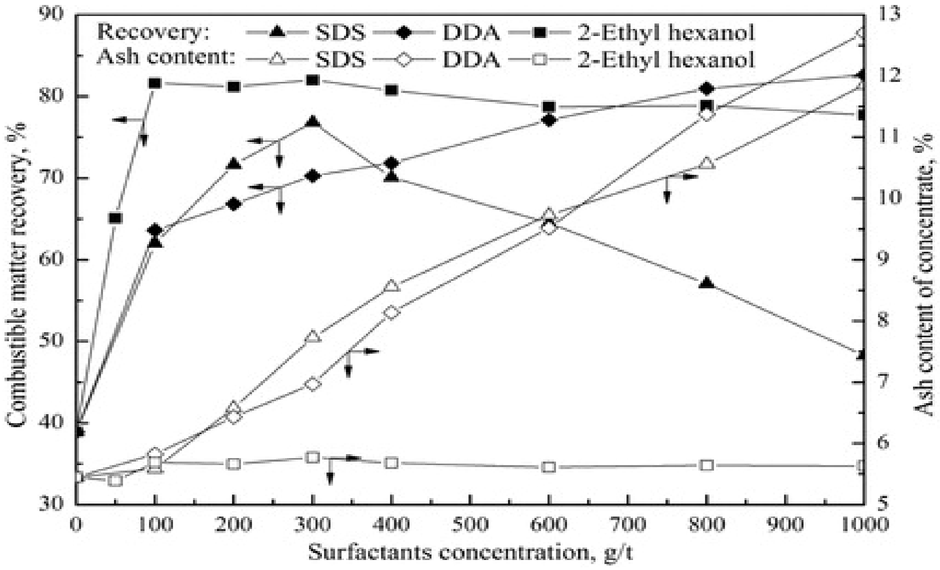

Figure 2-3: The effect of sodium dodecyl sulfate, cationic dodecyl amine and 2-ethyl hexanol on the combustible recovery of carbonaceous particles and the reduction of the ash in the ROM coal (Qu et al., 2015)

The effect of oily bubbles on the combustible recovery of sub-bituminous carbonaceous particles from the Daliuta coal preparation plant, Shendong mine area of China, was also studied by Liao et al. (2016). These carbonaceous particles were sieved to – 500 + 74 µm, and they comprised of ash, moisture and oxygen contents of 8.71 wt%, 16.91 wt% and 12.73 wt%, respectively. The recovery of the product carbonaceous particles increased with the collector dosage, with oily bubble flotation having the highest recovery (Figure 2-4). However, the ash reduction potential seemed to be compromised as the dosage increased. This might be due to the pulling of semi-hydrophobic carbonaceous particles towards the concentrate and therefore impacting the grade of the carbonaceous particles. However, the separation efficiency, which is defined as the difference between combustible recovery and ash recovery ranged between 45 to 50%, seemed to be high regardless of an increase in ash content as a function of collector dosage. The combustible recovery, ash recovery and separation efficiency were determined by using Equations 2-1, 2-2 and 2-3.

$$Separation\ efficiency = Combustible\ recovery - ash\ recovery \qquad \text{Equation 2-1}$$

$$Combustible\ recovery = \frac{M_C\,(100 - A_C)}{M_F(100 - A_F)} \times 100 \qquad \text{Equation 2-2}$$

$Ash\ recovery = \frac{M_C A_C}{M_F A_F} \times 100$ Equation 2-3

Where M_C is the mass of the clean coal (g), M_F represents the mass of the feed coal (g), A_C presents the ash content of the clean coal (%) and A_F denotes the ash content of the feed (%).

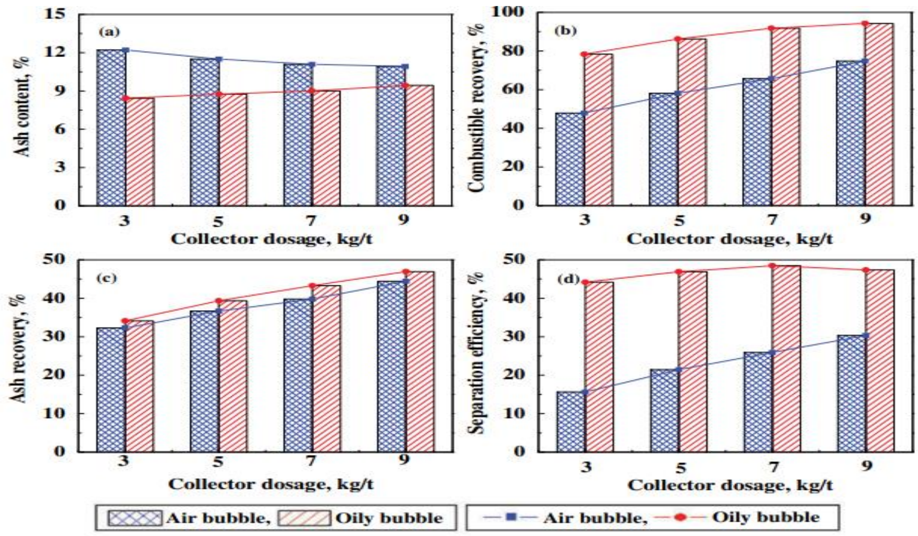

Figure 2-4: The effect of air and oily bubbles on the recovery of carbonaceous particles, the reduction of the ash in the ROM coal, ash recovery and the separation efficiency (Liao et al., 2016)

As indicated by Dey et al. (2013), Xia et al. (2013), Qu et al. (2015) and Liao et al. (2016), the presence of oxygen content within the coal particles initiates the high collector dosage. However, Zhang et al. (2020) conducted a study to evaluate the effect of oxidation on the beneficiation of coal particles of – 500 µm using microemulsion, which was prepared by mixing the cationic surfactant dodecyltrimethylammonium bromide (DTAB) and diesel. The feed ROM was collected from the Shendong mining area in China made up of ash and oxygen contents of 12.24% and 13.84%, respectively. The mixture of DTAB and diesel in a 1:2 ratio resulted in a high yield between 75% and 100% compared to the ratios of 1:5, 1:10 and 0:1. However, the ratio of 1:2 resulted in the second-highest ash content within the product carbonaceous particles concentrated (Figure 2-5).

This highest yield of between 75% and 100% could be regarded optimum with ash content of approximately 8%. However, optimum products depend on the end product’s specifications. As indicated, the clean coal yield saturation levels were experienced at high dosage of 8 kg/ton for the following ratios, 0:1, 1:2, 1:5 and 1:10. DTAB alone produced a coal product of lowest yield of 35%. Likewise, saturation levels for ash content seems to have resulted at 8 kg/ton of the microemulsions. There is a dissimilar trend for DTAB whereby a clean coal product with high ash contents of about 25% was achieved at doses of 2 kg/ton and 4 kg/ton. This might be due to the entrainment of inorganic mineral content. A better selectivity of clean coal from inorganic mineral content resulted from using the microemulsions.

In the current research, the HIP W/O emulsion binder prepared by mixing an emulsifier (Span 80) with kerosene and aqueous NaCl solution was used to float South African oxidised coal.

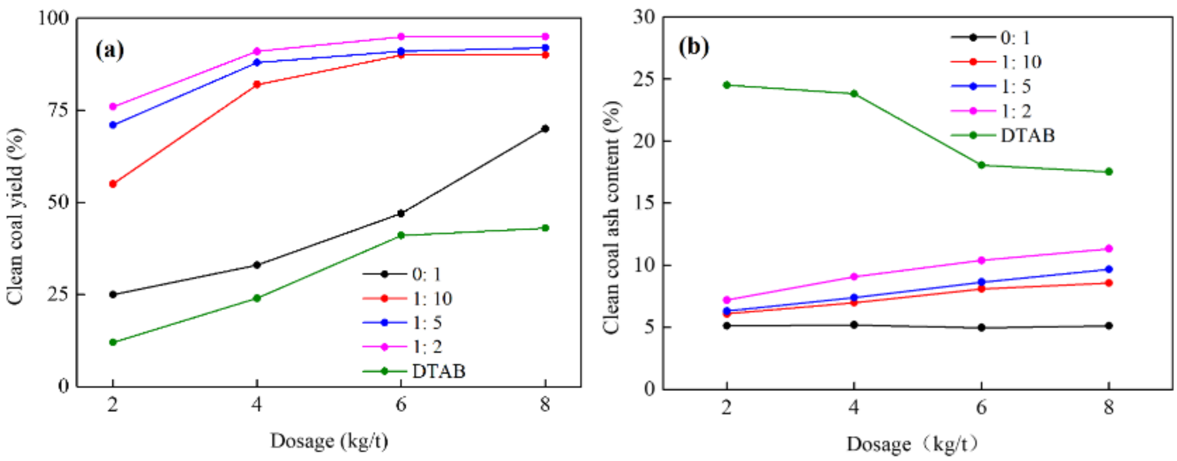

Figure 2-5: The effect surfactant dosages on the yield of the clean coal and the reduction of the ash in the ROM feed coal (kg/t) (Zhang et al., 2020)

2.2.2. Agglomeration process

It has been demonstrated by Horsfall et al. (1986), Liao et al. (2017), and Zhang et al. (2020) that froth flotation becomes ineffective when beneficiating – 75 µm coal particles. The study conducted by Peng et al. (2015) showed that the presence of inorganic mineral matters within the ultra-fine coal particles impacts the beneficiation of coarse (oversize) particles of + 74 µm. Carbonaceous ultra-fine particles, especially oxidised coal with different inorganic mineral content, has the following issues when subjected to froth flotation, using the traditional reagents:

I. The ultra-fine (undersize) particles with low inorganic mineral matter (or content) have strong adsorption to both the collector and frother. This is a challenge because the adsorption of the frother by the inorganic mineral matter reduces the amount of frother in the mix. This leads to a decrease in the bubbles' stability and, therefore, the coarse particles detach from the bubbles and the combustible recovery decreases. The carbonaceous particles' detachment gives the inorganic mineral matter a chance to attach to the air bubbles as a result of bubble surface area availability and therefore lead to an increased ash content (Akdemir and Sonmez, 2003; Das et al., 2010; Peng et al., 2015; Liao et al., 2017).

II. The ultra-fine coal particles with high inorganic mineral matter have also been demonstrated to have low adsorption to the frother. However, they have been found to have high collector adsorption. According to the literature, this is a challenge because the excessive adsorption of the collector leads to collector inadequacy and, therefore, impacts the recovery of coarse carbonaceous particles and the product ash reduction (Tao et al., 2000; Das et al., 2010; Liao et al., 2017).

To address the issue of beneficiating ultra-fine particles of – 75 µm, agglomeration was established as a modification to flotation, given that the particles must float before the process is complete. The agglomeration process is a technique that beneficiates ultra-fine coal particles by increasing their size, thereby forming clusters interspaced by the bridging agent (Wang et al., 2012; Sahinoglu and Uslu, 2015; Yadav et al., 2018). The cluster formation of the carbonaceous particles is evaluated by pouring the conditioned slurry into sieves that are greater than the size of the feed coal. This is substantiated by Laskowski and Yu (2000), who define the process as “size enlargement” and “liquid phase agglomeration”.

2.2.3. Selective agglomeration process

According to Bensley et al. (1977), the selective agglomeration process is based on the principle of oil-water mixture, which is also known as oil agglomeration. The technique uses pure oily collectors, including vegetable oils and neutral hydrocarbon oils such as kerosene and diesel, as collectors to agglomerate the carbonaceous ultra-fines (Dey et al., 2013; Xing et al., 2017; Kasomo et al., 2018; Zhang et al., 2020). However, it has been indicated by Wang et al. (2012) that the nature of the bridging agent and the presence of oxygen within the coal ultra-fines impact the success of the agglomeration. Wang et al. (2012) used kerosene and vegetable oil to beneficiate anthracite, bituminous and lignite coal or carbonaceous ultra-fines of – 75 + 53 µm. Equation 2-4 to Equation 2-6, was used in determining the efficiency of the process, by calculating the combustible matter recovery (CR), ash reduction (AR) and efficiency index (EI).

$$CR\ (\%) = \frac{Combustible_{agglomerates}\ (wt\%) \times Wt_{agglomerates}\ (g)}{Combustible_{feed}\ (wt\%) \times Wt_{feed}\ (g)} \times 100 \qquad \text{Equation 2-4}$$

$$AR\ (\%) = \frac{Ash_{agglomerates}\ (wt\%) \times wt_{agglomerates}\ (g)}{Ash_{feed}\ (wt\%) \times wt_{feed}\ (g)} \times 100 \qquad \text{Equation 2-5}$$

$$EI\ (\%) = CR\ (\%) + Ash\ (\%) \qquad \text{Equation 2-6}$$

An ash reduction of 88% with combustible recovery of 90% and an efficiency index of 180% was obtained from the beneficiation of anthracite ultra-fines from a Chongiqing mixed sample (Figure 2-6). The feed coal contained 11.9 wt% ash and oxygen content of 3.0 wt%. For the bituminous and lignite coal from Furong and Adaro, respectively, low separation efficiencies of 166% and 173% were obtained, respectively. These results were achieved by using kerosene as a collector. The results obtained from the use of vegetable oil is presented in Figure 2-7. The efficiency indices were 185%, 182% and 170% for the beneficiation of anthracite, bituminous and lignite carbonaceous ultra-fines, respectively. According to the authors, the high-efficiency indices achieved from vegetable oil are due to the hydrophilic oxygenated groups provided by the free acid or the aldehyde groups found in vegetable oils. However, the efficiency index for the beneficiation of ultra-fines from Adaro using kerosene was higher than when using vegetable oil (Wang et al., 2012).

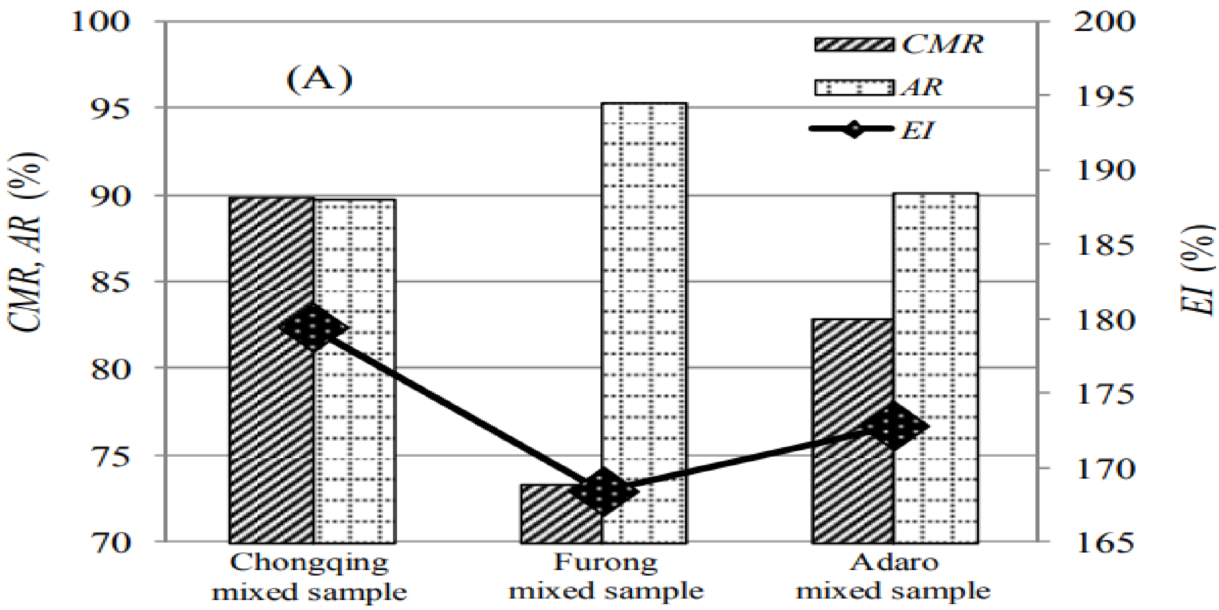

Figure 2-6: The effect of kerosene (A) on combustible matter recovery, the reduction of the ash in the ROM coal and the efficiency index (Wang et al., 2012)

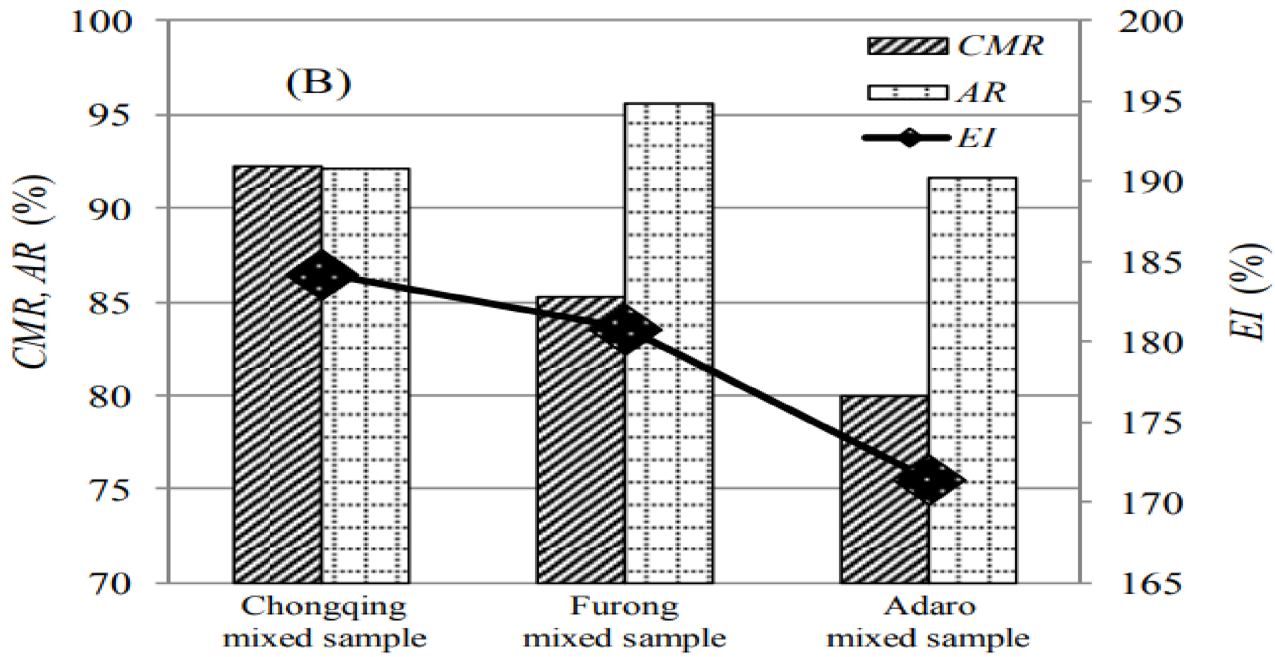

Figure 2-7: The effect of vegetable oil (B) on combustible matter recovery, the reduction of the ash in the ROM coal and the efficiency index (Wang et al., 2012)

Unlike Wang et al. (2012), waste soybean oil was used as a collector in the study carried out by Yadav et al. (2018). The effect of solid concentration, oil dosage and conditioning time on the combustible recovery of carbonaceous ultra-fines of about – 75 µm was investigated. Solid concentrations of 3 wt%, 6 wt% and 9 wt%, with a conditioning time of 15 minutes was used. The increase in the solid concentration led to increased collisions between the carbonaceous ultra-fines and the waste soybean oil. As a result, a high volume of carbonaceous ultra-fines adheres to the bridging agent and, therefore, the combustible recovery increases (Yadav et al., 2018). However, the ash reduction potential decreased with increasing solids concentration. In addition, Wang et al. (2012) indicated that the effectiveness of the bridging agents for beneficiating ultra-fines differ due to the chemical structures of the bridging agents.

Compatibility ensures the spreading of the bridging agent on the surface of coal during the agglomeration process (Mehrotra et al., 1983; Arkhipov et al., 2011; Marmur et al., 2017; Li et al., 2018). This spreading of the bridging agent is also known as the ultra-fines wettability, which is the ability of the bridging agent to wet the surface of coal ultra-fines. Therefore, the bridging agent replaces the water molecule and subsequently creates a contact angle with the coal ultra-fines (Dey, 2012). The failure of contact between the coal ultra-fines and the bridging agent due to the ultra-fines oxidation is well explained through the concept of hydrophobic effect (Mehrotra et al., 1983; Xia et al., 2013; Ozer et al., 2017).

The hydrophobic effect is known as the hydrophobic interaction or hydrophobic force. It is initiated when a hydrophobic collector spreads at the surface of the hydrophilic coal ultra-fines (Zeng et al., 2015; Ozer et al., 2017). Consequently, the coal particles and the bridging agent create a contact angle known to be greater than 90°. According to Zeng et al. (2015), Ozer et al. (2017) and Lu et al. (2019), the contact angle is also known as the wetting angle, and it measures the ability of the bridging agent to spread at the surface of carbonaceous ultra-fines. The formation of $\theta > 90°$ is due to the repulsive forces created at the boundary interface where the coal particles and the bridging agent meet (Ozer et al., 2017; Li et al., 2018; Lu et al., 2019). As a result, agglomerability becomes restricted because the water molecule replaces the collector at the surface of carbonaceous ultra-fines.

Lu et al. (2018) investigated the impact of the oxygen content within the coal ultra-fines on bridging agent replacement by water molecules at the surface of the ultra-fines. They used bituminous D and sub-bituminous coal ultra-fines – 74 µm from different mine sites in Shanxi Province, China. Generally, China classified sub-bituminous coal as coal comprises moisture content of 8.71%, volatile matter of 27.89%, ash content and fixed carbon of 16.91% and 46.49% respectively (Liao et al., 2016). In South Africa, D grade coals have calorific values of 24.5 MJ/kg, inherent moisture of 8%, ash content of 21%, 23% of volatile matter and total sulphur content of 1.5% (Steyn, 2010).

It was found that the spreading of the water molecule at the surfaces of the sub-bituminous and bituminous D coal ultra-fines with oxygen contents of 11.3% and 8.81%, respectively, was due to the contact angles being less than 90° (Figure 2-8). However, these results indicate that the coal ultra-fines' surface was highly oxygenated (hydrophilic), and the water molecule replaced the bridging agent at the surface of these ultra-fines. Consequently, the ultra-fine coal and the bridging agent formed a contact angle greater than 90°. In another study, kerosene was used as a collector to wet bituminous ultra-fine coal with different oxygen contents from the Liulin coal field, Taiyuan and Shanxi Provinces, China. As shown in Figure 2-9, the hydrophobic kerosene formed a contact angle of less than 90° with hydrophobic non-oxidised carbonaceous ultra-fines (fresh coal) with no spreading, while a contact angle greater than 90° was formed at the surface of hydrophilic oxidised carbonaceous ultra-fines (Lu et al., 2019).

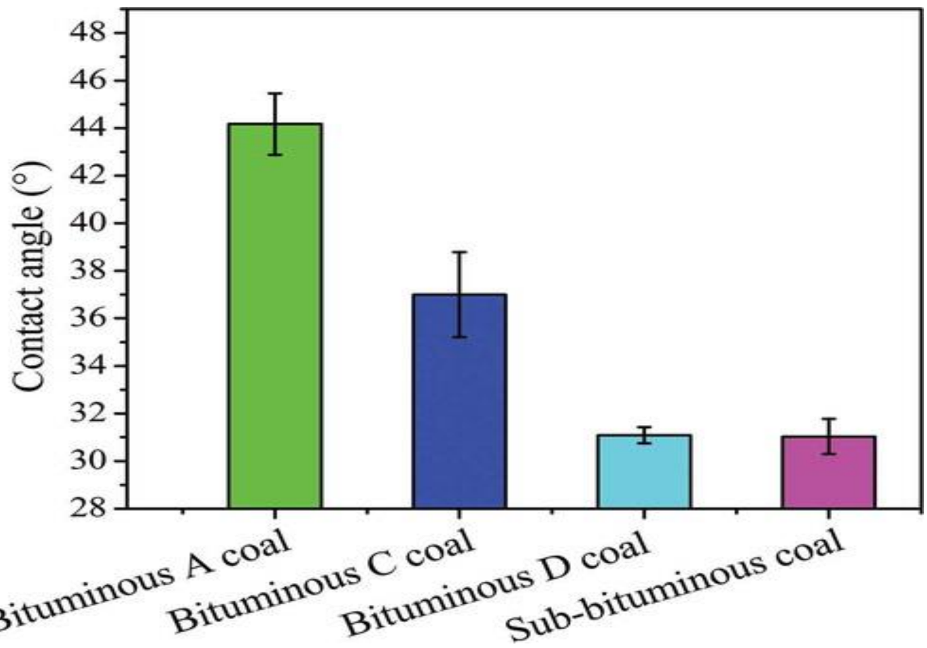

Figure 2-8: The contact angle between water molecules and ultra-fine carbonaceous particles of different ranks (Lu et al., 2018)

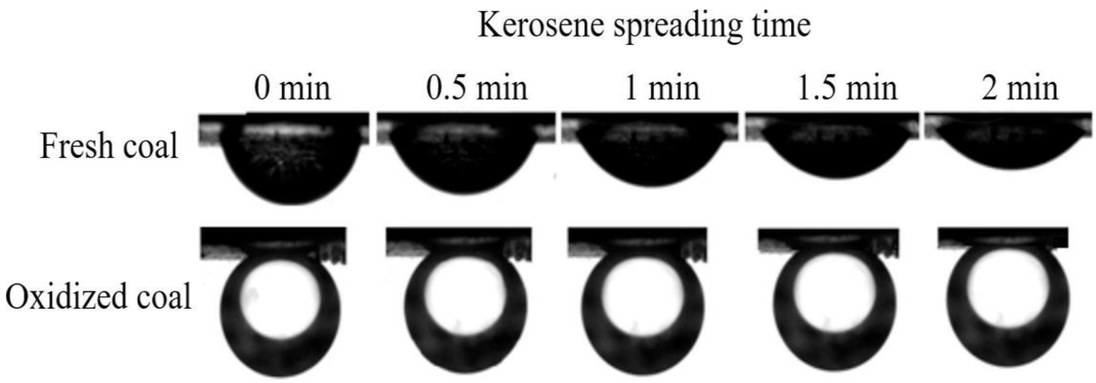

Figure 2-9: The spreading of kerosene at the surfaces of oxidised and non-oxidised carbonaceous ultra-fines (Lu et al., 2019)

2.2.3.1. The oxidation of ROM coal particles

As indicated in the studies carried out by Qu et al. (2015), Liao et al. (2016) and Lu et al. (2019), the presence of oxygen within the coal ultra-fines impacts the flotation and agglomeration processes. The oxygen content, along with other elements including carbon, sulphur, nitrogen and hydrogen, is modified because the coal is exposed to atmospheric air. These elements, especially carbon and oxygen, are essential because they determine the extent of oxidation. According to Ozer et al. (2017), Barma (2018) and Aich et al. (2019), the atmospheric exposure of coal ultra-fine initiates the production of hydrophilic oxygenated functional groups on the surface of the ultra-fines. These groups are responsible for developing oxidation stages depending on the degree that the particles are being exposed to atmospheric air. The first group formed in any coal particle is known as the hydroxyl (C–OH). Other groups found within the coal are carbonyl (–C=O) and carboxyl (O=C–OH). ROM coals are known to be less weathered and therefore comprise of C–OH groups. However, –C=O and O=C–OH occur when the coal particle is continuously exposed to the atmosphere (Perry and Grint, 1983; Pisupati and Scaroni, 1993; Barma, 2018; Li et al., 2018; Aich et al., 2019). The adsorption of these groups onto the surface of the coal particles is due to the loss of electrons and the instability within the particle.

The intensity of adsorption for hydrophilic oxygenated functional groups is used to determine the extent that the coal ultra-fines are being exposed to atmospheric air. As described by Xia et al. (2013), Netten et al. (2014) and Netten and Galvin (2018), ultra-fine coal particles are known to be hydrophobic (non-oxidised) naturally, while those which comprises of –C=O and O=C–OH groups are deemed hydrophilic (oxidised). Ultra-fine coal oxidation is a weathering process that occurs when the ultra-fines are stockpiled in open areas (Sarikaya and Ozbayoglu, 1990; Pisupati and Scaroni, 1993; Lu et al., 2018). According to Netten and Galvin (2018), the ultra-fines stored in water are less vulnerable to atmospheric exposure. This finding demonstrates a need for further study to determine the degree of oxidation of the ultra-fine coal particles stored in slurry ponds.

2.2.3.2. Determination of ROM coal oxidation

The hydrophobicity and hydrophilicity of coal particles can be determined using analytical methods and instruments such as ultimate analysis (using the CHN Analyzer), X-ray photoelectron spectroscopy (XPS) analysis, FTIR spectra and zeta potential (Sahinoglu and Uslu, 2015; Xing et al., 2017; Xu et al., 2017; Wagner et al., 2018). These techniques are used to predict the agglomerability of the coal fines and hence its combustible recovery, especially when the functional groups of the collectors are known.

(i). Ultimate analysis

In the case of ultimate analysis, the literature has demonstrated that the technique is used to determine the elemental composition of nitrogen (N), total carbon (TC), hydrogen (H) and oxygen (O) (Xing et al., 2017). Apart from the elemental composition, functional groups can also be determined using either XPS analysis or FTIR spectra. XPS analysis was used by Lu et al. (2018) to determine the –C=O and O=C–OH groups present on the surface of the coal with high oxygen content. This is illustrated by the bituminous D and sub-bituminous coal with oxygen contents of 8.81% and 11.23%, as shown in Table 2-3. These coals possess high contents of –C=O and O=C–OH groups (Table 2-4).

Table 2-3: The elemental analysis (%, air dry basis) of carbonaceous ultra-fine particles of different ranks (Lu et al., 2018)

Coal samples	N	C	H	S	O	C/O
Bituminous A coal	1.78	87.43	4.95	0.31	5.53	15.81
Bituminous C coal	1.59	86.21	5.01	0.48	6.70	12.87
Bituminous D coal	1.66	83.47	5.48	0.58	8.81	9.48
Sub-bituminous coal	1.97	81.02	5.47	0.31	11.23	7.22

Table 2-4: The contents of functional groups at the surface of ultra-fines (Lu et al., 2018)

Coal samples	Relative concentration ratios of different forms of organic C%			
	C–C/C–H	C–O–C/C–O	C=O	O=C–O
Bituminous A coal	83.77	12.46	3.77	0.00
Bituminous C coal	78.42	14.21	4.50	2.87
Bituminous D coal	73.12	16.80	5.79	4.29
Sub-bituminous coal	70.50	18.32	4.50	6.68

(ii). Fourier transformation infrared spectrometry (FTIR)

The FTIR spectrometry technique uses wavelength to illustrate the presence of oxygenated functional groups within the coal particles. The peaks created as a function of wavenumber and absorbance% represent different functional groups. The FTIR spectra results obtained by Wang et al. (2012) demonstrated that Andaro's ash-free coal is more oxidised compared to the Furong and Chongqing ash-free coals (Figure 2-10). This is indicated by the COOH found at the surface of the Andaro's ash-free coal corresponding to the wavenumber of 1,700 cm^{-1}. This is in line with the ultimate analysis data, which indicated that Andaro coal had an oxygen content of 31.5%. Compared to the oxygen contents of 3.0% and 10.5% found at the surface of the Chongqing and Furong coals, Andaro's coal was more oxidised (Wang et al., 2012).

The aliphatic groups are also used to evaluate the oxidation of coal ultra-fines because oxidation is known to decrease the carbon content of coal. This is substantiated by the ultimate analysis results obtained by Lu et al. (2018) whereby the sub-bituminous coal was deemed more oxidised than the bituminous A coal, which contained carbon and oxygen contents of

87.43% and 5.53%, respectively. While the sub-bituminous coal comprised of carbon and oxygen; 81.02% and 11.23%, respectively (Table 2-3).

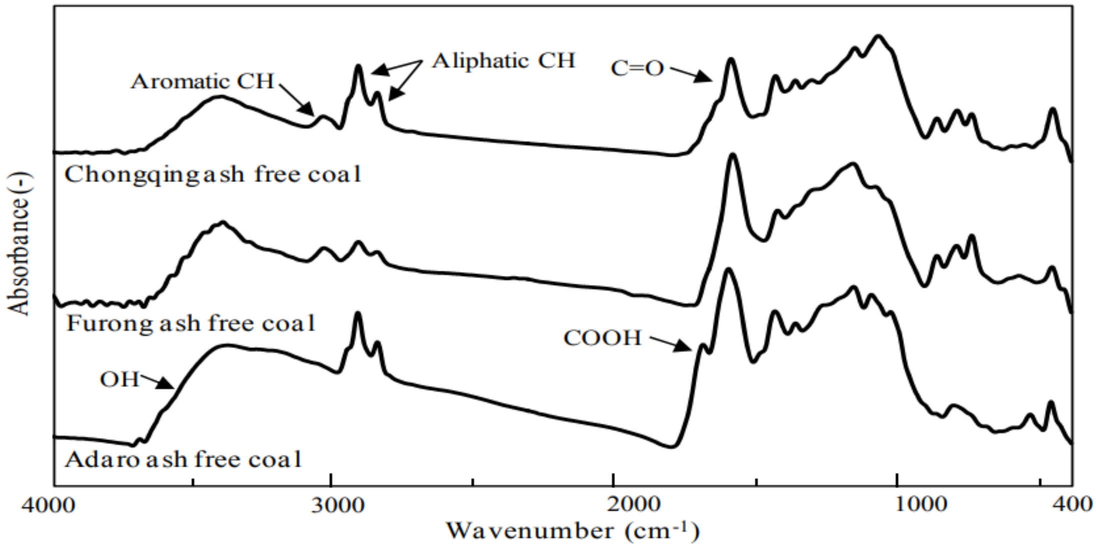

Figure 2-10: The FTIR spectra of the Chongqingash, Furong and Adaro ash-free coals (Wang et al., 2012)

(iii). Zeta potential

According to the literature, zeta potential is an electro-kinetic property, which is also used to examine the extent of oxidation in coal by evaluating the surface charge change. This is measured by evaluating the pH of the coal (Sarikaya and Ozbayoglu, 1990; Sen et al., 2009; Lu et al., 2019). In a study carried out by Dey et al. (2013), a promoter was used to neutralise the surface charges on the surface of an ultra-fine coal sample. The neutralisation of the charge is illustrated by the less negative values of zeta potential at various pH for the coal particle with a promoter (Figure 2-11). According to Sen et al. (2009), Ozer et al. (2017), Lu et al. (2018) and Lu et al. (2019), at neutral pH, the repulsive forces between the coal fines and the bridging agent are minimised. As a result, the compatibility of the coal fines with the bridging agent increases and lower bridging agent dosages are required. As seen in Figure 2-11, coal with no promoter has a more negative zeta potential value at various pHs than coal treated with a promoter. The negative zeta potential indicates the presence of negatively charged hydrophilic oxygenated function groups at the surface of the ultra-fine coal (Ozer et al., 2017).

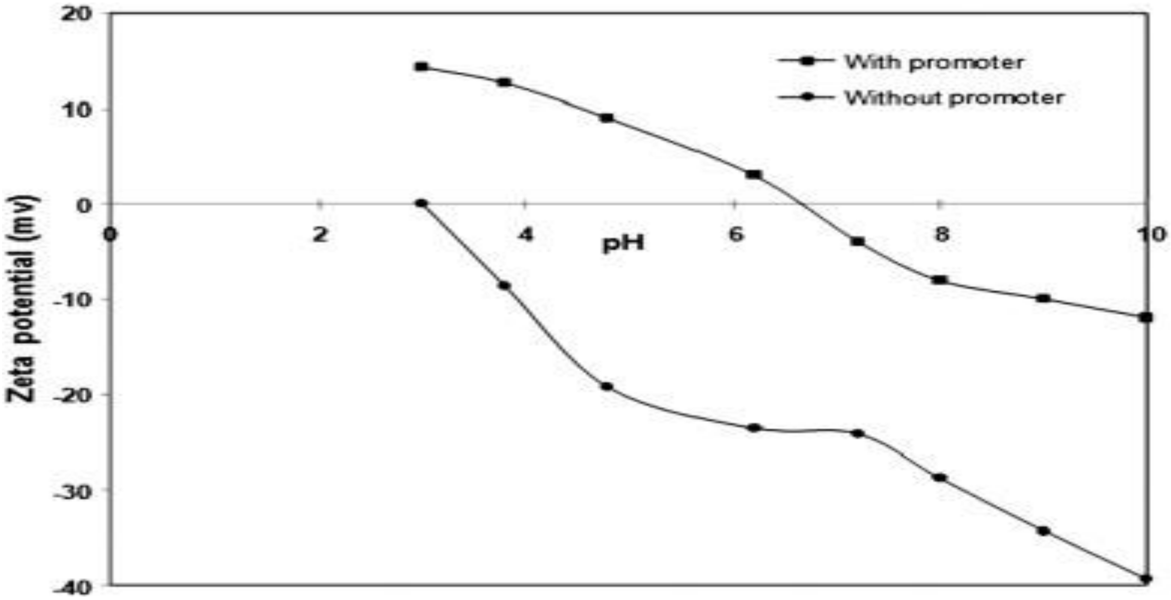

Figure 2-11: The effect of a promoter at the surface of carbonaceous ultra-fine at various pH (Dey et al., 2013)

Sahinoglu and Uslu (2015) indicated that with a known coal zeta potential and bridging agent, the yield of the agglomeration process could be predicted. In addition, the neutral pH of coal ultra-fines also leads to maximum recovery in the form of agglomerates. Several studies have conclusively shown that the zeta potential of the coal fine particles could be used to predict the required dosage of the reagents to mitigate the binding agent replacement potential on the surface of the coal (Sen et al., 2009; Lu et al., 2018; Lu et al., 2019).

2.2.4. Advanced agglomeration process

Given that the agglomeration process had been demonstrated to effectively beneficiate coal ultra-fines, the advanced agglomeration process, using HIP W/O emulsion binder was established to address the following issues:

I. To enhance the selectivity and, therefore, beneficiate both the hydrophobic and hydrophilic carbonaceous ultra-fine particles from the inorganic mineral matters.

II. To reduce the inorganic mineral matters within the product agglomerates. This is because the HIP W/O emulsion binder possesses the collector, frother and depressant characteristics.

III. To replace kerosene or diesel and therefore reduce the pure collector volumes for coal beneficiation.

According to Netten et al. (2014), Sahinoglu and Uslu (2015), Netten et al. (2016), Netten and Galvin (2018), Yadav et al. (2018) and Lu et al. (2019), the advanced agglomeration process does not differ much from the selective agglomeration process. The collector type and the use of W/O emulsion binder differentiate these two processes. It has been demonstrated that the advanced agglomeration uses the HIP W/O emulsion binder, which is also known to be a novel and economical binder. It selectively wets and binds to both the hydrophobic and the hydrophilic carbonaceous particles, thereby leaving the inorganic minerals un-wetted (Netten et al., 2017b; Netten and Galvin, 2018; Lu et al., 2019). Regardless of the benefits and the capabilities of the advanced agglomeration process, it has been demonstrated that the effectiveness of the process can be compromised if factors such as agitation time, selectivity, solids concentration, collector dosage and the degradation of the HIP W/O emulsion binder are not taken into consideration during beneficiation. These factors are also important when the emulsion is applied ***in the flotation process, as used in this study***, rather than the advanced agglomeration.

2.2.5. Emulsification

Emulsification is the mixing of water, collectors, electrolytes and emulsifiers using a homogeniser or stirrer for a certain period (Bensley et al., 1977; Borrow et al., 2018; Kasomo et al., 2018; Yadav et al., 2018). Subsequently, a *novel binder*, a viscous and gel-like substance, HIP W/O emulsion binder, was produced (Netten et al., 2015; Netten et al., 2016; Netten et al., 2017b; Netten and Galvin, 2018). The reagents and the emulsification process will be explained in the subsequent section.

2.2.5.1. Collectors

The selective agglomeration and froth flotation techniques use collectors such as vegetable oils (soy bean, canola, sunflower cotton seed and many more) and neutral hydrocarbon oils such as kerosene and diesel. However, the availability of these vegetable oils has been reported to be low, and the cost of these hydrocarbons, especially diesel, is high. This is another reason that motivated the establishment of the HIP W/O emulsion binder. According to Laskowski and Yu (2000), Netten et al. (2017a) and Netten and Galvin (2018), about 7.5 ml of either kerosene or diesel can be used to produce a 300 ml batch of HIP W/O emulsion binder. The reason behind this is explained later in the text.

2.2.5.2. Electrolytes

An electrolyte is a molecule that dissociates into cations and anions when dissolved in water. NaCl is a strong electrolyte that is hydrophilic and several authors have used it to prepare the HIP W/O emulsion binder. According to Netten and Galvin (2018) and Lu et al. (2019), NaCl assists in preventing phase inversion of the emulsion binder. Given that the HIP W/O emulsion degradation is an issue in the advanced agglomeration process, the rate or potential of degradation is evaluated by examining the conductivity change of the dissolved HIP W/O emulsion binder in water under mechanical stirring. This is because it has been demonstrated that the suspension of NaCl from the HIP W/O emulsion influences the conductivity.

2.2.5.3. Emulsifier

Emulsifies, also known as emulsifying agents or surfactants (Capes and Darcovichi, 1984; Ozer et al., 2017; Xing et al., 2017; Borrow et al., 2018), are categorised into several groups such as non-ionic, cationic, anionic and zwitterionic. All these groups are amphiphilic, meaning they comprise both water-hating (hydrophobic tail) and water-loving sites (hydrophilic head) (Ozer et al., 2017; Lu et al., 2019). The differences in their composition arise due to the hydrophilic head group type. According to Pichot (2012) and Qu et al. (2015), the head can either be neutral or charged depending on the emulsifier group; non-ionic (neutral), cationic (positive charge), anionic (negative charge) and zwitterionic (both positive and negative charges). Even though zwitterionic is compatible with other types, non-ionic emulsifiers have been demonstrated remarkable in the case of coal beneficiation (Capes and Darcovichi, 1984; Borrow et al., 2018). This is substantiated by Qu et al. (2015), who beneficiated carbonaceous particles using non-ionic 2-ethyl hexanol and found that this surfactant does not compromise the ash reduction potential like anionic SDS and cationic DDA.

Non-ionic emulsifiers are insoluble in water but soluble in organic liquids. This is due to the dominance of the hydrophobic alkyl chain, which renders the whole structure hydrophobic (Lu et al., 2019). Ozer et al. (2017) and Lu et al. (2019) indicate that these molecules are amphiphilic, and their hydrophilic heads are neutral. Span 80 is the most commonly used non-ionic emulsifier essential for the bridging agent preparation in the advanced agglomeration process. The molecule has a chemical structure of $C_{24}H_{44}O_6$ and is also known as sorbitan monooleate (Netten et al., 2014; Netten et al., 2016; Borrow et al., 2018; Netten and Galvin, 2018). The main reason behind the capabilities of Span 80 to dissolve organic liquids, mainly kerosene, is due to the hydrophobic bonds it forms with organic liquids (Lu et al., 2019).

2.2.6. The effect of emulsification on collector usage

According to the literature, the cost of collectors has been a major challenge to the beneficiation of coal ultra-fines. The objective is always to maximise the collector dosages without compromising the mass pull and the process of selectivity. As reported by Netten and Galvin (2018) and Lu et al. (2019), pure oily collectors are used for the beneficiation of fine coal, but given the structural changes of the coal due to atmospheric exposure, these collectors are ineffective (Ozer et al., 2017; Li et al., 2018; Lu et al., 2019). This means the affinity of the carbonaceous ultra-fines to attach to the air bubbles during flotation and therefore enhance the mass pull are compromised (Dell, 1953; Dell, 1964; Hu, 1975; Nicol et al., 1994; Sahu et al., 2019).

The HIP W/O emulsion binder was developed to decrease collector usage (Netten and Galvin, 2018; Lu et al., 2019). According to Cameron (2005), the HIP W/O emulsion binder is an emulsion that comprises more than a 74% volume fraction of water droplets as the dispersion phase. The HIP emulsions have been used for many years, mostly in food preparation, fuels, oil recovery and cosmetics (Cameron, 2005 and Abdulredha et al., 2018). For the beneficiation of coal ultra-fines, more than an 80% volume fraction of the dispersed phase is preferred due to the reduction in the organic liquids used for the emulsion binder preparation. The dispersion phase for HIP W/O is presented in Figure 2-12, where the impact of the dispersion phase on the size of the continuous phase films shows that the higher the volume of the dispersion phase (water molecules), the thinner the organic liquid films and therefore low organic liquids requirement. According to Netten and Galvin (2018), the water molecules occupy and fill the void spaces within the HIP W/O emulsion binder.

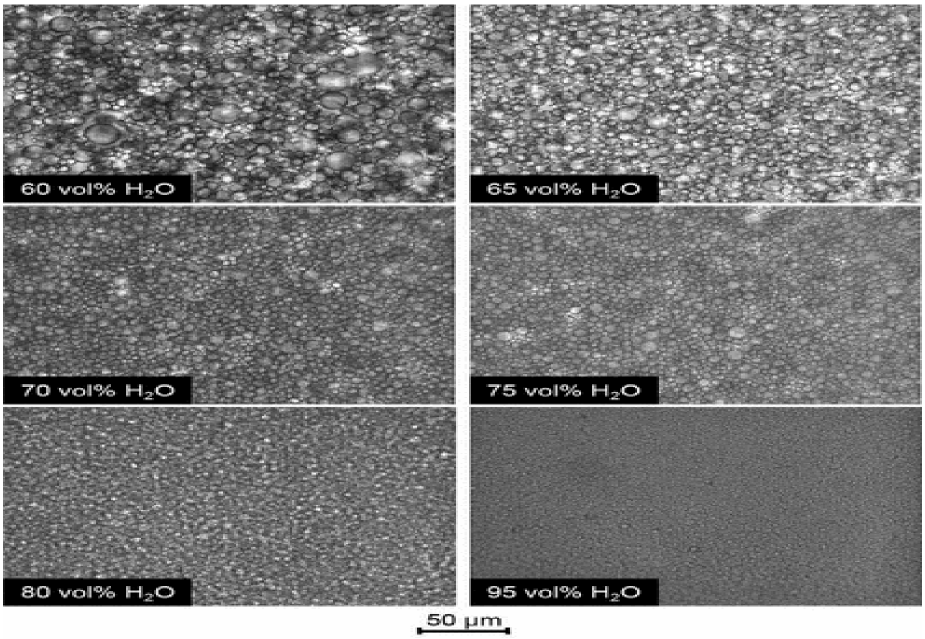

Figure 2-12: Microscopic images of a HIP W/O emulsion with various internal dispersion phase volume fractions (Netten et al., 2017b)

Apart from the internal phase, the emulsion binder comprises the continuous or external phase, which is made by mixing Span 80 with kerosene. The HIP W/O emulsion binder is termed W/O because the dispersion phase, which comprises water droplets, has been added to the continuous phase of organic liquids. It has been reported by Netten and Galvin (2018) and Lu et al. (2019) that 7.5 ml of kerosene, 7.5 ml of Span 80 and 285 ml of water can yield about 300 ml of viscous HIP W/O emulsion binder (Figure 2-13).

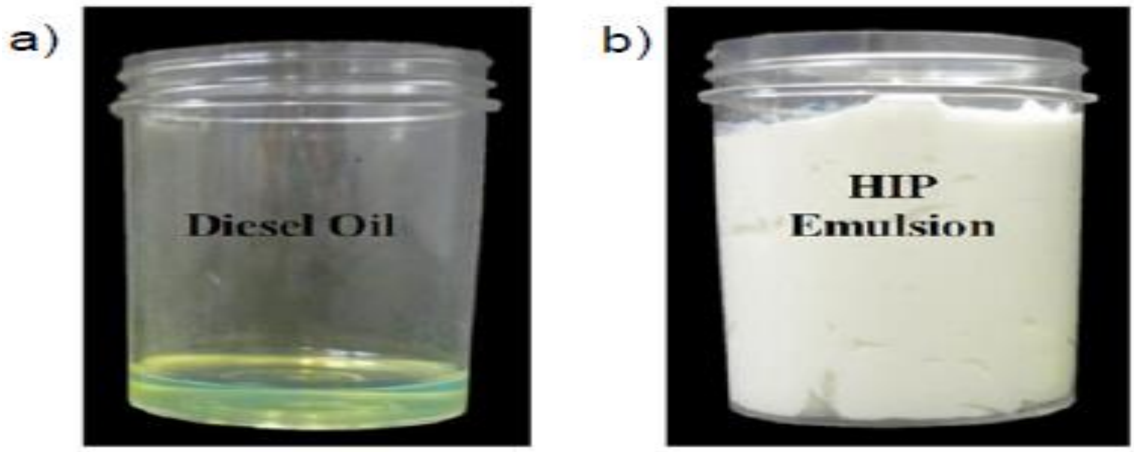

Figure 2-13: Diesel (a); HIP W/O emulsion (b) containing same volume of organic liquid (Netten et al., 2017b; Galvin and Netten, 2017; Borrow et al., 2018)

2.2.7. Factors affecting the advanced agglomeration and flotation process

2.2.7.1. Agitation time

There are two types of agitation regarding the floating of coal particles before agglomeration and froth flotation. These agitation times include the mixing time and the conditioning time. Based on the studies conducted by Lu et al. (2019) and Zhang et al. (2020), the latter is associated with the dispersion of the coal ultra-fines prior to adding the HIP W/O emulsion binder, while the former is the dispersion time for both the coal and the HIP W/O emulsion binder. The conditioning time has been reported to influence the floating of the carbonaceous particles from the coal ultra-fines. This is caused by the impact of the conditioning time on the stability of the emulsified binder HIP W/O. As demonstrated by Netten and Galvin (2018) and Lu et al. (2019), long conditioning times at agitation speeds of more than 1,000 revolutions per minute (rpm) has been reported to degrade the HIP W/O emulsion binder. For this reason, Netten et al. (2016) recommended conditioning the HIP W/O emulsion binder using minimum agitation times of between 5 seconds and 15 seconds. However, this also depends on the speed of agitation provided by the agglomeration or flotation unit.

As a result of poor conditioning time, the inversion could be compromised (Netten et al., 2016). The inversion time is defined as the time it takes to float the carbonaceous ultra-fines within the coal. It can also be defined as the time to form agglomerates or froths (Ozer et al., 2017; Lu et al., 2019). As reported by these authors, both the agitation speed of the agglomeration and flotation units and the conditioning time impact the floating of the carbonaceous ultra-fines from coal. However, the feed coal also influences the cell size, which dictates the speed of agitation.

The distribution of the floated carbonaceous ultra-fines (Figure 2-14) can either be narrow or wide depending on the particle size range of the carbonaceous clean product. According to Netten et al. (2014), wide size distribution, which is illustrated by the wideness of the curve, demonstrates the conditioning time of between 0 and 10 seconds (Figure 2-14). This wide distribution reflects the availability of different particle size fractions within the produced carbonaceous agglomerate under the set condition time (Netten and Galvin, 2018; Lu et al., 2019; Zhang et al., 2020). For instance, within the conditioning time of 10 seconds, the size range of the carbonaceous particles is between 20 µm and approximately 998 µm, whereas, at 0 seconds, 5 to about 980 µm particle size carbonaceous agglomerates or products are obtained.

In the case of a narrow distribution, the proportion of carbonaceous particles agglomerate is low. This is illustrated by the agitation times of 45 and 90 seconds (Figure 2-14).

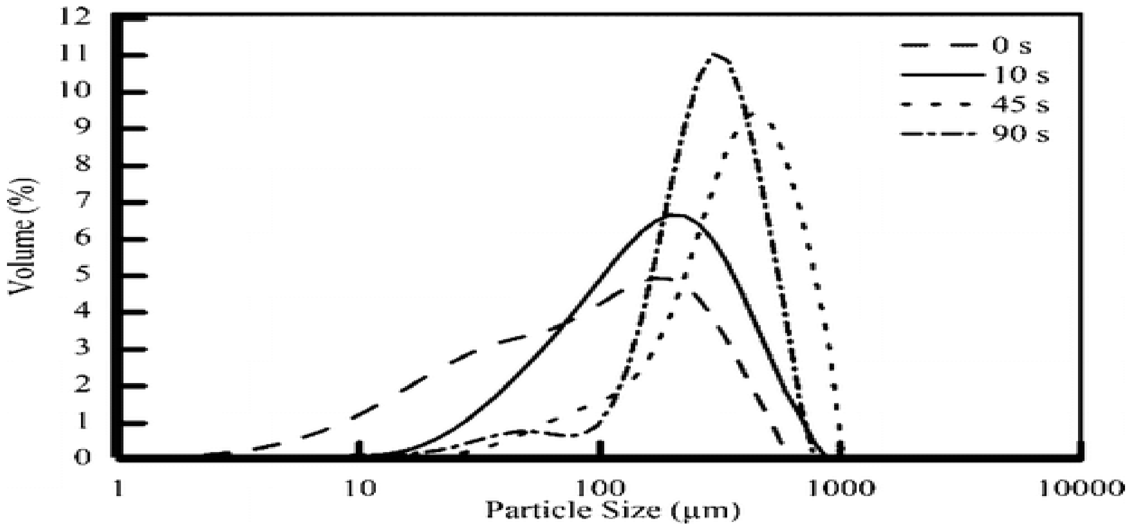

Figure 2-14: The effect of agitation time on the distribution of carbonaceous ultra-fines (Netten et al., 2014)

In addition to particle size distribution (PSD), mean diameter curves can also be used to monitor the sizes of the produced carbonaceous agglomerates. The mean diameter of the agglomerates increases with the inversion time up to the conditioning time of 40 seconds and then starts to decrease (Figure 2-15). Netten et al. (2014) reported that the decrease in conditioning times between 50 and 100 seconds is an indication of HIP W/O emulsion binder degradation. This is because the structural integrity of the emulsion binder is too weak to hold the agglomerated carbonaceous particles. The mean diameter is also known as the average diameter of the agglomerates, and is defined as the 50% (d_{50}), the representative of the agglomerate sizes (Netten et al., 2014).

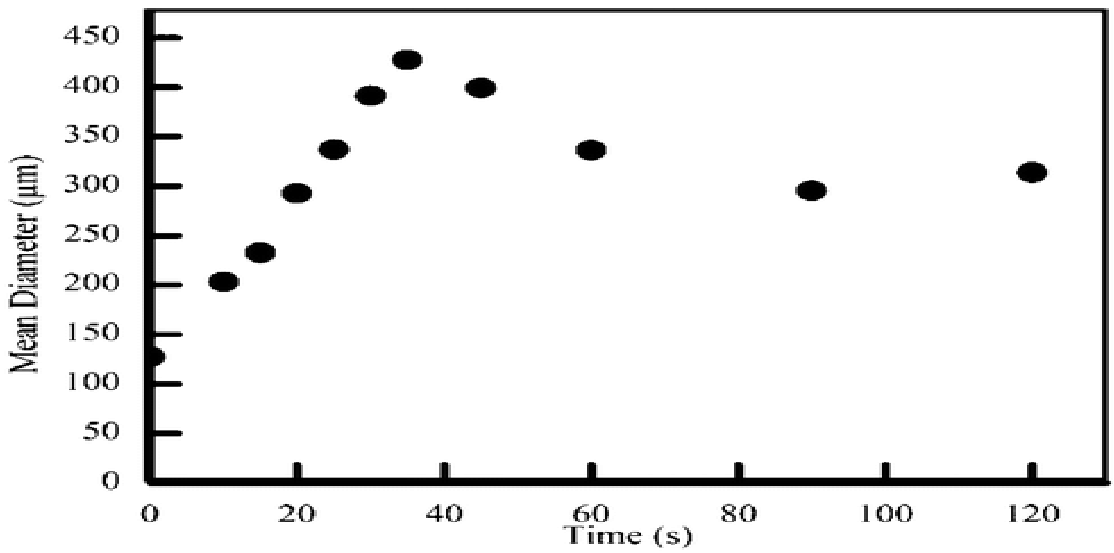

Figure 2-15: The average diameter (d_{50}) of the agglomerated carbonaceous ultra-fines as a function of agitation time (Netten et al., 2014)

2.2.7.2. Selectivity

Selectivity is the ability to differentiate the hydrophobic and hydrophilic carbonaceous ultra-fine particles from inorganic mineral matters prior to advanced agglomeration and froth flotation (Netten and Galvin, 2018; Lu et al., 2019). NaCl within the emulsion enhances the selectivity of carbonaceous ultra-fines from the feed ROM coal (Ozer et al., 2017). This is due to the ability of the NaCl to neutralise the surface charges of the coal when it gets dissolved in the dispersion phase. Despite the years of research, the percentage by weight (wt%) of NaCl required still seems debatable given that Netten et al. (2014), Netten et al. (2015), Netten et al. (2016) and Netten and Galvin (2018) used 3 wt% NaCl to beneficiate non-oxidised coal. Whereas, Lu et al. (2019) used 5 wt% NaCl as part of the dispersion phase. In the current study, the percentage composition of NaCl was varied to determine its influence on the grade and yield of the clean coal.

The surface neutralisation of coal particles is very important because it has been demonstrated to improve the selectivity of carbonaceous particles from the coal inorganic matters. The presence of clay minerals, including but not limited to silica (SiO_2), kaolinite [$Al_2Si_2O_5(OH_4)$], calcite ($CaCO_3$) and dolomite [$CaMg(CO_3)_2$], and oxygen in the chemical structure of these clay minerals can lead to the decrease in the selectivity potential before flotation and agglomeration (Sarikaya and Ozbayoglu, 1990; Qu et al., 2015; Borrow et al., 2018; Lu et al., 2019). Selectivity influences the quality and yield of the products produced by these two techniques. In terms of the ultra-fine coal beneficiation through advanced agglomeration, the ash content within the agglomerated product indicates the success of selectivity. That is, with HIP W/O emulsion binder, only the carbonaceous ultra-fines will be floated, leading to lower ash coal product compared to the traditional agglomeration and flotation processes where poor wetting oily collectors such as kerosene and diesel don't select or beneficiate oxidised carbonaceous ultra-fines effectively (Xia et al., 2013; Lu et al., 2019; Sahu et al., 2019; Zhang et al., 2020).

As indicated by Falcon and Ham (1988), Netten et al. (2014), and Netten and Galvin (2018), any beneficiation technique that can reduce the ash content to 20% from the feed coal with an ash content of more than 30% is deemed effective. However, this depends on the product specifications for the target market. For instance, the ash content of 20% and above are mostly used for electricity generations, particularly in South Africa. Power plants like Lethabo power station, requires coal feed with ash content ranging from 35% and 42% ash (Eskom, n.d.). Whereas agglomerated products with an ash content of less than 8% are regarded as high grade and are used for metallurgical applications. However, the fixed carbon, volatile matter and moisture contents of the clean coal has a significant role in the application of the coal.

As a result of poor selectivity, several beneficiation approaches were established, which include Dell's original release analysis, Dell's modified release analysis and tree analysis, to upgrade the floated and agglomerated product in terms of reducing the inorganic mineral matters (Dell, 1953; Dell, 1964; Hu, 1975 and Sahu et al., 2019). These analysis processes are similar, given that the objective is to enhance the process of selectivity. The differences arise in the modification of aeration rate, scrapping time and the impeller speed (Nicol et al., 1994; Bhattacharya et al., 2017). This is dictated by the products, either concentrate or tailings, reintroduced to the subsequent stages of froth flotation. The tree analysis consists of scavenger, cleaner and re-cleaner stages (Figure 2-16). The concentrate and tailing streams produced are mostly used to calculate the cumulative yield, achieved by adding the mass pulled to the agglomerated product.

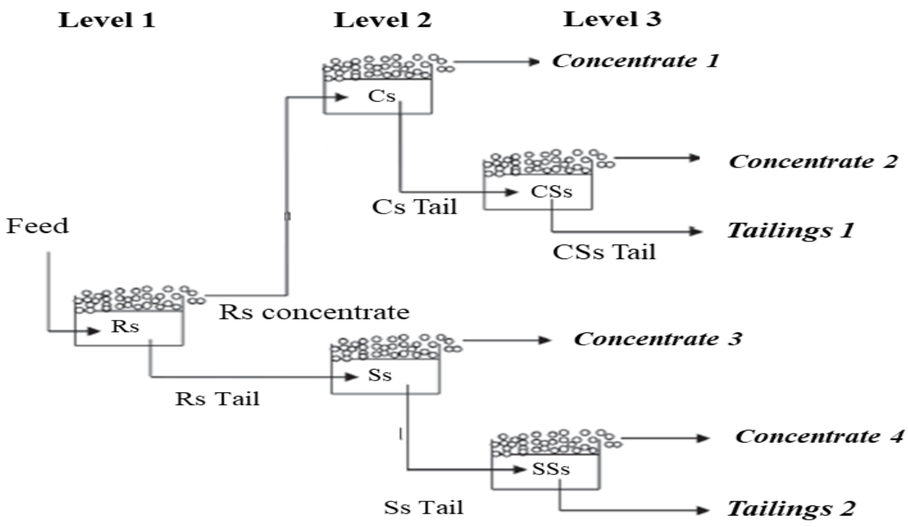

Figure 2-16: Tree analysis procedure (Nicol et al., 1994)
Rs: rougher stage; Cs: cleaner stage; CSs: cleaner scavenger stage; Ss: scavenger stage; SSs: scavenger scavenger stage

2.2.7.3. HIP W/O emulsion binder functional groups on selectivity

The HIP W/O emulsion binder could enhance the selectivity of the carbonaceous particles within the coal that are made hydrophobic and hydrophilic due to oxidation (Netten and Galvin, 2018; Lu et al., 2019). This is because the HIP W/O emulsion binder has hydrophobic and hydrophilic characteristics, leading to the chances of hydrogen bonding formation between the carbon present in the oxidised coal and the HIP W/O emulsion binder. However, the strength of the hydrogen bond formed will differ based on the extent to which the coal has been oxidised, which also reflect the amount of oxygen present in the coal (Lu et al., 2019).

As shown in Figure 2-17, the HIP W/O emulsion binder behaves differently in terms of spreading at the surfaces of the oxidised and non-oxidised carbonaceous ultra-fines. This is due to the different oxygen contents found within these ultra-fine coal particles. The HIP W/O emulsion is well distributed at the surface of oxidised coal with no sign of instabilities in the form of droplet aggregate. In the case of non-oxidised (fresh coal), the distribution of the HIP W/O emulsion binder is unstable (Figure 2-17).

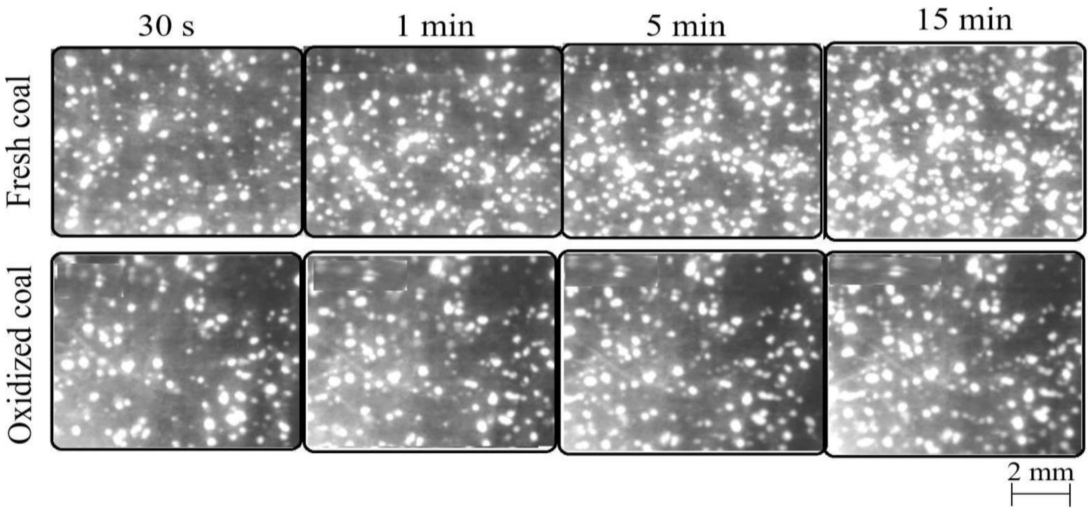

Figure 2-17: Micrographs of the HIP W/O emulsion binder droplets at different carbonaceous ultra-fine surfaces (Lu et al., 2019)

In a study carried out by Netten et al. (2016), non-oxidised ROM coal with 50% under -100 µm was beneficiated using the HIP W/O emulsion binder. A combustible recovery of 70% - 80% carbonaceous agglomerates with an ash content of 16 – 17% was achieved. This reduction was obtained from a feed coal with an ash content of 42%. An oxidised coal of – 74 + 38 µm was beneficiated in a flotation cell by Lu et al. (2019), and the author reported an increase in yield with the HIP W/O emulsion binder. However, the authors did not evaluate the effectiveness of the process in terms of ash reduction potential and combustible recovery. The absence of adequate literature on the advance agglomeration of both oxidised and non-oxidised ultra-fines coal using the same HIP W/O emulsion binder highlights the need for further study in this field.

2.2.7.4. Solid's concentration

The solids concentration of particles, also known as pulp density or bulk solids, impacts the recovery of carbonaceous ultra-fines and the ash reduction potential (Mohanty et al., 1998; Ozer et al., 2017). Mohanty et al. (1998) showed that solids concentration of 24 wt% yielded high combustible recovery and low ash content within the product agglomerates compared to the solids concentration of 16 and 8 wt%. As reported by the authors, higher solids concentration is essential in enhancing the selectivity of the process. This was also supported by Yadav et al. (2018); the increase in solids concentration enhanced the probability of collisions between coal ultra-fines and the bridging agent. Consequently, high volumes of carbonaceous ultra-fines within the coal adhered to the bridging agent, and the weak hydrophobic particles, which are unliberated, sink, and the grade improves (Yadav et al., 2018).

Wills (2006) demonstrated that the required feed for coal beneficiation through laboratory test work could be 250 g, 500 g, 1 kg or 2 kg. However, this is not a restriction, the size of the ROM feed and the water as indicated in Equation 2-7 depends on pulp density. Liao et al. (2017) beneficated coal feed of 120 g with pulp density of 7.4 wt%. A pulp density of 8 wt% was used by Qu et al. (2015). According to Wills (2006), the solids concentrations could be more than 40 wt%, however, there is literature inadequacy especially on the beneficiation of coal at laboratory scale. In terms of water requirements, this ensures proper dilution and therefore avoids under or over dilution of either the slurry or the collector. Poor dilution is problematic given that over dilution minimises the interaction of the coal particles with the reagents. As a result, the hydrophobicity enhancement of the carbonaceous particles within the coal is compromised. Therefore, carbonaceous particles end up sinking instead of floating. In terms of under dilution, it has been demonstrated that the particles weigh the bubbles and therefore initiate bubble-particle detachment (Mohanty et al., 1998; Wills, 2006).

$$C_{ws} = \frac{W_s}{W_s + W_w} \times 100 \qquad \text{Equation 2-7}$$

Where C_W is the solids concentration percentage, W_S represents the mass of the feed coal, and W_W indicates the water required for the mix.

An investigation into the effect of solid concentrations at 3 wt%, 9 wt% and 10 wt% to beneficiate ultra-fine coal at – 75 µm using waste soybean oil as a bridging agent was conducted by Yadav et al. (2018). Based on the study conducted by Mohanty et al. (1998), these solid concentrations are regarded to be very low. Yadav et al. (2018) found that the combustible recovery increased with solids concentration. At 3 wt%, the combustible recovery was 76.36%, while at 9 wt%, the recovery was 89.90%. However, the ash reduction potential was found to decrease with increasing solids concentration. This might be due to the high air bubble surface area, which allows the inorganic minerals and weak hydrophobic particles to be pulled to the concentrate (Mohanty et al., 1998).

2.2.7.5. Collector dosage

Collectors are the driving force for the separation of the inorganic minerals in coal from its organic. This is because they enhance the hydrophobicity of the carbonaceous particles within the coal and enhance the selectivity process. However, the dosage is influenced by the coal type or grade fed during the rougher stage. This implies that every feed coal has its own dosage requirements to be beneficiated effectively. As reported by Qu et al. (2015) and Peng et al. (2015), the collector dosage per ton of the feed primarily used is between 227 g/ton and 907 g/ton. Mohanty et al. (1998) used 200 g/ton, 750 g/ton, 1300 g/ton and 1850 g/ton dosage to beneficiate coal ultra-fines using release analysis. The lower dosages of 200 g/ton and 750 g/ton resulted in optimum separation in terms of ash reduction (Figure 2-18). ***The current study used 250 g/ton, 350 g/ton and 450 g/ton organic liquids (kerosene and Span 80) to prepare the HIP W/O emulsion binder***.

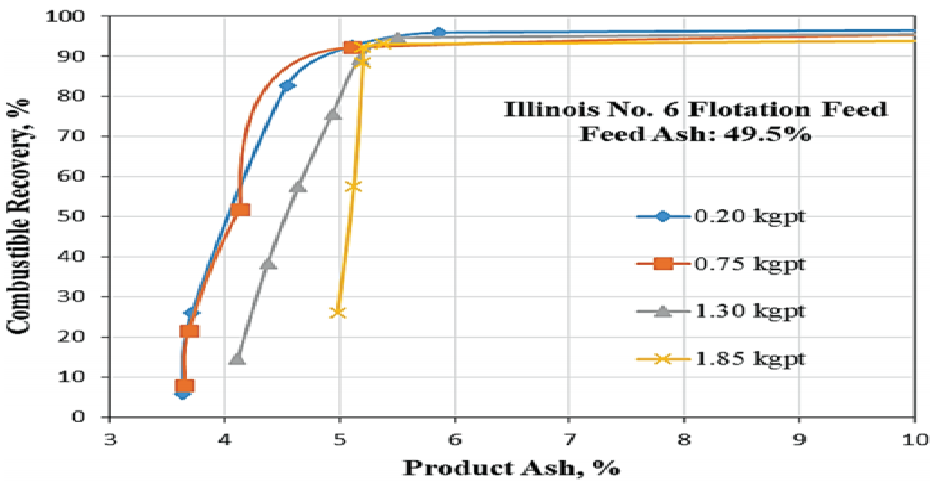

Figure 2-18: The effect of collector dosage on the combustible recovery and ash content within the concentrate (Mohanty et al., 1998)

Given that Mohanty et al. (1998) used collectors such as n-dodecane [$CH_3(CH_2)_{10}CH_3$] and still achieved the ash content of less than 10% within the clean coal product, it is expected that the HIP W/O emulsion binder will also reduce the ash content further, especially in coal with different oxygen contents. Additionally, Netten and Galvin (2018) have demonstrated that tree flotation produced a clean coal product with ash content of less than 10% from the feed ash content of 42% ash. This was high grade product compared to clean coal produced using agglomeration. According to the author, there might be entrainment of inorganic mineral contents within the agglomerates.

2.2.7.6. HIP W/O emulsion degradation

Despite the benefits of the advanced agglomeration process using HIP W/O emulsion, it has been demonstrated that the creation of stable HIP W/O emulsion binder is challenging, especially under mechanical stirring (Netten et al., 2016; Barma, 2018; Netten and Galvin, 2018; Lu et al., 2019). This is because of the force applied to the emulsion binder and, consequently, the oil films of the continuous phase break and initiate phase inversion (Borrow et al., 2018; Netten and Galvin, 2018). Phase inversion can be defined as the transformation of HIP W/O emulsion binder to HIP O/W emulsion binder (Borrow et al., 2018). In the study carried out by Netten et al. (2016), the conductivity of the HIP W/O emulsion as a function of emulsification time was used to evaluate the stability of the emulsion binder. The conductivity of the HIP W/O emulsion binder increased with an increasing conductivity up to 45 and 60 seconds, whereafter, the conductivity remained constant (Figure 2-19). This increase was because the suspending liquid of tap water comprised high quantity of NaCl (Borrow et al., 2018).

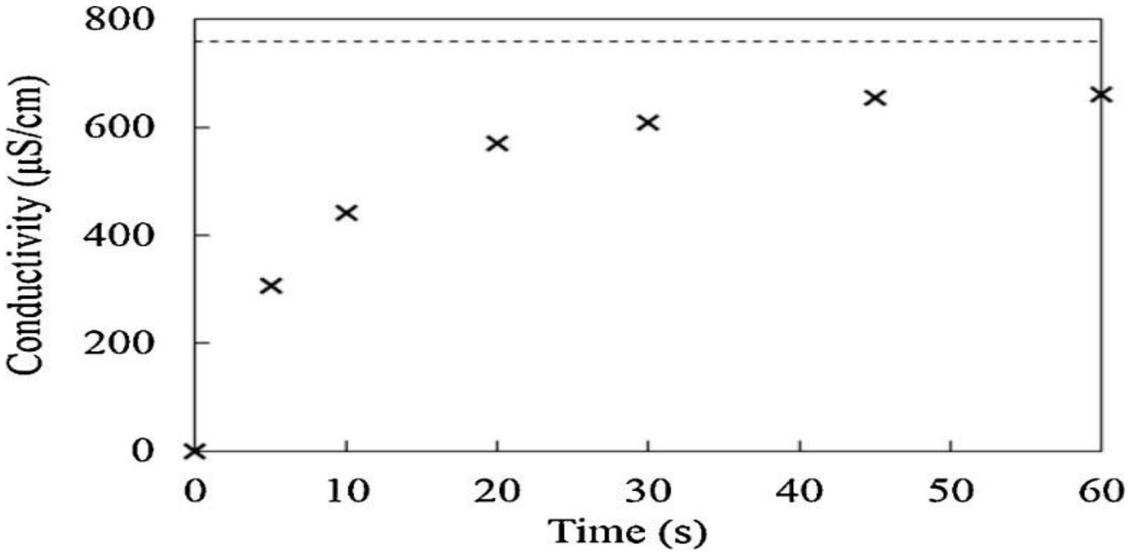

Figure 2-19: The conductivity of HIP W/O emulsion binder as a function of emulsification time (Netten et al., 2016)

The maximum conductivity limit was greater than 700 µS/cm (Figure 2-19). This was obtained by measuring the conductivity of the dispersion phase during the HIP W/O emulsion binder preparation. According to Netten et al. (2016) and Borrow et al. (2018), the maximum conductivity limit indicates the maximum level of NaCl in tap water, which corresponds to the conductivity that must be obtained to complete the degradation of the HIP W/O emulsion binder throughout the advance agglomeration process. This demonstrates that the maximum limit for the HIP W/O emulsion binder prepared using NaCl concentrations of 3 wt% and 5 wt% will differ. Without any experimental backup, it can be assumed that the rate of degradation for the HIP W/O emulsion binder prepared with 5 wt% NaCl might be slower compared to that prepared with 3 wt% NaCl. Knowing that the degradation rate of HIP W/O emulsion binder is associated with different NaCl concentrations will assist in avoiding unexpected rapid rate of degradation for both the batch and continuous steady-state advanced agglomeration process.

The thinness of the continuous phase film depends on the volume of the internal phase (Netten and Galvin, 2018; Lu et al., 2019). Lu et al. (2019) found that the HIP W/O emulsion binder did not experience degradation after 10 minutes of conditioning at 15,000 rpm. However, Netten et al. (2016) reported opposite results, given that the degradation of the HIP W/O emulsion binder occurred with an increasing conditioning time. Netten et al. (2016) used a waring blender operated at the speed of 22,000 rpm to condition the HIP W/O emulsion binder for 60 seconds, and the HIP W/O emulsion binder was inverted in less than 30 seconds. This agrees with the results obtained by Borrow et al. (2018) who conditioned the binder within 5 to 30 seconds. The variation in results from the studies might be due to the dissimilar volume of the internal phase and the concentration of the NaCl (Netten et al., 2016; Borrow et al., 2018 and Lu et al., 2019). Netten et al. (2016) and Borrow et al. (2018) used the dispersion phase of 95% aqueous solution with 3 wt% NaCl, whereas Lu et al. (2019) used the dispersion phase of 85% aqueous solution with 5 wt% NaCl.

From these findings, it can be deduced that at a constant agitation speed and NaCl concentration, the emulsion binder with the dispersion phase of 95% by volume (vol%) will experience degradation easily compared to the binder with 85 vol% of the dispersion phase. Netten et al. (2016) and Borrow et al. (2018) reported that this might be due to the failure of the continuous phase oil films to handle the applied force for extended conditioning times, with 60 seconds being the maximum. The volume of the continuous phase might contribute to the conditioning times for the beneficiation of coal fines using kerosene within the range of 0 and 120 seconds, as indicated by Netten et al.'s. (2016) study. It has been reported that kerosene can be conditioned for long periods of time because it has thick oil films. Therefore, it can handle the stress provided by agitation (Laskowski and Yu, 2000; Netten and Galvin, 2018).

Thus, both advanced agglomeration and flotation using HIP W/O emulsion binder will operate effectively at certain conditioning times before degrading. However, this depends on the agitation speed provided by the agglomeration and flotation units. Too much force applied to the HIP W/O emulsion initiates binder degradation. In terms of the minimum agitation times, it has been reported that the fragmentation of the HIP W/O emulsion binder is minimised. Therefore the emulsion becomes insufficient for the agglomeration of the carbonaceous ultra-fines, and the mean diameter of the agglomerates tends to decrease (Figure 2-15) (Netten and Galvin, 2018). The HIP W/O emulsion binder must fragment into small gel-like pieces, which has been reported to act as a "scaffolding onto which carbonaceous particles can deposit" (Netten et al., 2014, p. 10662).

2.3. Conclusion

This review presents different beneficiation processes for the concentration of coal. It has been demonstrated that the carbonaceous ultra-fines, which are considered discards or tailings, can be re-beneficiated from the coal dump to upgrade its value or quality. In addition, the collector usage can be reduced by employing the HIP W/O emulsion binder. However, each beneficiation process has limitations and failures regarding the ash reduction potential. Thus ongoing research aims to establish new processes that are cost-effective and can benefit oxidised coal. The newly developed HIP W/O emulsion binder has an issue with binder degradation. However, understanding the degradation mechanisms of the emulsion will enable the successful enrichment of the ultra-fine using the W/O HIP emulsion binder, both in flotation and agglomeration processes.

CHAPTER 3: MATERIALS AND EXPERIMENTAL PROCEDURES

3.1. Introduction

This chapter sets out the detailed experimental method used in this research for the upgrading of coal discard by the advanced W/O HIP emulsion binder technique. Using this approach, the effectiveness of the W/O HIP emulsion binder and kerosene for the beneficiation of organic carbonaceous coal particles with different oxygen contents was investigated. The information regarding the discard coal preparation and characterisation, the HIP W/O emulsion preparation and the beneficiation test procedures as indicated in Figure 3-1 are provided.

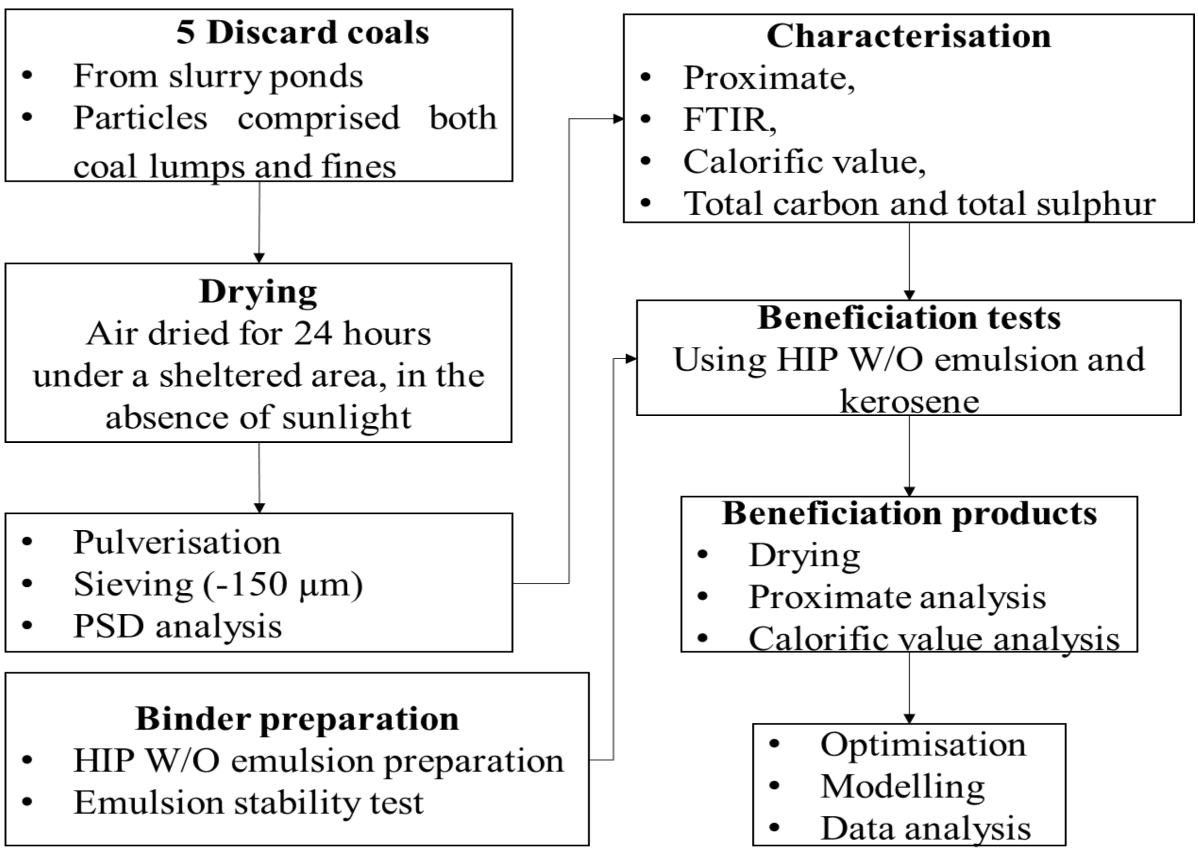

Figure 3-1: Experimental flowchart

3.2. The coal preparation and characterisation

Five discard coal feeds dumped for about 20 to 30 years were collected from different mines in Witbank and used in this study. The greyish discard coals 2 and 4, sampled from outside of the stockpile were exposed to severe atmospheric conditions. Meanwhile, discard coals 1, 3 and 5 were sampled from inside the stockpile (Figure 3-2). The as received coals were a bit moist, with the ultra-fines clogged to form coal lumps. The samples were air dried for 24 hours in a sheltered area, in the absence of sunlight.

After drying, the coal feeds were further crushed, pulverised sub-sampled using a riffle splitter. The pulverized samples were screened using 212 µm sieve for the following analyses including the particle size distribution, total sulphur and total carbon, proximate, calorific value and FTIR. For the beneficiation test, screened sample (-150 µm) was sub-sampled to 250 g coal stored in an airtight sample bag.

Figure 3-2: Different discard coal feeds

3.2.1. The coal characterisation procedures

3.2.1.1. Particle size distribution

Malvern Mastersizer 2000 with a Hydro 2000MU dispersion unit was utilized to determine the particle size distribution of the pulverised coal samples. The following steps were followed:

- Distilled water of about 800 ml was placed into the sample dispersion unit.
- The pump of the equipment was switched on and operated at the speed of 3000 rpm to ensure that the sample remain suspended inside the distilled water.
- A background measurement was evaluated to ensure that the equipment was ready for analysis. Any of the coal samples were then added to the distilled water in increments until the lazer obstruction range was between 10 – 20%.
- Once the analysis was complete, the equipment was cleaned by replacing the slurry water with clean distilled water.

3.2.1.2. Total sulphur and total carbon analysis

The total sulphur and total carbon analysis were performed according to ASTM D 4239-14:2015 using LECO CHN 628 integrated with 628 S module. About 1 g of the samples were measured and placed into a crucible. The crucibles were placed in a furnace for the determination of sulphur and total carbon.

3.2.1.3. Proximate analysis

Leco TGA 701 was used to determine the proximate analysis of the coal discards in accordance with ASTM - D5142 (ASTM, 2009). The following steps were followed to ensure effective analysis:

- Approximately 1 g of the coal samples was placed into a ceramic crucible.
- To determine the inherent moisture, the ceramic crucibles were left uncovered. Nitrogen gas was used and the coal samples were analysed at 25°C to 107°C using a ramp rate of 6°C/min.
- Once inherent moisture determination was complete, the TGA's cover opened and the crucibles were covered with ceramic lids. The same nitrogen gas was used to determine volatile matter and the temperature was raised from 107°C to 950°C at a ramp rate of 43°C/min.
- Subsequently, temperature was reduced below 600°C, and the crucible lids were removed. In oxygen atmosphere, the temperature was then raised to 750°C at a heating rate of 3°C/min to determine ash content of the coal discards.
- To determine a fixed carbon content, Equation 3-1 was used:

$$Fixed\ carbon\ = 100 - (Volatile\ matter\ + Ash) \qquad \text{Equation 3-1}$$

3.2.1.4. Calorific value

A Leco AC500 bomb calorimeter was used to measure the heat energy content in accordance with the ASTM D5865-04 standard (ASTM, 2019). For analysis, about 1 g of the coal discards was required and the test was repeated to confirm the results. The analysis were conducted in an oxygen environment at high pressure. The following steps were followed:

- Approximately 1 g of the coal particles was weighed and placed into a crucible.
- The crucible was then placed on a sample holder that is connected to the lid of the bomb (combustion vessel).

- A fuse wire (10 cm) was connected to the sample holder with the remaining fuse placed above the crucible without making contact.
- The combustion vessel was then closed with its lid. Subsequently, the bomb was charged with oxygen gas up to a pressure of 3000 kPa.
- The oxygen filled bomb was carried using tongs and placed at the centre of a 2 L bucket of distilled water, with the vessel fuse leads connected to the loading mechanism to start the analysis.
- The analysis was repeated twice for confirmation.

3.2.1.5. FTIR analysis

The FTIR measurements of the coal discards were performed using Perkin Elmer FTIR Spectrometer - Spectrum Two to determine the functional groups of the coal samples and the reagents used for beneficiation. The analysis was carried out within a transmittance mode, at the wavelength range of 4000 - 450 cm^{-1}. Approximately 0.2 g of the samples were used and placed on the instrument diamond attenuated total reflectance (ATR) accessory. A pressure was applied on the sample by knob and subsequently a spectrum was displayed on the computer screen.

3.2.2. Models of coal preparation and characterisation equipment

Table 3-1: Table of equipment

Pulveriser

A milling equipment with removable pot was enclosed inside a chamber to minimise the noise created during operation. The coal particles were placed between the ring bows and therefore impacted to generate fines.

Image: (FLSmith, n.d) and (Alibaba, n.d.)

Riffle splitter

Static sampling device was used to sample the as received coal to get a representative coal feed. The device comprised an inlet whereby the coal was fed on top and then flowed through the knife edges and alternate openings to the two collecting bins.

Malvern Mastersizer 2000

The analytical technique was used to determine the particle size distribution (PSD) of the coal particles. The equipment comprised a Hydro 2000MU dispersion unit.

Image: (MalvernMastersizer, n.d.)

Leco TGA 701

An analytical equipment which was used to conduct the proximate analysis to determine the ash content, inherent moisture, fixed carbon, total carbon content of the coal sample.

Image: (MARC, n.d.)

Leco AC 500 oxygen bomb calorimeter

Was used to determine the calorific value (heating value) of the coal discards.

Image: (LECO, n.d.)

Perkin Elmer FTIR Spectrometer - Spectrum Two

The degree of oxidation of the five coal samples and the reagents were determined using the equipment indicated. The results were displayed on a computer screen.

Image: (Abdulsam, 2019.)

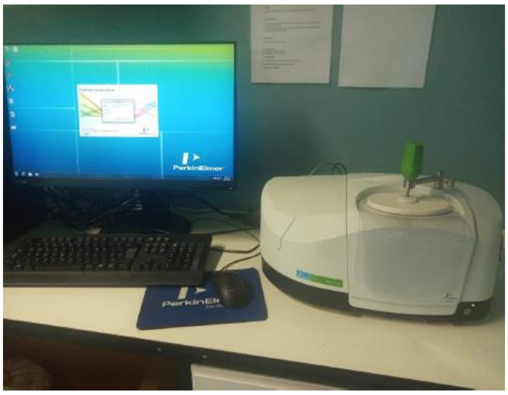

3.3. Emulsion preparation

The hydrophobic binders (W/O emulsion) were prepared in a 300 ml batch by using the following reagents (organic liquids) including kerosene and Span 80 also known as the Sorbitan monooleate (SMO), chemically represented as $C_{24}H_{44}O_6$ (Lu et al., 2019). NaCl was also used and therefore dissolved in tap water to produce dispersed aqueous NaCl solution phase (95% by volume) of different NaCl concentrations (3 and 5 wt%), as shown in Figure 3-3 (Mashaba and Bada, 2021). The remaining 5% by volume of the W/O emulsion binder denotes the continuous phase and comprised the organic liquids at different ratios (Figure 3-3).

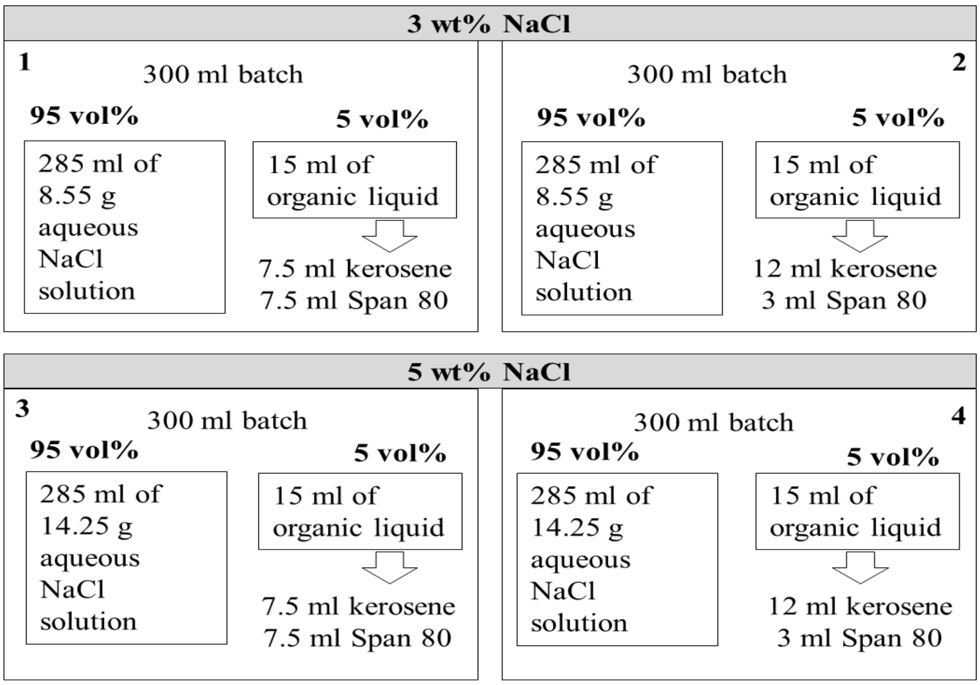

Figure 3-3: Outline for the HIP W/O emulsion preparation

The organic liquids; the SMO and kerosene were mixed in a Kenwood Chef stand mixer to produce a white, milky, and viscous emulsion binder (Figure 3-4). Phase inversion was not encountered because the prepared NaCl solution was added gradually (7.5 ml) every 15 seconds. In the study conducted by Netten and Galvin (2018), the increments approximating 15 ml were added to the mixture of organic liquids. This is because the 15 ml aqueous solution accounts half the total organic liquids (Span 80 and kerosene) used.

Figure 3-4: Preparation of the emulsion binder

3.3.1. Emulsion stability test

The degradation or stability of W/O emulsion during beneficiation is essential, therefore, was assessed with a conductivity meter (WTW LF 340) to verify their stability by evaluating a change in conductivity of the emulsion binders. For stability determination, 8 g of the W/O binders from each set was dispersed in tap water (500 ml). The test was performed in a mechanical floatation cell and operated at 1000 rpm with varying stirring speed between 0 and 25 minutes. Subsequently, the conductivity of the suspending liquid was measured after the set agitation time (Mashaba and Bada, 2021).

3.4. Beneficiation tests

The beneficiation tests on five discard coal feeds were conducted using a mechanical flotation cell which did not require external air flow rate. The rotating impeller that was positioned at the bottom of the vertical shaft (Figure 3-6A) created enough air flow to generate flotation air bubbles. A coal slurry was prepared using 25 wt% coal and therefore dispersed inside 1.5 L flotation cell at the speed of 1,000 rpm for two minutes. The scavenger, cleaner and re-cleaner stages, as indicated in Figure 3-5, were mixed for two minutes under the same speed. The process was batch whereby each stage was carried out after the completion of the initial stage. The emulsion binder and kerosene doses of 1.5 g, 2.0 g and 2.5 g were utilized and the conditioning time of 30 seconds was applied (Mashaba and Bada, 2021). These reagent masses were converted to 5 kg/ton, 7 kg/ton and 9 kg/ton, respectively, using Equation 3-2:

$$Reagents\ dosages\ (kg/ton) = \frac{mass\ of\ HIP\ emulsion\ or\ kerosene}{mass\ of\ dry\ coal} \quad \text{Equation 3-2}$$

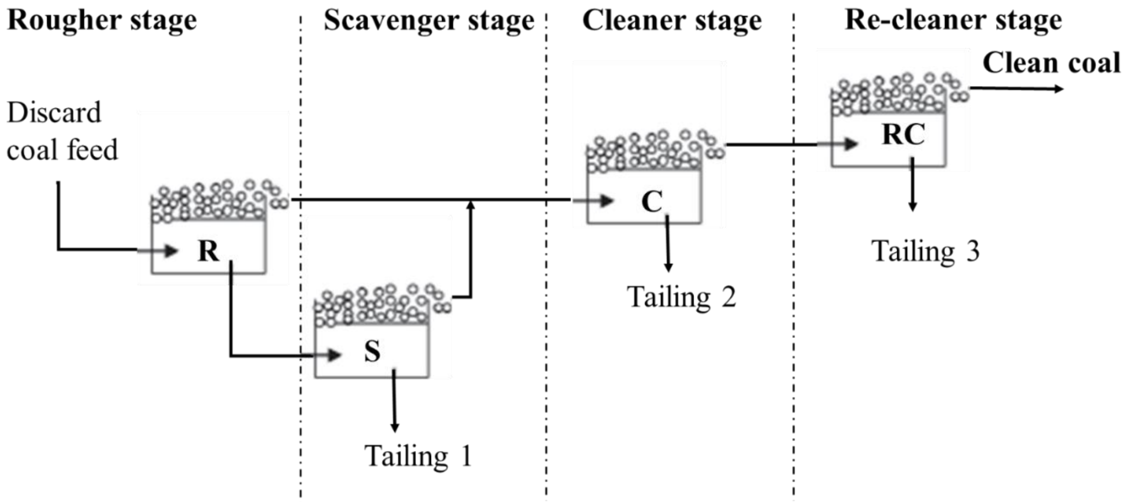

Figure 3-5: Representation of the stages for the froth flotation tests (Nicol et al., 1994)
R - rougher cell, S - scavenger cell, C – cleaner, RC - re-cleaner cell.

The Span 80 and kerosene in the emulsion binder accounted for 5 vol% of the reagent dosages (Equation 3-3), and the remaining 95 vol% was NaCl solution (Figure 3-3). The equivalent organic liquid dosages of Span 80 and kerosene were 0.25 kg/ton, 0.35 kg/ton and 0.45 kg/ton as derived from Equation 3-3. 100% kerosene was used, without the addition of tap water as indicated by Equation 3-4.

$$Organic\ liquids\ within\ the\ emulsion\ (kg/ton) = binder\ (kg/ton) \times (5\ vol\%)$$

Equation 3-3

$$Organic\ liquid\ within\ kerosene\ (kg/ton) = kerosene\ (kg/ton) \times (100\ vol\%)$$

Equation 3-4

After floating and scrapping, the floated carbonaceous ultra-fines were scrapped within 30 seconds to avoid the instability of the flotation froth. Subsequently, the floated clean coals and the rejected minerals (tailing product) as illustrated in Figure 3-6, were oven dried (50 °C) for 15 hours (Figure 3). The ash content of the dried products along with the combustible recovery, yield and ash rejection was determined using Equations 3-5, 3-6, 3-7 and 3-8.

$$Ash\ (\%) = \frac{Residue\ remaining\ after\ burning\ (g)}{Initial\ weight\ of\ carbonaceous\ ultra{-}fines\ (g)} \times 100$$

Equation 3-5

$$Yield\ (\%) = \frac{Weight\ of\ floated\ carbonaceous\ product}{Total\ feed\ weight} \times 100$$

Equation 3-6

$$Combustible\ recovery\ (\%) = \frac{M_C\,(100-A_C)}{M_F\,(100-A_F)} \times 100$$

Equation 3-7

$$Ash\ rejection\ (\%) = 100 - (Cumulative\ yield \times (\frac{Cumulative\ ash\ (\%)}{Feed\ ash\ (\%)}))$$

Equation 3-8

Where M_c is the mass of the floated clean coal (g), M_F is the mass of the feed discard coal (g), A_C is the ash content of the floats (%) and A_F is the ash content of the coal feed (%).

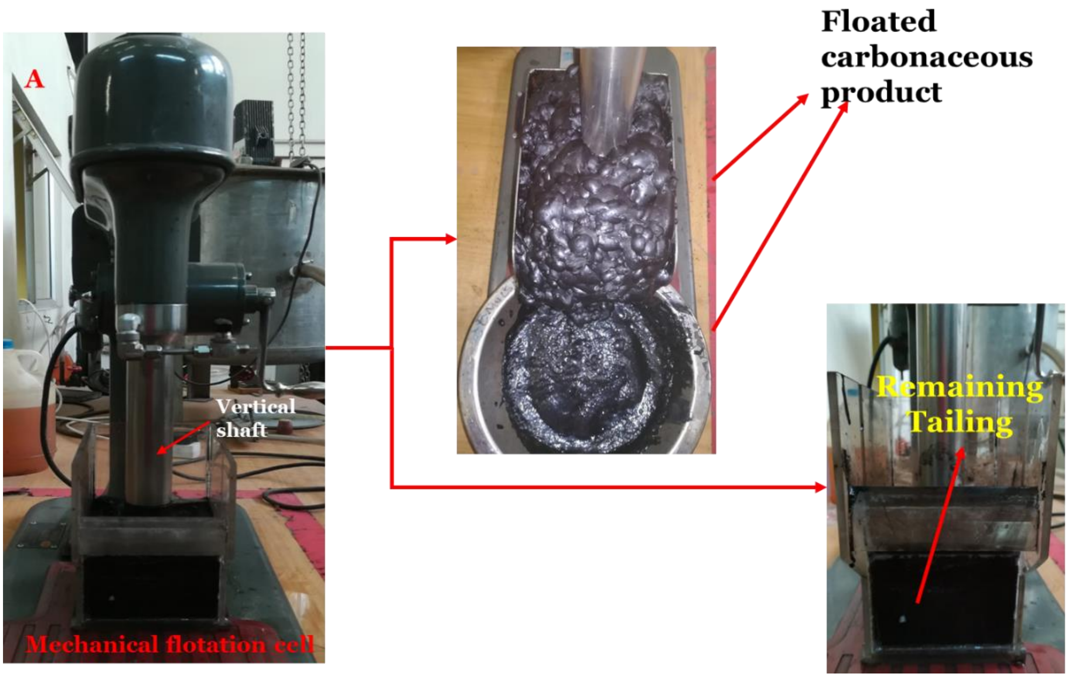

Figure 3-6: Representation for the froth flotation tests conducted (A – Mechanical flotation cell model)

3.5. Optimisation and modelling

The two highly weathered discard coals with ash contents of 48.71% and 41.71% were used to examine the influence of HIP W/O emulsion binder dosage (A) and agitation speed (B) on the attribute of the clean coal achieved. The experimental test runs were designed using Design-Expert software (version 11) through the RSM and central composite design. A design matrix of 13 experimental test runs was obtained under one-factorial points, one axial points and five central points, which were repeated five times to achieve an accurate estimate of experimental error (Zhao et al., 2011; Abdulsalam et al., 2019). The design matrix of the experiment on the influence of two numerical or input factors on the two highly weathered discard coals is indicated in Table 3.2. As indicated in Figure 3-7, the schematic representation differs from Figure 3-5. This is because a re-recleaner stage was applied to further enhance the quality of the clean coal product by further reducing its ash content (Figure 3-7).

The HP W/O emulsion binder doses of 5 kg/ton, 7 kg/ton and 9 kg/ton were used. This enabled the floating of the clean coal particles to the concentrate. From observation, HIP W/O emulsion dosages of less than 5 kg/ton produced minimum froth which restricted the scrapping of the clean product and therefore the produced concentrate was insufficient for analysis. In the study conducted by Zhang et al. (2020), microemulsion doses of 2 kg/ton, 4 kg/ton, 6 kg/ton and 8 kg/ton were used to beneficiate coal discards of less than 0.5 mm from Shendong Mining area in China. So it can be concluded that doses vary from each study due to the nature of the coal feeds.

Table 3-2: Experimental design matrix for the optimisation test

Run	Coded factors		Actual factors	
	A	B	A: Dosage (kg/ton)	B: Agitation speed (rpm)
1	0	0	5	1500
2	0	-1	7	1200
3	1	1	9	1800
4	1	-1	9	1200
5	0	1	7	1800
6	-1	1	5	1800
7	1	0	9	1500
8	0	0	7	1500
9	-1	0	5	1500
10	0	0	7	1500
11	-1	0	5	1200
12	0	0	7	1500
13	0	0	7	1500

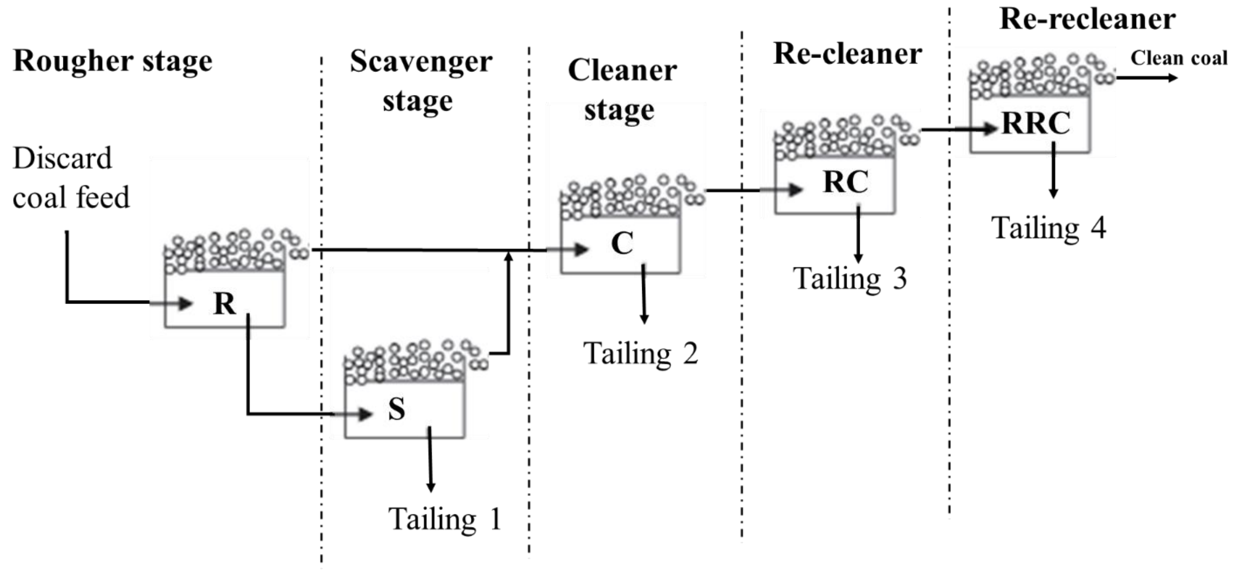

Figure 3-7: Representation of the stages for the froth flotation tests
R - rougher cell, S - scavenger cell, C - cleaner, RC - re-cleaner cell, RCC - re-re-cleaner.

3.6. Summary

This chapter presents the techniques used to characterise the discard coal feeds, the procedure followed in preparing the emulsion binder and the beneficiation technique used. The analytical methods, including the PSD, proximate, calorific value, total sulphur and total carbon, were used to determine the physico-chemical properties of the discard coals (− 150 µm). The extent of weathering of the coal discards was examined using FTIR. The experimental design of the optimisation study, using Design-Expert software for discard coal 2 and 3, was outlined. The results of the experiments and the discussion thereof are presented in Chapter 4.

CHAPTER 4: RESULTS AND DISCUSSION

4.1. Coal characteristic

4.1.1. Physico-chemical properties and extent of coal weathering

The PSD of the coal discards is presented in Figure 4-1 and the abundance of particle sizes within size fraction are represented by volume percentage. The percentage coal passing 150 µm was 96% for discard coal 1, and 84%, 93%, 78% and 92% for coal discards 2, 3, 4 and 5, respectively. Discard coal 1, followed by coal 3 and 5, was the softest coal, with 96% passing through the 150 µm screen (Figure 4-1). The difference in the PSD curves for these coal samples may be attributable to the difference in hardness and friability (Isaac, 2019).

From the proximate analysis test, the ash content, inherent moisture, volatile matter and fixed carbon of coal discards were determined. The ash content of discard coal 1 was found to be 29.34%, with discard coal 2, 3, 4, and 5 consisting of 48.71%, 41.71%, 28.63% and 33.32% ash, respectively. The calorific value from the five coal sample ranged between 8 and 21 MJ/kg with discard coal 2 having the lowest calorific value classified as Grade D III according to the South African Coal Standard Classification. The total carbon results indicate that discard coals 1, 4 and 5 have a total carbon content of more than 50% (Table 4-1). On the other hand, discard coal 2 comprised the lowest total carbon content of 24.9% followed by discard coal 3 with the total carbon content of 43.7%. As indicated in the study conducted by Maledi (2017), coal with high ash contents is known to have low volatile matter contents. The author used four coals with coal C comprising high ash content of 68.3% and lowest volatile matter and inherent moisture of 13.9% and 2.0%, respectively. The results achieved by Maledi (2017) are not in agreement with the results achieved for discard coal 2 in this study. Discard coal 2 was found to have a high volatile content of 26.79%, which could be caused by the presence of highly volatile inorganic minerals associated with this discard. Further study is required to ascertain the reason behind this anomality.

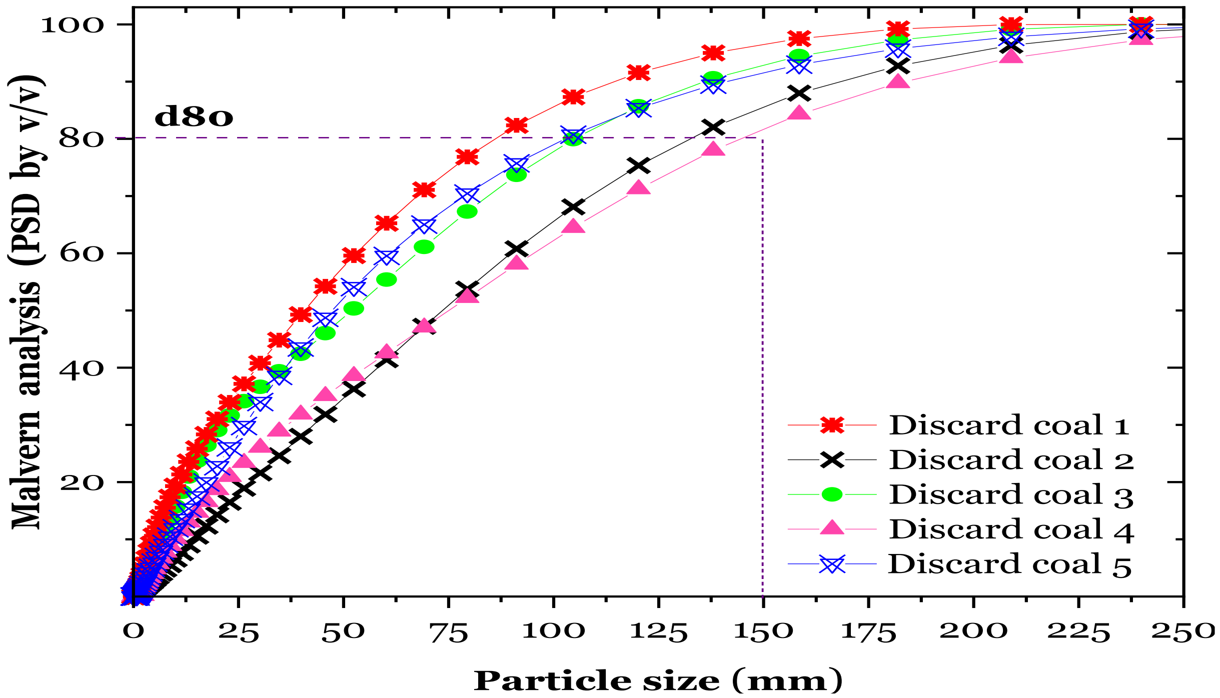

Figure 4-1: The particle size distribution of the coal discards determined with Malvern analyzer

Table 4-1: The physico-chemical properties of the discard coal feeds

Coal sample	Proximate analysis (air dry basis)				Total sulphur and carbon analysis (dry basis)		Calorific value (MJ/kg)
	Ash content %	Fixed carbon %	Volatile matter %	Inherent moisture %	Total carbon %	Total sulphur%	
Discard coal 1	29.34	43.29	23.40	3.02	54.50	0.87	20.94
Discard coal 2	48.71	17.79	26.79	5.80	24.9	3.04	8.48
Discard coal 3	41.71	35.58	20.79	7.36	43.7	1.29	16.29
Discard coal 4	28.63	43.83	22.88	5.71	55.95	1.00	20.61
Discard coal 5	33.32	40.68	22.63	5.51	51.45	0.43	18.55

4.1.2. Fourier transformation infrared spectra for the raw coal and the reagents (emulsion binder and kerosene)

The extent of weathering of the five coal samples was determined using FTIR. The FTIR spectra for the samples were interpreted based on the previous investigation conducted by Wang et al. (2012) and Jing et al. (2019). As indicated in Figure 4-2, the important regions of the spectra are the functional region (4000 - 1500 cm^{-1}) and the fingerprint region (1500 - 500 cm^{-1}). Discard coal 2 has the most pronounced peak intensity at 4000 - 4500 cm^{-1}, which demonstrates the significant amount of OH groups at the surface of the coal. This also indicates that discard coal 2 is highly oxidised relative to discard coal 3, 4, 5 and 1 (Figure 4-2). The colour of discard coal 2 (Figure 3-2) concurs that this discard was more exposed to weather elements, suggesting that this coal has been dumped for longer than the other coals.

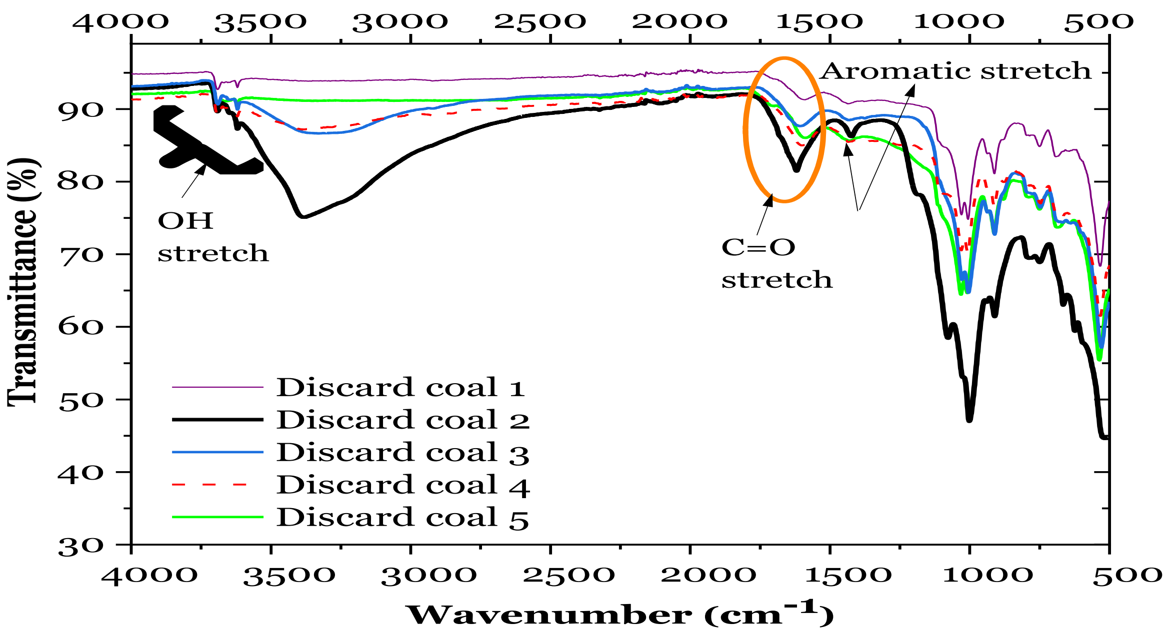

Figure 4-2: Fourier transformation infrared spectra of the discard coal feeds

Figure 4-3 presents the infrared spectra for reagents (collectors): the HIP W/O emulsion binder and kerosene used to beneficiate the as-received discard coals. This was to examine the presence of the C-H aliphatic, O-H and C=O groups on the surface of the collectors. At the surface of the HIP W/O emulsion binder, there are C-H aliphatic, O-H stretch and C=O groups demonstrating that W/O emulsion is an emulsifier comprising both hydrophilic and hydrophobic groups and thus binds with weathered coal. Kerosene was found to be a hydrophobic hydrocarbon, as evidenced by the presence of the only aliphatic stretched C-H at 2837-2967 cm^{-1} (Figure 4-3).

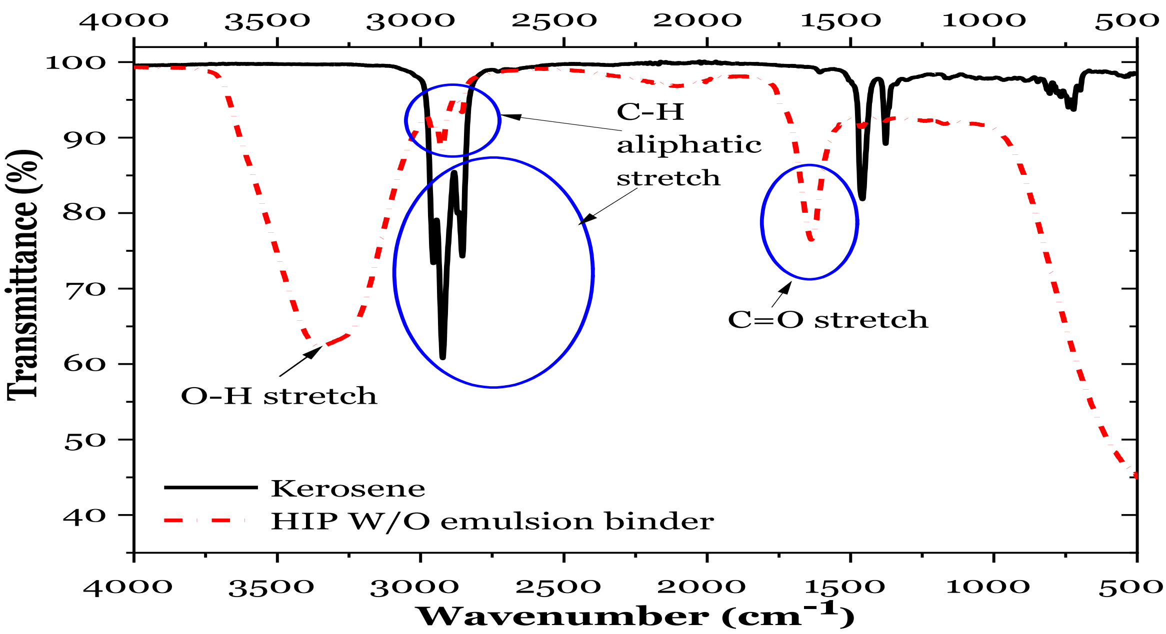

Figure 4-3: The FTIR spectra for the collectors used for beneficiation

4.2. Stability of the HIP W/O emulsion binder

The results of the conductivity test of the four emulsion binders prepared at different volume ratios of organic liquids and NaCl concentrations are presented in Figure 4-4. The conductivities increased with an increasing agitation time, and this is due to the stress created by the applied force (mechanical agitation) on the emulsion binders. As a result, phase inversion occurred due to the breakdown of the kerosene and the Span 80's oil films, resulting in the release of NaCl to the suspending liquid phase (Borrow et al., 2018; Netten and Galvin, 2018). The conductivity of emulsion binder 4 continues to increase until 20 to 25 minutes, with conductivity remaining almost constant. This increase is due to the large quantity of NaCl released into the tap water suspension liquid phase. This finding is similar to that of Borrow et al. (2018) on the stability of different dosages of emulsion binder.

According to Table 4-2, the HIP W/O binder 1 produced the cleanest coal product based on the initial beneficiation test conducted using different binder ratios. A clean coal product with an ash content of 11.76% and highest heat value of 28.61 MJ/kg was obtained for binder 1. The degradation achieved by this binder at the lowest conductivity might be responsible for its stability. Likewise, mixing the Span 80 and kerosene in equal proportion (binder 1) is also expected to enhance the bonding and consequently the binder's viscosity and stability (Netten et al., 2016; Borrow et al., 2018). Emulsion binders (Binder type 4, 3 and 2), which degraded faster, with higher conductivities, produced clean coal with high ash content (Figure 4.4 and Table 4.2) due to deterioration or phase inversion (Netten et al., 2016).

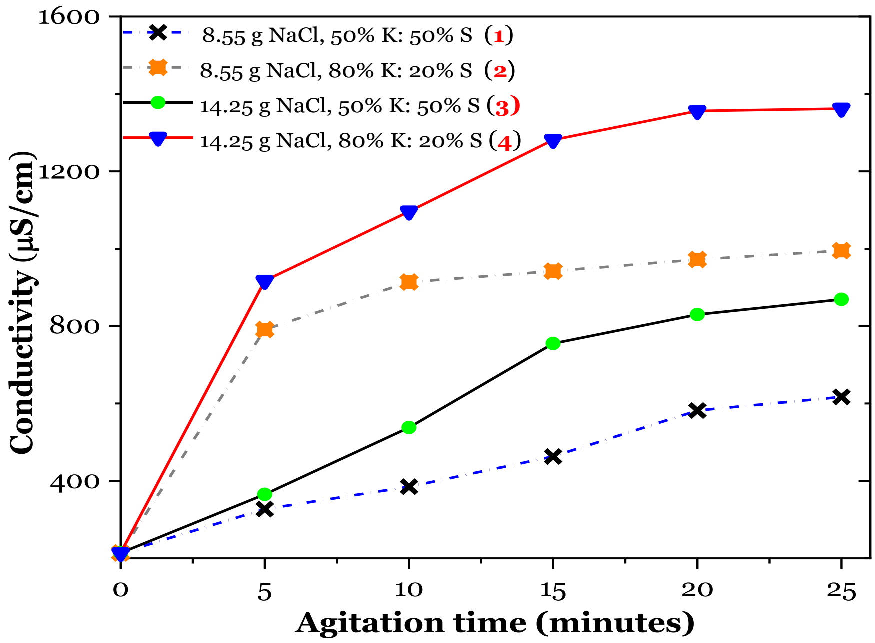

Figure 4-4: The conductivities of the HIP W/O emulsion binders
(S: Span 80; K: kerosene).

Table 4-2: The physico-chemical properties of the floated clean coal produced from all binders

Binder type	**5 kg/ton**		**7 kg/ton**		**9 kg/ton**	
	Ash (%)	CV (MJ/kg)	Ash (%)	CV (MJ/kg)	Ash (%)	CV (MJ/kg)
1	**11.76**	**28.61**	13.71	26.85	18.46	26.26
2	18.88	25.94	19.55	25.68	20.00	25.58
3	17.87	26.03	19.18	25.98	20.83	25.37
4	19.10	25.55	21.01	25.41	21.57	25.18

CV: calorific value

The degradation and non-stability of the emulsion binder at higher dosages led to an increase in the coal yield (Figure 4-5) and a reduced coal calorific value (Table 4-2). According to Netten et al. (2014) and Netten and Galvin (2018), this is due to the phase inversion that separates the Span 80 and kerosene. Consequently, the hydrophilic inorganic minerals absorb kerosene and, therefore, become hydrophobic and report to the floated clean coal product (Peng et al., 2015). A clean coal product of low yield and high calorific value of 28.61 MJ/kg and 26.03 MJ/kg was achieved using 5 kg/ton of the emulsion binder 1 and 3, respectively. This suggests that a low rate of emulsion degradation hinders the attachment of inorganic minerals to the clean coal and the detachment of carbonaceous ultra-fines from the froth. According to Netten et al. (2015), this is because the binder is sufficient to sustain its structure. On the basis of the results of the preliminary test, binder 1 was selected for the beneficiation of the entire coal tested.

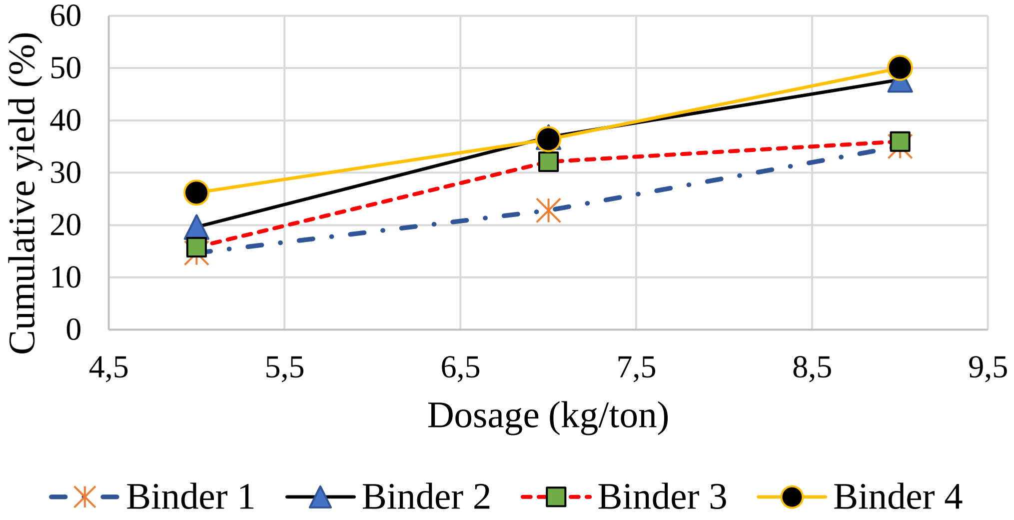

Figure 4-5: The carbonaceous ultra-fines yield achieved under different dosages of different emulsion binders

4.3. Influence of collector dosages on the washability (flotability) and ash rejection of discard coal 1

Figure 4-6 presents the cumulative yield and ash content of the clean coal concentrate achieved by beneficiating the as received coal 1 under various concentrations (5 kg/ton, 7 kg/ton and 9 kg/ton) of kerosene and the emulsion binder 1. A feed coal of 29.34% ash was upgraded with emulsion binder 1 at 5 kg/ton, 7 kg/ton and 9 kg/ton to 20.68%, 21.06% and 23.65%, respectively. The corresponding cumulative yields of 40%, 64.81% and 87.23% were produced from the same sample. With kerosene at similar doses (5 kg/tonne, 7 kg/tonne and 9 kg/tonne), a clean coal concentrate with an ash content of 21.14%, 22.38% and 28.09% and cumulative yield of 55.42%, 78.79% and 94.21% were recovered, respectively.

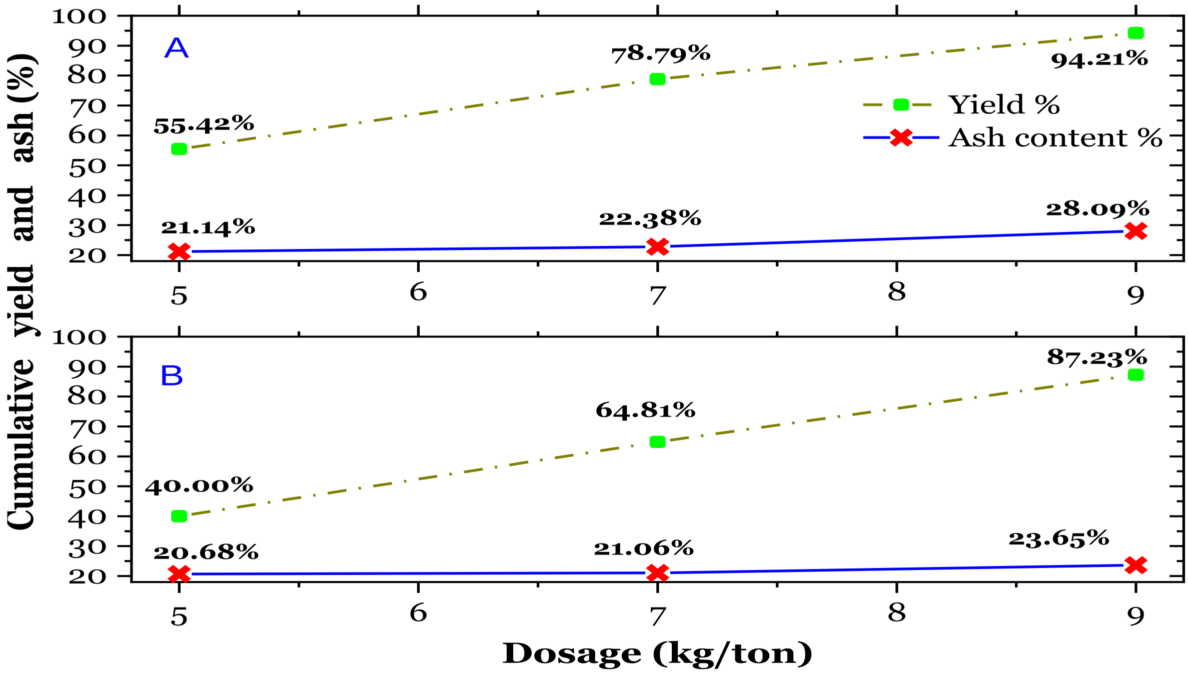

Figure 4-6: Influence of kerosene (A) and HIP W/O emulsion (B) on a clean coal product yield and ash content

The floated clean products produced from the rougher stage were further upgraded using 5 kg/ton, 7 kg/ton and 9 kg/ton emulsion and kerosene. As seen in Figure 4-7, the cleanest floated concentrate with 11.76% ash was produced using 5 kg/ton of emulsion. The lowest ash content of 17.47% was achieved from 5 kg/ton kerosene (Figure 4-8). Similar to the product yield, the combustible recovery of the particles, along with their ash content, increased as the HIP W/O emulsion binder and kerosene concentration increased. According to Netten and Galvin (2018), the increase noted might be due to the binder sufficiency, which enhanced the floatability and pulled the semi-hydrophobic carbonaceous particles to the concentrate, thereby lowering the grade of the carbonaceous particles. The HIP W/O emulsion binder produced coal with higher quality than that from kerosene (Figures 4-7 and 4-8) due to its ability to float coal particles rendered hydrophilic due to weathering.

Figure 4-8 presents the washability curve achieved by using kerosene. As indicated, similar trend to the HIP W/O emulsion binder was experienced and the combustible recovery of the clean coal product increased with an increase in kerosene dosages. Additionally, the clean coal yield was found to be proportional to kerosene dosages. The results agree with the results achieved by Lu et al., 2019 up to a certain dosage. This might be due to the laboratory oxidised coal used by the author.

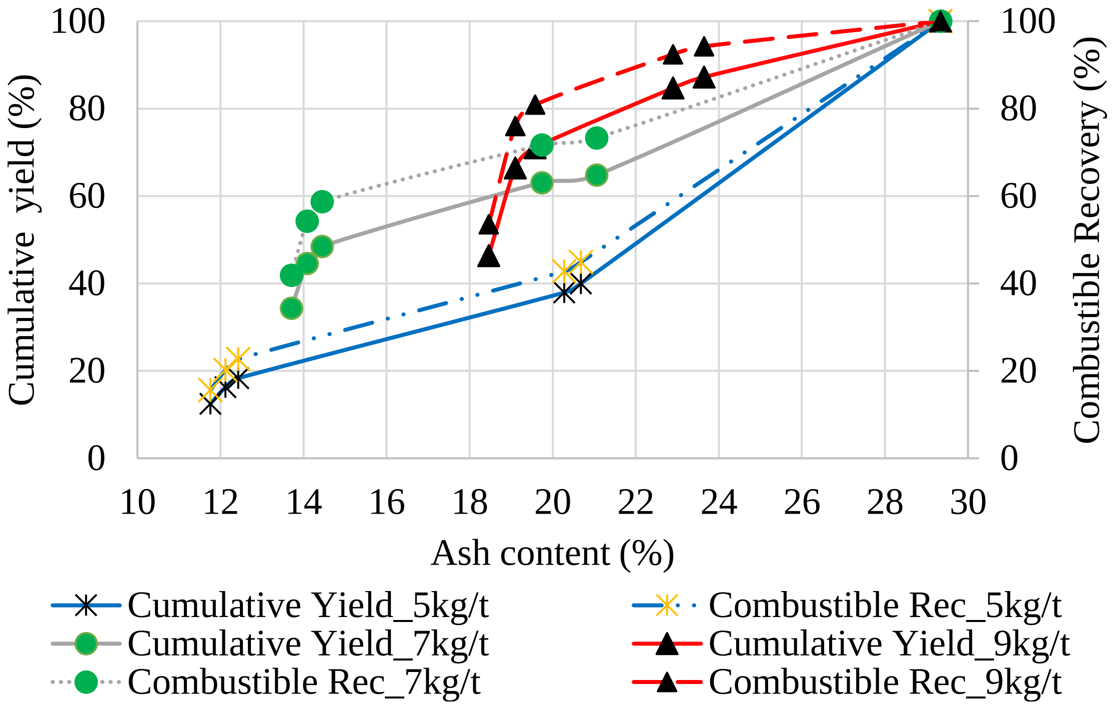

Figure 4-7: Impact of HIP W/O emulsion dosages on the cumulative yield and ash content of the feed coal 1

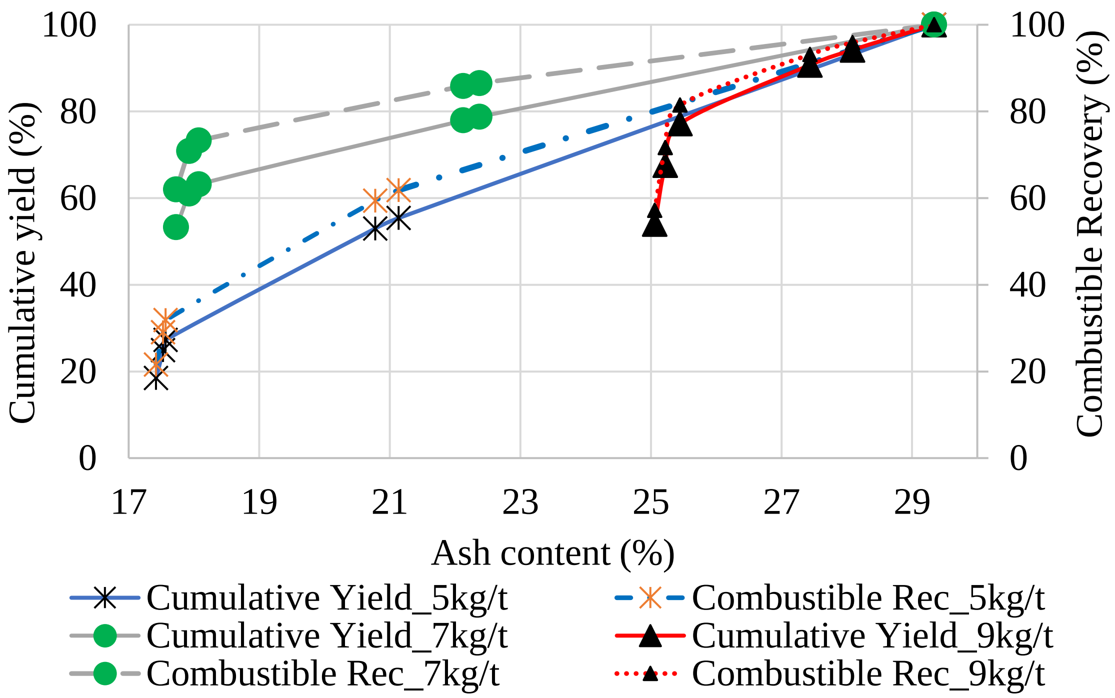

Figure 4-8: Impact of kerosene concentrations on the cumulative yield and ash content of the feed coal 1

The extent to which the HIP W/O emulsion binder and kerosene were able to select the carbonaceous particles from the inorganic minerals within the discard coal was evaluated using ash rejection percentage (Equation 3-7). Figure 4-9 represents the ash percentages rejected from reporting to the floated concentrate under second cleaning stage of froth flotation. The highest ash rejection of 94.99% was achieved for the discard coal under 5 kg/ton of emulsion. At 5 kg/ton of kerosene, 89.03% of ash was rejected from reporting to the clean coal product. As a result of low inorganic mineral content within the clean coal produced under 5 kg/ton of HIP W/O emulsion binder, the discard coal feed calorific value was upgraded from 20.94 MJ/kg to 28.61 MJ/kg.

On the other hand, a clean coal product with a heating value of 26.42 MJ/kg was achieved with kerosene under the same concentration (Figure 4-10). With the outcome of the washability and ash rejection results from discard coal 1, the other discard coals (2, 3, 4 and 5) were only subjected to HIP W/O emulsion at 5 kg/ton. The data used to plot the washability curves is presented in Appendix A.

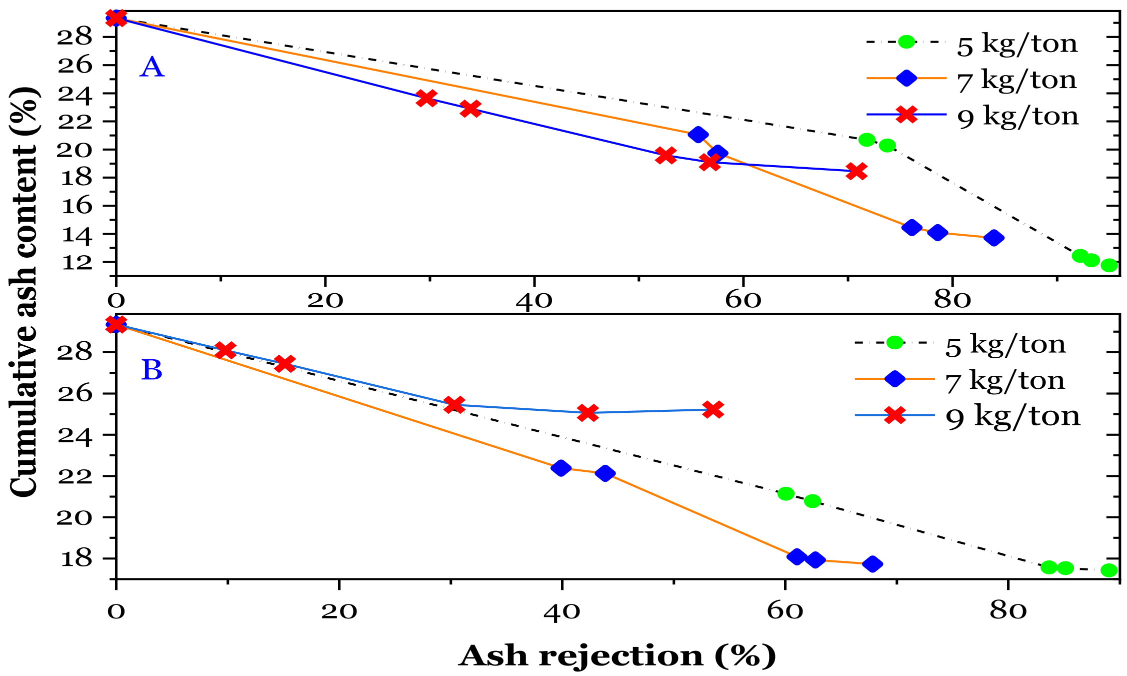

Figure 4-9: The rejection of inorganic minerals from reporting to the floated carbonaceous product at different HIP W/O (A) and kerosene (B) dosages

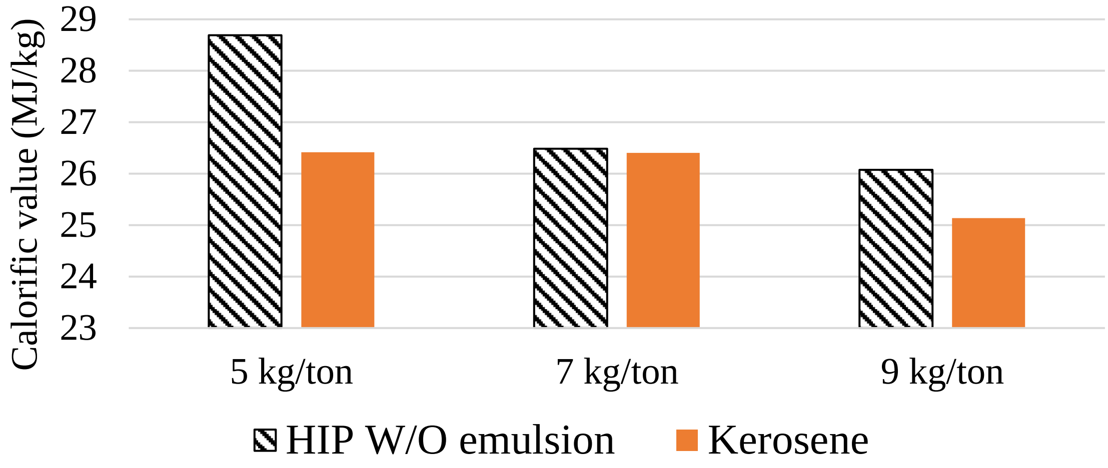

Figure 4-10: The calorific values of the clean coal products

4.4. Impact of 5 kg/ton of the emulsion binder on the washability of discard coal 2, 3, 4 and 5

The washability curves for the beneficiation of coal 2, 3, 4 and 5 at the same emulsion concentration (5 kg/ton) that coal 1 was subjected to is depicted in Figure 4-11. A clean coal with a combustible recovery of 2.5% and 6.14% and ash content of 31.16% and 17.23% were obtained for coal 2 and 3, respectively. On the other hand, a combustible recovery of 3.08% and 4.02% with an ash content of 12.12% and 12.70% was achieved for discard coal 4 and 5, respectively. A clean coal product with a combustible recovery of 15.61% and 11.76% ash was achieved for discard coal 1. The nature and degree of weathering of the coal could be responsible for the difference in ash content and yield of the clean coal products achieved.

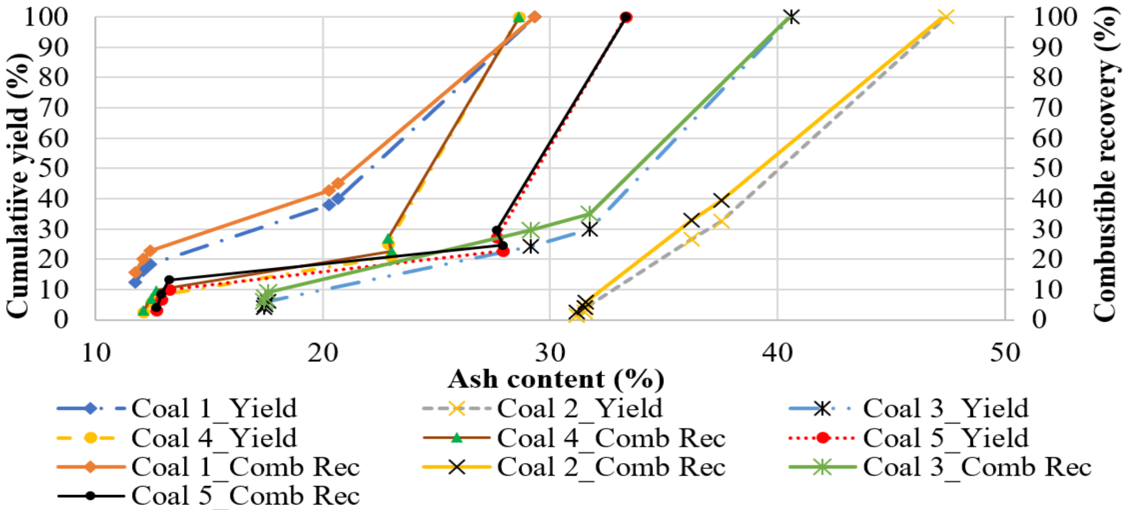

Figure 4-11: Effect of HIP W/O emulsion concentration (5 kg/ton) on the cumulative yield, combustible recovery (Comb Rec) and ash content of the clean coal products

Table 4-3 presents the calorific value of the floated clean coal product under the emulsion concentration of 5 kg/ton. A higher calorific value increment was achieved for discard coal 2 and 3. The increase in the grade of both coals might be due to the high abundance of the OH groups found on their surfaces. According to Lu et al. (2019), HIP W/O emulsion is noted to prevent the entrainment of inorganic minerals in the floated clean coal product. In addition, it can lead to the formation of strong bonds with the oxygenated functional groups in the weathered coal.

As a result of the efficiency of the emulsion, the highest calorific value increase of 9.68 MJ/kg was achieved from the beneficiation of discard coal 2 which was improved from the feed calorific value of 8.48 MJ/kg to 18.16 MJ/kg. According to the South African Standard Classification of Coals, this floated clean coal falls within D III grade coal. This product meets the specifications of some of the Eskom power plants, such as the Lethabo power plant. On the other hand, the clean coal obtained from discard coal 1 and coal 4 has a calorific value of 28.61 MJ/kg and 27.62 MJ/kg. They can be classified as Grade A and Grade B, respectively. The products obtained for discarded coal 3 and 5 have heating values of 25.77 MJ/kg and 26.28 MJ/kg, respectively (Table 4-3).

Table 4-3: The calorific value of the clean coal products of discard coal feeds

	Coal discards				
Calorific value (MJ/kg)	**1**	**2**	**3**	**4**	**5**
Discard coal	20.94	8.48	16.29	20.61	18.55
Clean coal	28.61	18.16	25.77	27.62	26.28
CV increment	7.67	9.68	9.48	7.01	7.73

CV= calorific value

4.5. Experimental design and statistical analysis

This section presents the regression models of discard coal 2 and 3 developed using RSM to evaluate the influence of input variables: HIP W/O emulsion binder dosage (A) and agitation speed (B) on the attribute of the clean coal achieved. The relevance of the study was to use the laboratory flotation test results to generate mathematical regression equations for future analysis. These equations can be used to predict the responses of ash content and calorific value with respect to the yield of clean coal products as applied to discard coal 2 and 3. Additionally, the influence of the input variables is represented graphically by 3D responses and contour plots obtained from the Design expert software.

4.5.1. Regression model development for discard coal 2 using the HIP W/O emulsion

The calorific value of the clean coal product decreases with the increase in HIP W/O emulsion binder dosage (Table 4-4). However, the calorific value (grade) increased as the flotation speed increased at constant emulsion concentration. According to Netten et al. (2014), this is because vigorous agitation enhances the fragmentation of the emulsion binder. The abundance of the small gel-like pieces of emulsion binder created by fragmentation is essential because the emulsion pieces act as a "scaffolding onto which carbonaceous particles can deposit" (Netten et al., 2014). As previously stated, an increase in the emulsion binder concentration enhances the floatability of semi-hydrophobic carbonaceous particles to the concentrate, thereby leading to low-grade coal products (Netten and Galvin., 2018).

The emulsion binder at 5 kg/ton did not experience degradation (Table 4-4). The calorific value of the clean coal product continues to increase (18.76 to 19.45 MJ/kg) with increasing agitation speed. This demonstrates that the structural integrity of the emulsion binder was still strong during beneficiation binding the carbonaceous ultra-fines to the concentrate. Netten et al. (2014) demonstrated the emulsion breakdown by a reduction in clean coal agglomerate diameter. This was due to the weakened structure of the binder under the agitation speed of 22,000 rpm.

Table 4-4: Experimental results achieved for discard coal 2

Run	**Factor 1** Dosage (kg/ton)	**Factor 2** Agitation speed (rpm)	**Response 1** Ash content (%)	**Response 2** Calorific value (MJ/kg)
1	7	1500	34.22	18.54
2	7	1200	34.40	18.33
3	9	1800	33.17	18.50
4	9	1200	34.74	18.05
5	7	1800	32.30	18.97
6	**5**	**1800**	**31.51**	**19.45**
7	9	1500	34.88	18.11
8	7	1500	34.36	18.55
9	5	1500	33.51	18.90
10	7	1500	34.20	18.45
11	5	1200	33.56	18.76
12	7	1500	34.25	18.54
13	7	1500	34.33	18.56

The F-values and p-values obtained from the Analysis of Variance (ANOVA) were evaluated for the significance of the models (Table 4-5 & 4-6). The F-value measures how much of the difference between the data points and sample mean are within the residual mean square. This led to the determination of the p-value. This p-value regulates whether the alternative or null hypothesis is true (Hou et al., 2013). For this study, the alternative hypothesis was confirmed to be true. Agitation speed and emulsion dosage significantly impacted the ash content and the heating value of the clean coal product achieved, whereas the null hypothesis stated otherwise. For the alternative hypothesis to be true, the p-value of the model and the input factors must be less than 0.05 (Chattopadhyay et al., 2015; Hembrom and Suresh, 2018).

The F-value of 243.10 for calorific value (Table 4-6) was less than 330.11 achieved for the ash content (Table 4-5). However, the p-values for both model responses were found to be less than 0.05. This confirms that the emulsion dosage and agitation speed significantly influenced the heating value and ash content of the clean product. As per Equations 4.1 to 4.4 and Tables 4-5 and 4-6, the quadratic model was achieved for both ash content and the calorific value. This was due to the significance of the model terms A, B, AB, and B^2. Whereas, A^2 was found insignificant for both ash content and calorific value due to the p-values greater than 0.05. The A^2 term was not eliminated from the model equation (Equation 4.1) for ash content since it has minimal impact on the relationship between the adjusted correlation (Adj. R^2) of 0.9928 and predicted correlation (Pred. R^2) of 0.9718 (Table 4-5). This was proven by the achieved Adj. R^2 and Pred. R^2 difference of 0.021, which is less than 0.2 (Sharma et al., 2012). Likewise, the exclusion of A^2 was found to increase the p-value of the AB term from 0.0239 to 0.0348, which makes it closer to the p-value's threshold limit of 0.05. Therefore, A^2 was included in the regression model equation for the ash content (Equation 4.1).

For the calorific value model (Table 4-6), removing the insignificance A^2 term increased the Adj. R^2 and Pred. R^2 from 0.9861 to 0.9878 and 0.9671 to 0.9742, respectively. However, R^2 decreased from 0.9919 to 0.9918, and both experimental and actual values are shown to fit according to the lack of fit p-value of 0.6647, which is greater than 0.05. The adequate precision, which measures the model's accuracy by evaluating if the sample data is distributed around the sample mean, also increased from 47.7826 to 55.7106. Based on this value, it can be concluded that the models for calorific value and ash content are accurate given their adequate precision of 55.7106 and 60.1007, respectively. These ratios are greater than 4, therefore desirable, and demonstrates the accuracy and precision of sample data for the response surface models (Behera et al., 2018; Abdulsalam et al., 2019).

Table 4-5: ANOVA results for the surface model of ash content for discard coal 2

Source	Sum of Squares	df	Mean Square	F-value	p-value	Remark
Model	11.53	5	2.31	330.11	<0.0001	Sig.
A	2.95	1	2.95	422.97	<0.0001	
B	5.45	1	5.45	780.80	<0.0001	
AB	0.0576	1	0.0576	8.25	0.0239	
A^2	0.0226	1	0.0226	3.24	0.1149	
B^2	2.42	1	2.42	346.11	<0.0001	
Residual	0.0489	7	0.0070			
Lack of Fit	0.0294	3	0.0098	2.01	0.2546	Not sig.
Pure Error	0.0195	4	0.0049			
Cor Total	11.58	12				
R^2	0.9958					
Adj. R^2	0.9928					
Pred. R^2	0.9718					
Adeq. Precision	60.1007					

Df - degree of freedom; A: HIP W/O emulsion dosage; B: Agitation speed; Cor. Total – the total Sum of Squares corrected for the mean; Adeq. Precision – Adequate Precision; Sig. – Significant

Table 4-6: ANOVA results for the surface model of calorific value for discard coal 2

Source	Sum of Squares	df	Mean Square	F-value	p-value	Remark
Model	1.62	4	0.4049	243.10	<0.0001	Sig.
A	1.00	1	1.00	600.68	<0.0001	
B	0.5281	1	0.5281	317.07	<0.0001	
AB	0.0144	1	0.0144	8.65	0.0187	
B^2	0.0766	1	0.0766	46.00	0.0001	
Residual	0.0133	8	0.0017			
Lack of Fit	0.0052	4	0.0013	0.6349	0.6647	Not sig.
Pure Error	0.0081	4	0.0020			
Cor. Total	1.63	12				
R^2	0.9918					
Adj. R^2	0.9878					
Pred. R^2	0.9742					
Adeq. Precision	55.7106					

Df - degree of freedom; A: HIP W/O emulsion dosage; B: Agitation speed; Cor. Total – the total Sum of Squares corrected for the mean; Adeq. Precision – Adequate Precision; Sig. – Significant

The quadratic regression model equations for both coded and actual equations for future analysis of the input factors and output responses are presented as Equations 4.1 to 4.4. However, it should be noted that the input factors show a different effect on the response equations as demonstrated by the coefficients of coded and actual equation terms. This is because the intercept of input factors is not considered the centre of the design space for the actual equation. Therefore, the coefficients within the actual equations cannot be used to study the impact of emulsion dosage and the agitation speed on ash content and calorific value (Stat-Ease, n.d). As indicated in coded equations (Equations 4.1 and 4.2), emulsion binder dosage has positive and negative coefficients for ash content and calorific value, respectively.

According to Behera et al. (2018) and Yadav et al. (2018), the negative coefficients indicate the antagonist effect. Whereas the positive coefficients demonstrate a synergistic effect on the output responses. In this study, the minus sign of B demonstrates that an increase in agitation speed decreases the ash content. While the positive sign on the calorific value equation illustrates an increase in calorific value due to increased agitation speed.

Coded equations

$$Ash\ (\%) = 34.28 + 7.02 \times 10^{-1}A - 9.53 \times 10^{-1}B + 1.20 \times 10^{-1}AB - 9.05 \times 10^{-2}A^2 - 9.36 \times 10^{-1}B^2 \qquad \text{Equation 4.1}$$

$$Calorific\ value\left(\frac{MJ}{kg}\right) = 18.52 - 4.08 \times 10^{-1}A + 2.97 \times 10^{-1}B - 6.0 \times 10^{-2}AB + 1.54 \times 10^{-1}B^2 \quad \text{Equation 4.2}$$

Actual equations

$$Ash\ (\%) = 14.19 + 3.68 \times 10^{-1}A + 2.66 \times 10^{-2}B + 2.0 \times 10^{-4}AB - 2.26 \times 10^{-2}\ B^2 - 1.0 \times 10^{-5}\ B^2 \quad \text{Equation 4.3}$$

$$Calorific\ value\left(\frac{MJ}{kg}\right) = 21.27 - 5.42 \times 10^{-2}A - 3.44 \times 10^{-3}B - 1.0 \times 10^{-4}AB + +1.71 \times 10^{-6}B^2 \quad \text{Equation 4.4}$$

Table 4-7 presents the experimental (actual) and the predicted values obtained using the regression modelling equations. There is a strong correlation between the experimental and predicted values, as indicated by the Adj. R^2 of 0.9928 and 0.9878 for ash content and calorific value.

Table 4-7: Experimental and predicted values of the experimental design responses for coal 2

Run	**Dosage (kg/ton)**	**Agitation speed (rpm)**	**Ash content (%)**		**Calorific value (MJ/kg)**	
			EV	PV	EV	PV
1	7	1500	34.22	34.28	18.54	18.52
2	7	1200	34.40	34.29	18.33	18.38
3	9	1800	33.17	33.12	18.50	18.51
4	9	1200	34.74	34.78	18.05	18.03
5	7	1800	32.30	32.39	18.97	18.97
6	**5**	**1800**	**31.51**	**31.48**	**19.45**	**19.43**
7	9	1500	34.88	34.89	18.11	18.12
8	7	1500	34.36	34.28	18.55	18.52
9	5	1500	33.51	33.48	18.90	18.94
10	7	1500	34.20	34.28	18.45	18.52
11	5	1200	33.56	33.62	18.76	18.73
12	7	1500	34.25	34.28	18.55	18.52
13	7	1500	34.33	34.28	18.56	18.52

EV = experimental value; PV = predicted value

In Figure 4-12, the straight line demonstrates the predicted values, whereas the data points illustrate the experimental values. There is a good fit between the values, as indicated by the closeness of the data points and the straight line. The clustered data points observed on the regression lines for both figures present the actual and predicted values for the centre points of the design matrix.

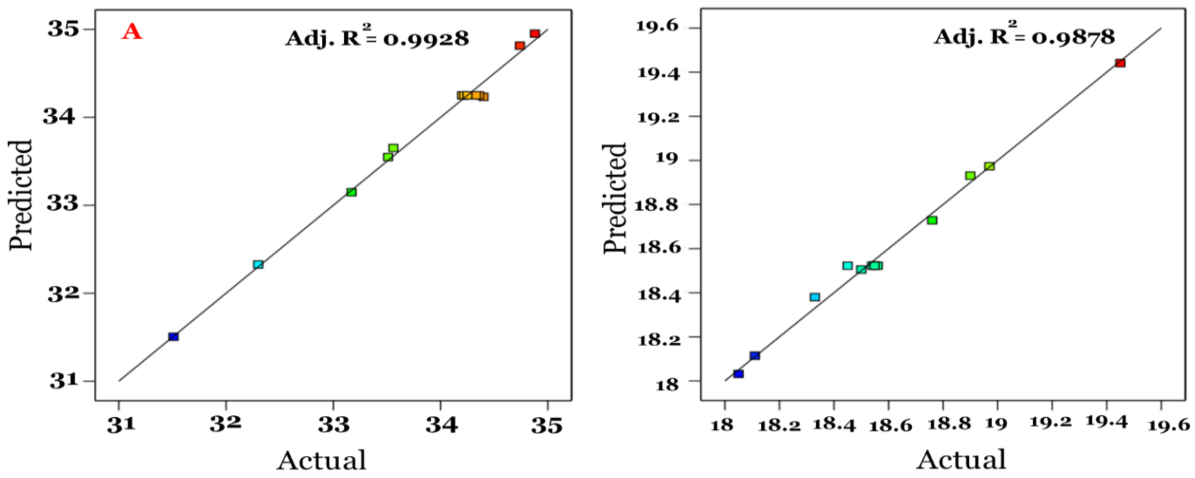

Figure 4-12: A linear regression plots for ash content (A) and calorific value (B) of discard coal 2

Figure 4-13 presents an internally studentized residuals plot, which studies the connection between the experimental and actual values by measuring their residuals (difference). It is referred to as internal because all the data points within the analysed sample are evaluated. According to the literature, it is difficult to compare data points with different residuals, especially with a threshold limit (Sharma et al., 2012; Behera et al., 2018). Therefore, the studentized model was introduced whereby the residuals are divided by the standard deviation of the sample data. The studentized residuals plots were used to evaluate the presence of outliers, defined as the data points that exceed the constant line of +3 and -3 (Figure 4-13). There were no outliers within the sample data for both ash content and calorific value, and there is only one data point with zero residual. This indicates a zero variance, which means that the experimental and predicted values are equal. Negative residuals demonstrate that the predicted values are greater than the actual values, whereby positive residual states the opposite (Sen and Swaminathan, 2004; Zhao et al., 2011; Abdulsalam et al., 2019).

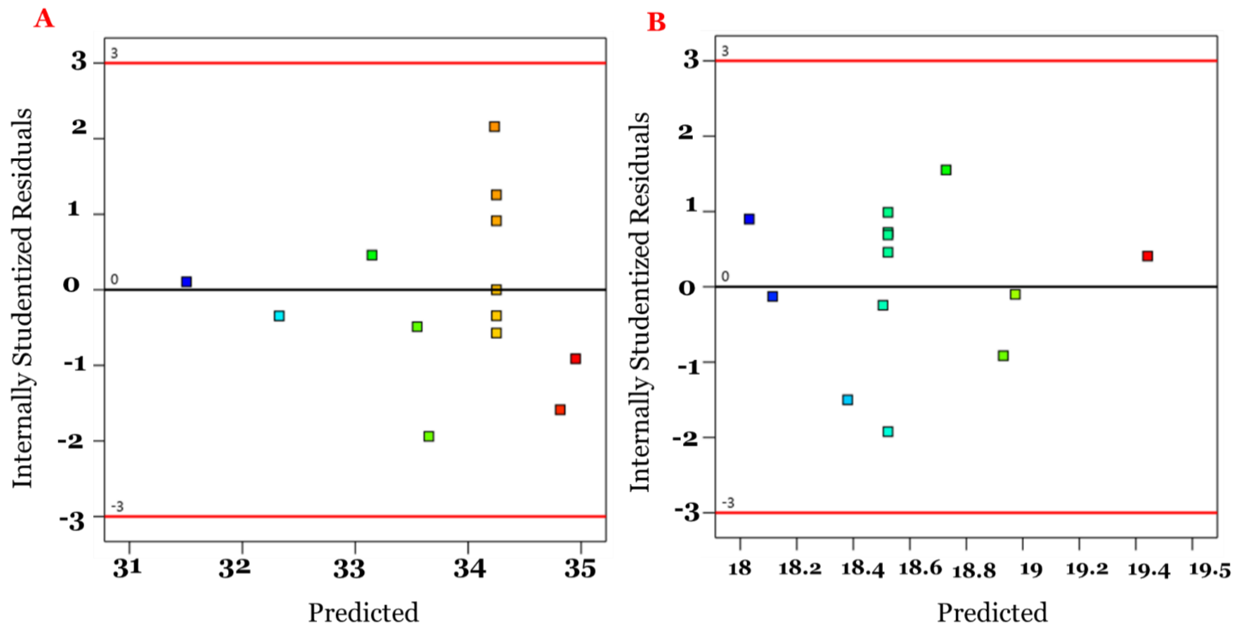

Figure 4-13: Studentized residuals plot for ash content (A) and calorific value (B) of discard coal 2

The 3D (3-dimensional) surface and contour (2-dimensional surface) plots for ash content and calorific value are presented in Figures 4-14 and 4-15. The ash content 3D plot has a concave shape, whereas the convex shape was achieved for the calorific value. This is due to the positive and negative AB terms within the regression models of ash content (Equation 4.1) and calorific value (Equation 4.2), respectively. The curvature of the 3D plots is also different, with ash content having a greater curvature. This is due to the presence of both the A^2 (9.05×10^{-2}) and B^2 (9.36×10^{-1}) terms within the model equation of ash content (Equation 4.1). On the other hand, only the B^2 ($1.54 \times 10^{-1} B^2$) term is within the calorific value model (Hou et al., 2013; Yadav et al., 2018; Abdulsalam et al., 2019).

As previously stated, the terms A and B are mainly used to investigate the impact of input variables on surface response. Based on the regression model equations (Equations 4.1 and 4.2), emulsion dosage (B) has a negative coefficient of 9.53×10^{-1} and a positive coefficient of 2.97×10^{-1} within the ash content and calorific value equations, respectively. It illustrates that at constant dosage, increasing agitation speed reduces the ash content and thus increases the calorific value. The emulsion binder dosage of 5 kg/ton and agitation speed of 1800 rpm produced a floated clean coal concentrate with 31.51% ash and heating value of 19.45 MJ/kg.

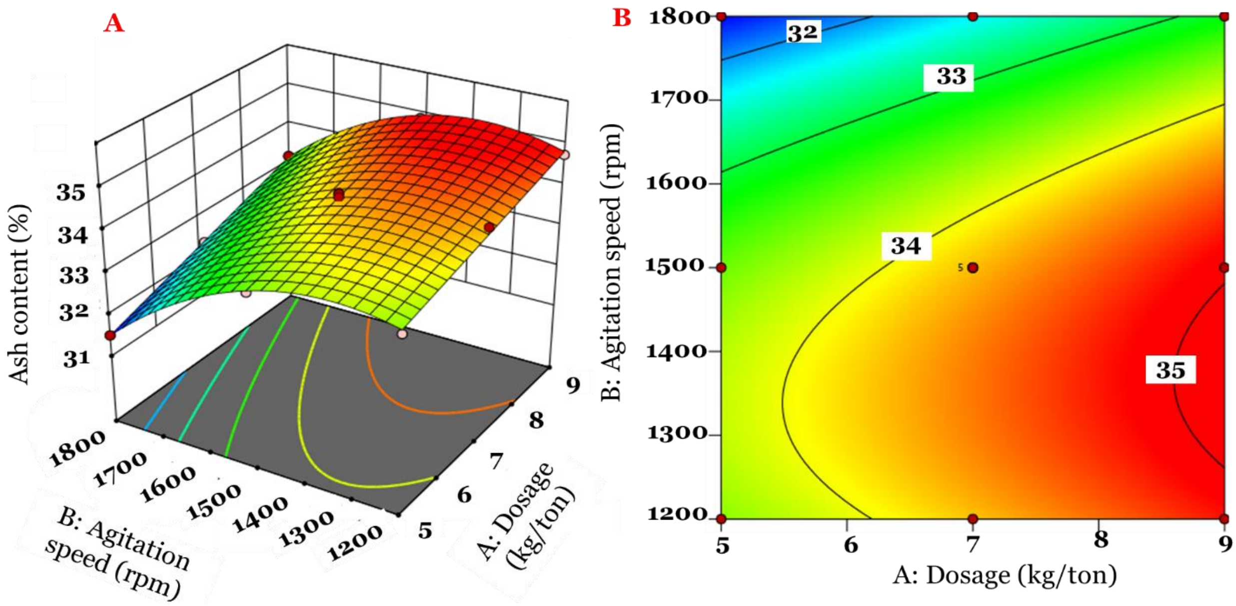

Figure 4-14: 3D surface (A) and contour plot (B) of ash content of discard coal 2

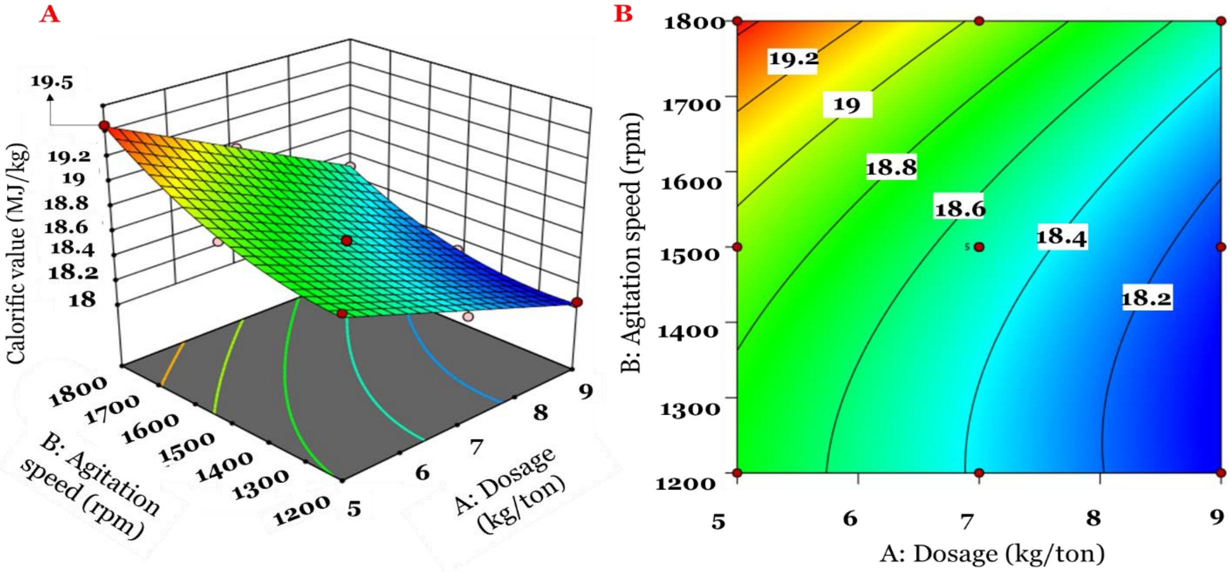

Figure 4-15: 3D surface (A) and contour plot (B) of calorific value of discard coal 2

Upon completing the data analysis and evaluation, the data were optimised such that input factors and response surface constraints were established (Table 4-8). The objective was to examine which input factors will yield predicted values with maximum and minimum calorific values and ash content, respectively. The input factors ranged from 5 kg/ton and 1200 rpm as lower limits to 9 kg/ton and 1800 rpm as upper limits.

Table 4-8: Process parameters used for optimisation of discard coal 2 using HIP W/O emulsion

Constraints	**Goal**	**Lower limit**	**Upper limit**
Dosage (A)	Is in range	5	9
Agitation speed (B)	Is in range	1200	1800
Ash content (%)	Minimise	31.51	34.88
CV (MJ/kg)	Maximise	18.05	19.45

CV= calorific value

The software yielded solutions comprising of different desirability as indicated in Table 4-9. Solution 1 was selected and regarded optimal due to the highest achieved desirability value of 0.997. A clean coal product with the predicted calorific value of 19.43 MJ/kg and the lowest ash content of 31.48% was achieved. As indicated in Table 4-9 and Figure 4-16, this was achieved under 5 kg/ton of the HIP W/O emulsion concentration and the agitation speed of 1800 rpm. The error percentage was calculated using Equation 4-5, and 0.10% was achieved for ash content and 0.10% for the calorific value. This suggests that the experimental values agree with the predicted values (Behera et al., 2018; Abdulsalam et al., 2019).

$$Percentage\ of\ absolute\ error\ (POAE) = \frac{Experimental - Predicted}{Experimental} \times 100 \quad \text{Equation 4-5}$$

Table 4-9: The optimised solutions for discard coal 2 surface responses

Number	**Dosage (kg/ton)**	**Agitation speed (rpm)**	**Ash (%)**	**Calorific value (MJ/kg)**	**Desirability**	**Remark**
1	**5.00**	**1800.00**	**31.48**	**19.43**	**0.997**	Selected
2	5.01	1800.00	31.48	19.42	0.996	
3	5.10	1800.00	31.53	19.42	0.986	
4	5.00	1789.27	31.58	19.42	0.978	
5	5.21	1800.00	31.58	19.39	0.969	
6	5.00	1200.00	33.62	18.73	0.425	
7	5.00	1211.91	33.65	18.73	0.421	
8	5.00	1246.04	33.72	18.74	0.411	
9	5.00	1305.00	33.79	18.76	0.407	
10	5.00	1285.72	33.77	18.76	0.407	

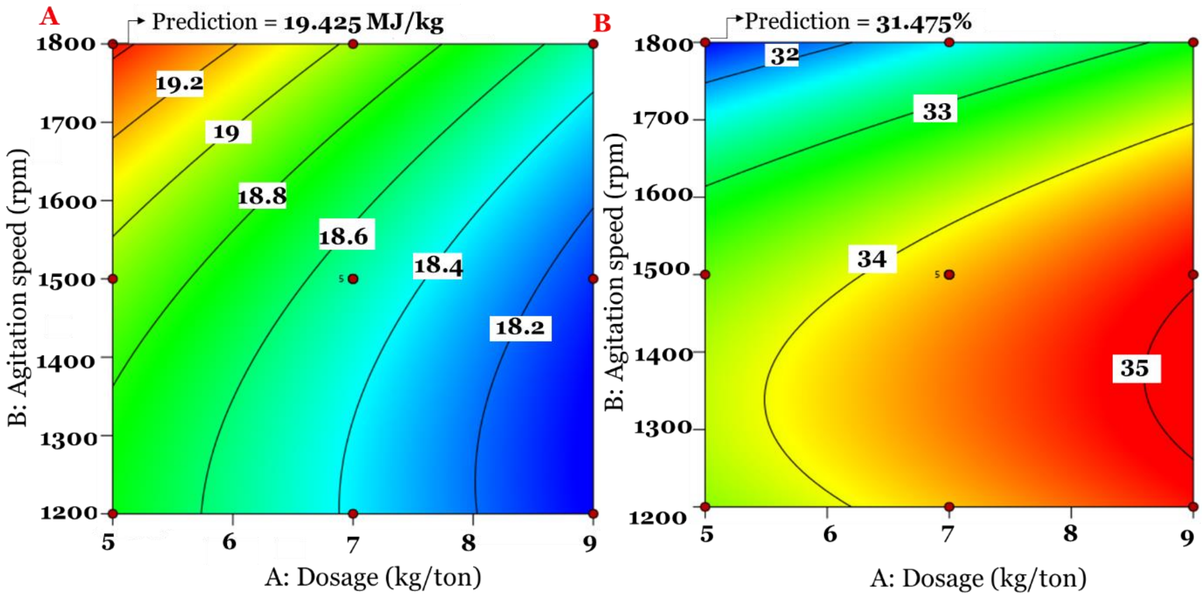

Figure 4-16: Contour plot of the calorific value (A) and ash content (B) of coal 2

Table 4-10 presents the model confirmation table. A post-analysis was performed whereby the emulsion dosage of 5 kg/ton and agitation speed of 1800 rpm were selected as confirmation points. Post experiment results with ash content of 31.48% and heating value of 19.47 MJ/kg were achieved and analysed by the software to validate the regression models. This was to confirm the model by evaluating if the observed ash content and calorific value are closer to the predicted mean of 31.48% and 19.43 MJ/kg, respectively (Stat-Ease, n.d; Teimouri, 2020). The model was confirmed and can be used to make predictions, as applied to discard coal 3.

Table 4-10: Model confirmation results for discard coal 2

Response	Predicted mean	Predicted median	Observed	95% PI low	95% PI high
Ash content (%)	31.48	31.48	31.48	31.21	31.74
Calorific value (MJ/kg)	19.43	19.43	19.47	19.32	19.57

PI: Probability interval

4.5.2. Regression model development for discard coal 3 using the HIP W/O emulsion

The influence of the emulsion concentration and agitation speed on ash content and calorific value of clean coal produced from the beneficiation of discard coal 3 are presented in this section. The experimental results obtained from the beneficiation test are shown in Table 4-11. Similar to the results achieved for discard coal 2, the heating value of the floated clean coal concentrates from discard coal 3 were found to increase with the agitation speed. On the other hand, the increase in the emulsion binder concentration was found to lower the grade of the floated clean coal.

Table 4-11: Experimental results achieved for discard coal 3

Run	**Factor 1** Dosage (kg/ton)	**Factor 2** Agitation Speed (rpm)	**Response 1** Ash content (%)	**Response 2** Calorific Value (MJ/kg)
1	7	1500	14.86	26.66
2	7	1200	18.56	25.76
3	9	1800	14.36	27.13
4	9	1200	19.43	25.48
5	7	1800	13.47	27.60
6	**5**	**1800**	**12.83**	**28.12**
7	9	1500	15.74	26.16
8	7	1500	14.77	26.70
9	5	1500	13.99	27.04
10	7	1500	14.76	26.77
11	5	1200	17.20	26.13
12	7	1500	14.90	26.64
13	7	1500	14.88	26.66

Tables 4-12 and 4-13 present the results from the ANOVA analysis. There was a significant impact from the emulsion binder dosage and agitation speed on ash content and heating value of the clean coals obtained. This was confirmed by the p-values of < 0.0001 for the surface model of ash content and calorific value. The Pred. R^2 and Adj. R^2 for ash content was 0.9881 and 0.9973 (Table 4-12), whereas 0.9832 and 0.9938 were achieved for the calorific value (Table 4-13). There was an agreement between the Pred. R^2 and Adj. R^2 for these surface models as indicated by the difference of less than 0.2 for ash content (0.0092) and calorific value (0.0106). The lack of fit was considered insignificant in relation to the ash content and calorific value. This demonstrates a good fit between the experimental and the predicted values. Therefore the models can be used for predictions (Sharma et al., 2012; Abdulsalam et al., 2019).

As previously mentioned, the adequate precision of a model must be more than 4 (Stat-Ease, n.d; Behera et al., 2018). An adequate precision of 98.9 was obtained for the ash content compared to 69.5 for the calorific value. However, there is low data point discrimination for both responses, given the achieved precision of more than 4. From the quadratic models obtained for the responses, A^2 and B^2 were insignificant for calorific value, whereas only A^2 is unimportant for ash content. These terms were not removed because they violate the alternative hypothesis by increasing the p-value of the AB term and making it insignificant.

As in discard coal 2, it was found that increasing the agitation speed enhanced the quality of the clean coal for discard coal 3 by lowering its ash content and increasing its heating value. This correlates with the negative coefficient of the agitation speed (B) for ash content and a positive coefficient in the calorific value equation (Equations 4.6 and 4.7). The emulsion binder has a positive and negative coefficient for ash content and calorific value, respectively. The constant term of 14.85 and 26.67 (Equations 4.6 and 4.7) for ash content and calorific value, respectively, demonstrates the intercept of A and B, regarded as the centre point within the design space (Stat-Ease, n.d).

Coded equations

$$Ash\ (\%) = 14.85 + 9.47 \times 10^{-1}A - 2.45B - 1.33 \times 10^{-1}AB - 3.34 \times 10^{-2}A^2 + 1.12B^2$$

Equation 4.6

$$Calorific\ value\left(\frac{MJ}{kg}\right) = 26.67 - 4.13 \times 10^{-1}A + 9.07 \times 10^{-1}B - 7.50 \times 10^{-2}AB - 3.24 \times 10^{-2}A^2 + 4.76 \times 10^{-2}B^2$$

Equation 4.7

Actual equations

$$Ash\ (\%) = 48.97 + 9.2210^{-1}A - 4.38 \times 10^{-2}B - 2.21 \times 10^{-4}AB - 8.36 \times 10^{-3}A^2 + 1.20 \times 10^{-5}B^2$$

Equation 4.8

$$Calorific\ value\left(\frac{MJ}{kg}\right) = 23.06 + 9.43 \times 10^{-2}A + 2.31 \times 10^{-3}B - 1.25 \times 10^{-3}AB - 8.10 \times 10^{-3}A^2 + 5.29 \times 10^{-7}B^2$$

Equation 4.9

Table 4-12: ANOVA results for the surface model of ash content for discard coal 3

Source	Sum of Squares	df	Mean Square	F-value	p-value	Remark
Model	45.40	5	9.08	889.05	<0.0001	Sig.
A	5.38	1	5.38	526.47	<0.0001	
B	36.02	1	36.02	3526.21	<0.0001	
AB	0.0702	1	0.0702	6.88	0.0343	
A^2	0.0031	1	0.0031	0.3025	0.5994	
B^2	3.44	1	3.44	337.13	<0.0001	
Residual	0.0715	7	0.0102			
Lack of Fit	0.0548	3	0.0183	4.37	0.0942	Not Sig.
Pure Error	0.0167	4	0.0042			
Cor. Total	45.47	12				
R^2	0.9984					
Adj. R^2	0.9973					
Pred. R^2	0.9881					
Adeq. Precision	98.9445					

Df - degree of freedom; A: HIP W/O emulsion dosage; B: Agitation speed; Cor. Total – the total Sum of Squares corrected for the mean; Adeq. Precision – Adequate Precision; Sig. – Significant

Table 4-13: ANOVA results for the surface model of calorific value for discard coal 3

Source	Sum of Squares	df	Mean Square	F-value	p-value	Remark
Model	5.99	5	1.20	383	<0.0001	Sig.
A	1.03	1	1.03	327.89	<0.0001	
B	4.93	1	4.93	1577.68	<0.0001	
AB	0.0225	1	0.0225	7.20	0.0314	
A^2	0.0029	1	0.0029	0.9282	0.3674	
B^2	0.0063	1	0.0063	2.00	0.2001	
Residual	0.0219	7	0.0031			
Lack of Fit	0.0112	3	0.0037	1.39	0.3679	Not Sig.
Pure Error	0.0107	4	0.0027			
Cor. Total	6.01	12				
R^2	0.9964					
Adj. R^2	0.9938					
Pred. R^2	0.9832					
Adeq. Precision	69.5003					

Df - degree of freedom; A: HIP W/O emulsion dosage; B: Agitation speed; Cor. Total – the total Sum of Squares corrected for the mean; Adeq. Precision – Adequate Precision; Sig. – Significant

The experimental and the predicted values achieved by beneficiating discard coal 3 with as received ash content of 41.71% are shown in Table 4-14. There is a good correlation between the experimental and predicted values, as also indicated by the Adj. R^2 of 0.9973 and 0.9938 for ash content and calorific value, respectively.

Table 4-14: Experimental and predicted values for discard coal 3

Run	**Dosage (kg/ton)**	**Agitation speed (rpm)**	**Ash content (%)**		**Calorific value (MJ/kg)**	
			EV	PV	EV	PV
1	7	1500	14.86	14.85	26.66	26.67
2	7	1200	18.56	18.42	25.76	25.81
3	9	1800	14.36	14.30	27.13	27.10
4	9	1200	19.43	19.46	25.48	25.44
5	7	1800	13.47	13.52	27.60	27.62
6	**5**	**1800**	**12.83**	**12.67**	**28.12**	**28.08**
7	9	1500	15.74	15.77	26.16	26.22
8	7	1500	14.77	14.85	26.70	26.67
9	5	1500	13.99	13.87	27.04	27.05
10	7	1500	14.76	14.85	26.77	26.67
11	5	1200	17.20	17.31	26.13	26.12
12	7	1500	14.90	14.85	26.64	26.67
13	7	1500	14.88	14.85	26.66	26.67

EV = experimental value; PV = predicted value

Figures 4-17 and 4-18 present linear regression and studentized residual plots. As seen in Figure 4-17, most of the data points are on the straight line, demonstrating a strong correlation between the experimental and predicted values. As previously stated, the clustered data points denote experimental and predicted values for centre points of the design matrix. There are no outliers in terms of ash content and calorific value (Figure 4-18). This demonstrates that the calculated mean for the data set is not biased; therefore, these surface response models can be used for predictions.

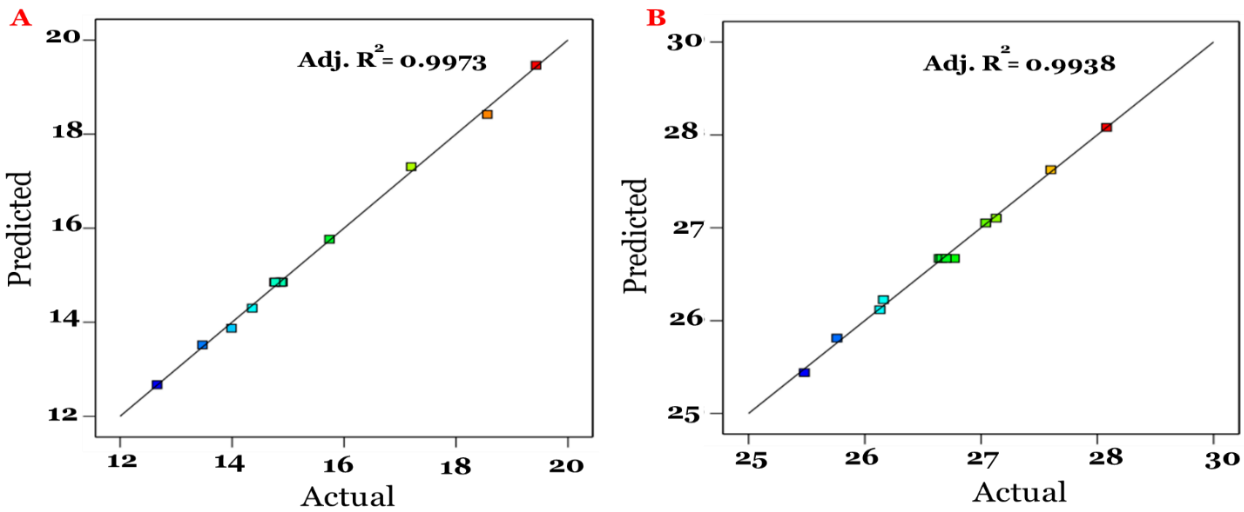

Figure 4-17: A linear regression plots for ash content (A) and calorific value (B) of discard coal 3

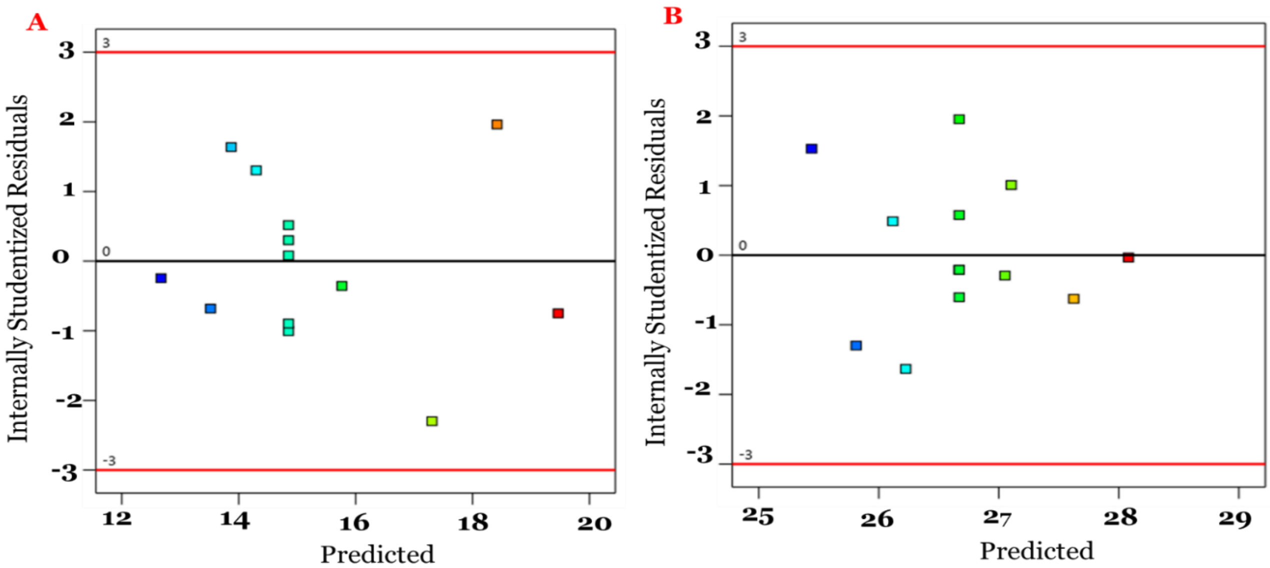

Figure 4-18: Studentized residual plots for ash content (A) and calorific value (B) of discard coal 3

The 3D and contour plots for the regression models of ash content and calorific value are presented in Figures 4-19 and 4-20. The data points represented by the circles are well fitted on the surface plots, demonstrating a strong correlation (Figure 4-19A and 4-20A). The data points under the surface response plot demonstrate low experimental values, whereas the data above indicates high experimental values compared to the predicted values (Setsepu et al., 2021). The surface 3D plot for ash content has a convex shape, whereas a flat shape was obtained for calorific value. This might be due to the insignificance of A^2 and B^2 terms within the regression model of calorific value (Table 4-13). In addition, the coefficients of the squared terms, especially the B^2 of 4.76×10^{-2} within the calorific value equation, is very small compared to B^2 of 1.12 for ash content, leading to minimal impact on the curvature of the surface response (Equations 4.6 and 4.7). The 3D surface plot of ash content for discard coal 2 is concave (Figure 4-14), whereas that for discard coal 3 has a convex shape (Figure 4-19). This is due to the positive and negative AB terms obtained for the ash content models for discard coal 2 (Equation 4.1) and 3 (Equation 4.6), respectively (Hou et al., 2013; Yadav et al., 2018).

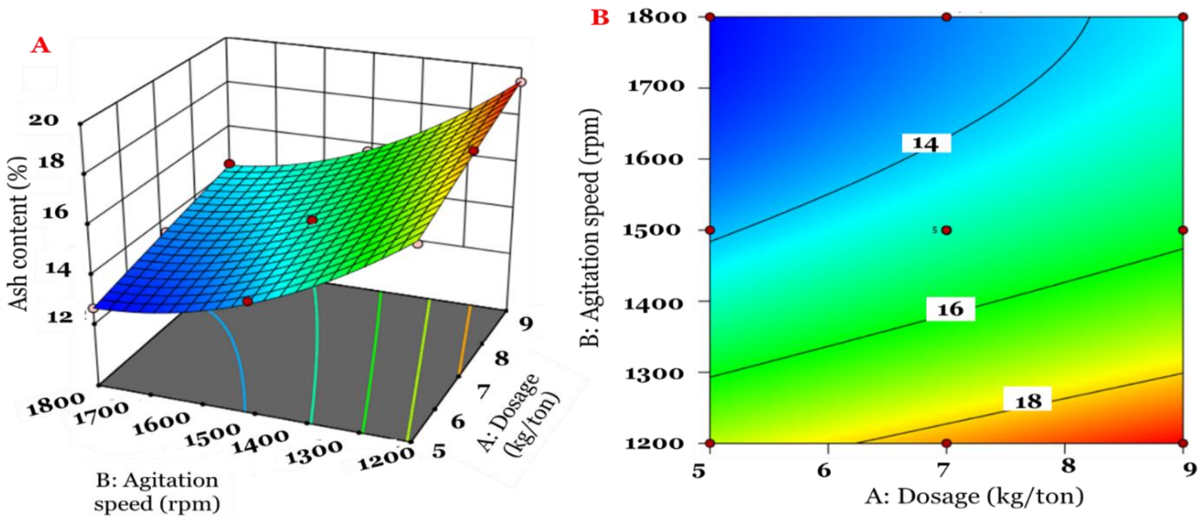

Figure 4-19: 3D surface (A) and contour plot (B) of ash content of discard coal 3

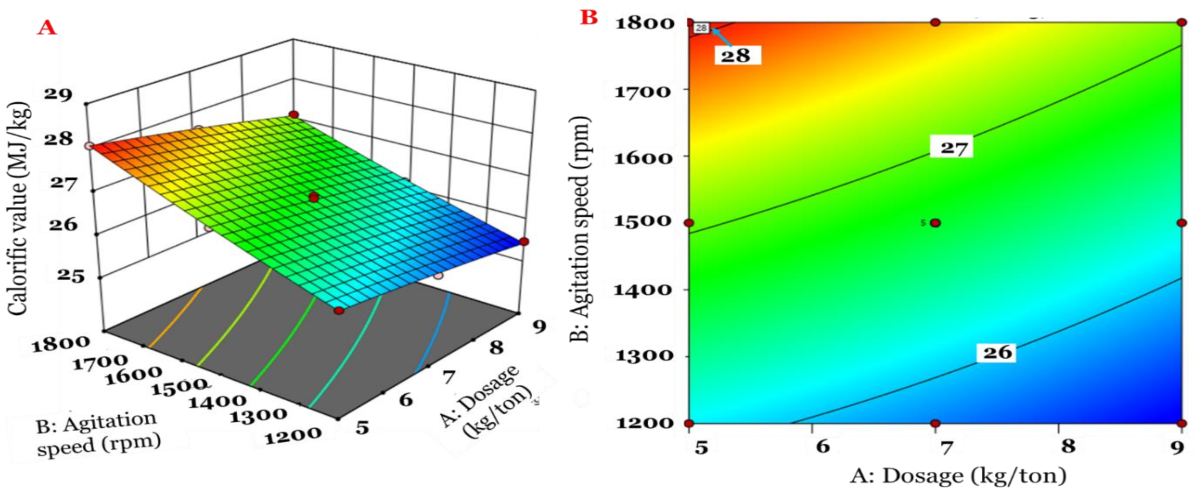

Figure 4-20: 3D surface (A) and contour plot (B) of the calorific value of discard coal 3

The data for discard coal 3 was optimised, whereby the input factors and response surface constraints were established (Table 4-15). This was to evaluate which input factors can yield a clean coal product with minimum ash content and high heating value.

Table 4-15: Process parameters used for the optimisation of discard coal 3

Constraints	Goal	Lower limit	Upper limit
Dosage (A)	Is in range	5	9
Agitation speed (B)	Is in range	1200	1800
Ash content (%)	Minimise	12.83	19.43
CV (MJ/kg)	Maximise	25.48	28.12

CV= calorific value

Of the yielded optimisation solutions, solution 1 was desirable because it resulted in a floated clean coal of 12.67% ash and a calorific value of 28.08 MJ/kg. As indicated in Table 4-16 and Figure 4-21, this was achieved under 5 kg/ton of the W/O collector concentration and the agitation speed of 1800 rpm. The error percentage of 1.24% and 0.14% was achieved for ash content and the calorific value, respectively.

Table 4-16: The obtained optimised solutions for discard coal 3 under HIP W/O emulsion

Number	Dosage (kg/ton)	Agitation speed (rpm)	Ash content (%)	Calorific value (MJ/kg)	Desirability	Remark
1	**5.00**	**1800.00**	**12.67**	**28.08**	**0.999**	Selected
2	5.00	1797.47	12.67	28.07	0.998	

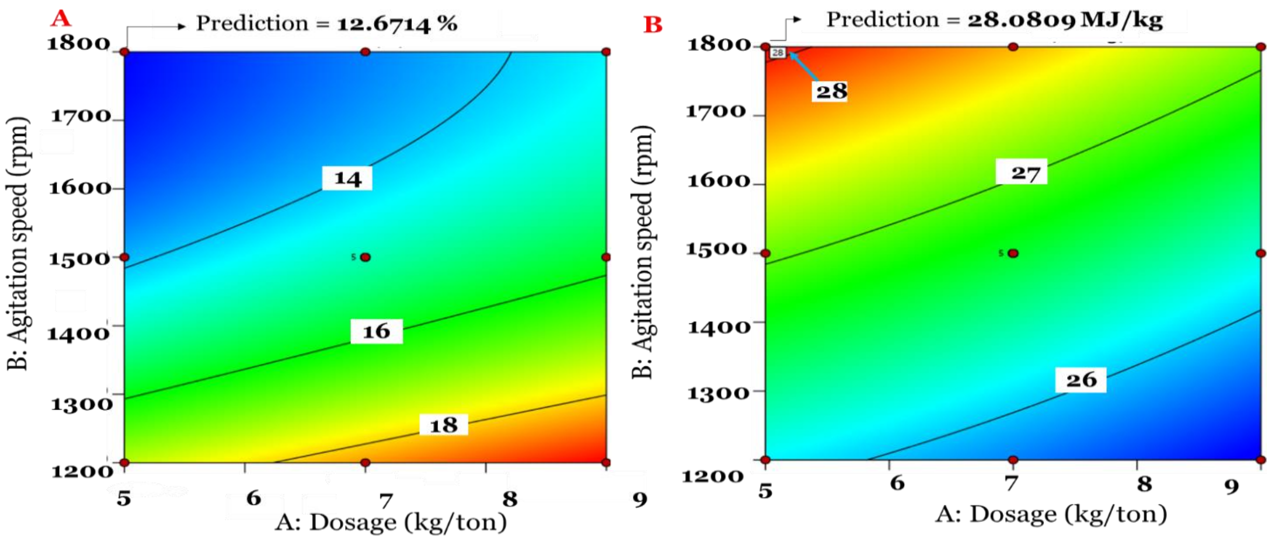

Figure 4-21: Contour plot of ash content (A) and calorific value (B) of discard coal 3

Table 4-17 presents the model confirmation table achieved after post-analysis of the suggested experimental run. The emulsion binder dosage of 5 kg/ton and flotation agitation speed of 1800 rpm produced floated clean coal with 12.87% ash and a heating value of 28.03 MJ/kg was achieved under 5 kg/ton and 1800 rpm. This was used as a validation point for the regression model equation, and it was found to be close to the predicted sample mean of 12.67% ash and the calorific value of 28.08 MJ/kg. The model was confirmed.

Table 4-17: Model confirmation results for discard coal 3

Response	Predicted mean	Predicted median	Observed	95% PI low	95% PI high
Ash content (%)	12.67	12.67	12.87	12.35	12.99
Calorific value (MJ/kg)	28.08	28.08	28.03	27.90	28.26

PI: Probability interval

4.5.3. Summary for regression model development

Regression model equations of surface responses for discard coals 2 and 3 were developed to make predictions. From this study, the agitation speed of 1800 rpm and HIP W/O emulsion dosage of 5 kg/ton was found optimal since it produces a floated clean coal concentrate with minimum ash content and maximum heating value.

4.6. Application of optimal conditions on discard coal 2 and 3 under kerosene

The optimal conditions of 5 kg/ton and 1800 rpm obtained from the optimisation study performed with an emulsion binder were utilised in beneficiating coal discard 2 and 3 with kerosene. This was to investigate the response of kerosene on ash content and heat content of clean product produced from the beneficiation of coal discards. A clean coal product with calorific values of between 19.05 MJ/kg and 27.20 MJ/kg was produced from discard coal 2 and 3 from a feed coal with 8.49 MJ/kg and 16.29 MJ/kg, respectively.

On the other hand, the W/O emulsion technology resulted with floated clean coal concentrate comprising the calorific value of 19.45 MJ/kg (Table 4-4 and 4-7) and 28.12 MJ/kg (Table 4-11 and 4-14) from discard coal 2 and 3, respectively. The HIP W/O emulsion binder and kerosene can both beneficiate weathered coal that has been dumped for decades. However, kerosene required an abundance of pure kerosene (without any modification by the addition of water) to enhance the floatability of the carbonaceous ultra-fines within the coal discard. This agrees with the literature showing that for effective separation under pure oils, the oil dosage of 10 to 20 wt% is required (Garcia et al., 1995; Dickinson et al., 2015; Netten et al., 2016). This is because the availability of hydrophilic oxygenated functional groups within discard coal enhances the potential of the air bubbles to repel the carbonaceous particles within the coal and therefore decreases the rate of attachment (Sarikaya and Ozbayoglu, 1990; Li et al., 2018). In comparison, the W/O HIP emulsion binder requires only 0.25 kg/ton of organic oil, while 5 kg/ton of pure kerosene is necessary to beneficiate the same coal.

CHAPTER 5: CONCLUSIONS AND RECOMMENDATIONS

5.1. Conclusions

In this study, the potential of the advanced HIP W/O emulsion binder was evaluated as an alternative technique to beneficiate weathered coal. Five South African coal discards slurry deposited for about 20 to 30 years and sourced from the Witbank coalfields were beneficiated using this technique. The study was inspired by the potential of the emulsion binder to beneficiate weathered coal particles with reduced amounts of organic liquids compared to traditional beneficiation that requires high doses of organic reagents like kerosene. The discard coal preparation and characterisation, the HIP W/O emulsion binder preparation, the beneficiation test, optimisation and modelling were conducted. With the determination of the physico-chemical properties of the coals, the degree of oxidation, and the response of collectors on coal discard products can be evaluated. Additionally, the laboratory analysed ash contents and calorific values for discard coals 2 and 3 were optimised and modelled to develop mathematical equations that can be used to make predictions. Different clean coal products were obtained and characterised in terms of their grades.

<u>The following conclusions were drawn from this study:</u>

I. Weathered coal discards are characterised by the presence of OH groups within their chemical structures. Discard coal 2 followed by discard coal 3 were found to be the most weathered discards. This agrees with the results achieved by Wang et al. (2012) who found the most weathered coal to possess intense peaks of OH groups.

II. Based on stability tests, the most stable binder was emulsion binder 1, followed by 3, 2 and 4. Emulsion binder 1 comprising 8.55 g NaCl, and Span 80 and kerosene in equal proportions resulted with floated high quality clean coal comprising 11.76% ash and heating value of 28.61 MJ/kg. The most non-stable emulsion binder 4 produced a clean coal product with high yield.

III. The beneficiation tests conducted under different concentrations (5 kg/ton, 7 kg/ton and 9 kg/ton) of the emulsion binder and kerosene showed that the increase in dosage is inversely proportional to the calorific value and directly proportional to clean coal yield.

- A floated clean coal concentrate of 11.76% ash, calorific value of 28.61 MJ/kg and 15.61% yield was achieved under 5 kg/ton of emulsion binder. In contrast, 17.47% ash, calorific value of 26.42 MJ/kg and a yield of 21.59% was achieved using 5 kg/ton of kerosene. These clean coal products were obtained by beneficiating discard coal 1 with a feed ash content of 29.34% and calorific value of 20.94 MJ/kg. The yields obtained are less than 50%, which could be because the tests were performed on a batch scale and that feed used was 250 g. In addition, the yield and grade are inversely proportional so that high yields of more than 50 % may be obtained with high ash contents and low calorific values for the clean coal product.

IV. The optimum concentration of 5 kg/ton of the emulsion binder was likewise used to beneficiate another four coal discards; discard coal 2, 3, 4 and 5.
   - The feed calorific values of 8.48 MJ/kg and 16.29 MJ/kg increased to 18.16 MJ/kg and 25.77 MJ/kg for discard coal 2 and 3, respectively.
   - The beneficiation of discard coal 4 and 5 increased the feed calorific values from 20.61 MJ/kg and 18.55 MJ/kg to 27.62 MJ/kg and 26.28 MJ/kg, respectively.

V. The study's optimisation and modelling indicated that the W/O HIP emulsion concentration is inversely proportional to the calorific value. In addition, the agitation speed of the flotation unit was found to be directly proportional to the calorific value of clean coal product produced by three-stage cleaning. The variation of agitation speed when using emulsion is novel. In previous studies the ability of W/O HIP emulsion collector was evaluated by using either 1500 rpm or 22,000 rpm. This depends on the beneficiation unit used.
   - A clean coal concentrate with an ash content of 31.51% and heating value of 19.45 MJ/kg was produced from coal 2 using 5 kg/ton of emulsion and an agitation speed of 1800 rpm. The feed coal's ash content and calorific value were 48.71% and 8.48 MJ/kg, respectively.
   - The feed ash content of 41.71% and heating value of 16.29 MJ/kg for discard coal 3 was upgraded to a floated concentrate with an ash content and heating value of 12.83% ash and 28.12 MJ/kg, respectively using 5 kg/ton of emulsion and 1800 rpm.
   - A 5 kg/ton kerosene concentration produced clean coal product with the heating value of 19.05 MJ/kg and 27.20 MJ/kg for discard coal 2 and 3, respectively.

In summary, emulsion binder 1 proved to be the superior binder, comprising 8.55 g NaCl, 50% kerosene and 50% Span 80. Compared to pure kerosene, requiring 5 kg/ton to produce clean coal products, the HIP W/O emulsion binder used only 0.25 kg/ton of the organic liquids (kerosene and Span 80) therefore demonstrated its economic viability since about 95 vol% of organic liquids was substituted by tap water. This research has established that weathered discard coal from South African coalfields deposited (slurry ponds) for decades can be upgraded into a high-quality product. As indicated, the approach is economically viable in terms of the different grades of clean coal obtained, which could be used for different applications. However, yields are low, in particular for high-quality clean coal products. The coal discards can be beneficiated at large scale using HIP W/O emulsion binder, however, flotation banks, filtration systems and pumps will be required or the use of an agglomeration cell at higher agitation speed.

5.2. Recommendations

Based on the success of this study which demonstrated that the W/O HIP emulsion collector can be used as a cost-saving reagent for coal beneficiation under froth flotation, the stated recommendations are proposed for future research:

I. The HIP W/O emulsion binder process should be conducted under agglomeration with the same weathered coal at an intense agitation speed of about 22,000 rpm since agitation speed has a significant influence on the HIP W/O emulsion process.

II. Pilot-scale tests using an emulsion binder should be conducted in a continuous agglomeration plant to examine the proficiency of the W/O HIP emulsion in beneficiating coal discards.

III. Economic viability assessment for the beneficiation of coal discards using the W/O HIP emulsion collector in comparison to traditional reagents.

REFERENCES

Abdulredha, M. M., Hussain, S. A. and Abdullah, L. C., 2018. Overview on petroleum emulsions, formation, influence and demulsification treatment techniques. *Arabian Journal of Chemistry,* Volume 13, pp. 3403 - 3428.

Abdulsalam, J., Mulopo, J., Oboirien, B., Bada, S. and Falcon, R., 2019. Experimental evaluation of activated carbon derived from South Africa discard coal for natural gas storage. *International Journal of Coal Science Technology,* 6(3), pp. 459 - 477.

Abdulsalam, J., (2019). *Development of Activated Carbons from South African Coal Waste for Application in Natural Gas Storage*. Doctor of Philosophy. University of the Witwatersrand, Johannesburg, South Africa. [Online] Available at: https://scholar.google.com/citations?user=soG36tYAAAAJ&hl=en. [Accessed 14 January 2022].

Aich, S., Nandi, B. K. and Bhattacharya, S., 2019. Effect of weathering on physico-chemical properties and combustion behavior of an Indian thermal coal. *International Journal Science Technology,* 6(1), pp. 51 - 62.

Akdemir, U. and Sonmez, I., 2003. Investigation of coal and ash recovery and retrainment in flotation. *Fuel Processing Technology,* Volume 81, pp. 1 - 9.

Alibaba, n.d. *MZ-100 Grinding mill*. [Online] Available at: https://www.alibaba.com/product-detail/lab-sample-pulveriser-grinding-mill-for_1600074552274.html. [Accessed 14 January 2021].

Arkhipov, V. A., Paleev, D. Y., Patrakov, Y. F. and Usanina, A. S., 2011. Determination of contact angle on the coal surface. *Journal of Mining Science,* 47(5), pp. 561 - 565.

Aslan, N. and Unal, I., 2011. Multi-response optimization of oil agglomeration with multiple perfomance characteristics. *Fuel Processing Technology,* Volume 92, pp. 1157 - 1163.

ASTM, 2009. *Standard Test Methods for Proximate Analysis of the Analysis Sample of Coal and Coke by Instrumental Procedures.* [Online] Available at: https: //www.astm.org-/Standards/D5142.htm. [Accessed 15 January 2022].

ASTM, 2019. *Standard Test Method for Gross Calorific Value of Coal and Coke.* [Online] Available at: https://www.astm.org/Standards/D5865.htm. [Accessed 15 January 2022].

Atasoy, Y. and Spottiswood, D. J., 1995. A study of particle separation in a spiral concentrator. *Minerals Engineering,* 8(10), pp. 1197 - 1208.

Bada, S. O., Falcon, R. M. S. and Bergmann, C. P., 2016. Co-firing potential of raw and thermally treated Phyllostachys aurea bamboo with coal. *Energy Sources, Part A: Recovery, Utilization, and Environmental Effects,* 38(10), pp. 1345 - 1354.

Barma, S. D., 2019. Ultrasonic-assisted coal beneficiation: A review. *Ultrasonics - Sonochemistry.*

Behera, S. K., Meena, H., Chakraborty, S. and Meikap, B. C., 2018. Application of response surface methodology (RSM) for optimization of leaching parameters for ash reduction from low- grade coal. *International Journal of Mining Science and Technology,* Volume 28, pp. 621 - 629.

Bensley, C. N., Swanson, A. R. and Nicol, S. K., 1977. The effect of emulsification on the selective agglomeration of fine coal. *International Journal of Mineral Processing,* Volume 4, pp. 173 - 184.

Benusa, M. D. and Klima, M. S., 2008. An Evaluation of a Two-Stage Spiral Processing. *International Journal of Coal Preparation and Utilization,* Volume 28, p. 237–260.

Benusa, M. D. and Klima, M. S., 2009. An Evaluation of a Two-Stage Spiral Processing. *International Journal of Coal Preparation and Utilization,* Volume 29, pp. 49 -67.

Bhattacharya, S., Jyoti, D., Sahu, L., Dey, S. and Singh, H B., 2017. Flotation of Low Volatile Coking Coal Fines. *Indian Instituate of Metallurgy,* 70(2), pp. 421 - 432.

Borrow, D. J., van Netten, K. and Galvin, K. P., 2018. Ultrafine particles recovery using thin permeable films. *Frontiers in Chemistry,* Volume 6, pp. 1 - 8.

Boylu, F., Tali, E., Cetinel, T. and Celik, M. S., 2014. Effect of fluidizing characteristics on upgrading of lignitic coals in gravity based air jigs. *International Journal of Mineral Processing,* Volume 129, pp. 27 - 35.

Boylu, F., Çinku, K., Çetinel, T., Karakaş, F., Güven, O., KaraağaçlIoğlu, I. E. and Çelik, M. S., 2015. Effect of coal moisture on the treatment of a lignitic coal through a semi-pilot-scale pneumatic stratification jig. *International Journal of Coal Preparation and Utilization,* 35(3), pp. 143 - 154.

Bu, X., Nia, C., Xie, G., Peng, Y., Ge, L. and Sha, J., 2017. Preliminary study on foreign slime for the gravity separation of coarse. *International Journal of Mineral Processing,* Volume 160, pp. 76 - 80.

Cameron, N. R., 2005. High internal phase emulsion templating as a route to well-defined porous polymers. *Polymer,* 46(5), pp. 1439 -1449.

Capes, C. E. and Darcovichi, K., 1984. A survey of oil agglomeration in wet fine coal processing. *Powder Technology,* Volume 40, pp. 43 - 52.

Chagwedera, K. M., Bada, S. O. and Falcon, R. M., 2018. Evaluation of alternative solid media for coal beneficiation using an air dense-medium fluidized bed. *Journal of Southern African Institute of Mining and Metallurgy,* Volume 118, pp. 883 - 890.

Chary, G. H. and Dastidar, M. G., 2012. Investigation of optimum conditions in coal - oil agglomeration using Taguchi experimental design. *Fuel,* Volume 98, pp. 259 - 264.

Chattopadhyay, U. S., Kalyani, V. K., Venugopal, R. and Charan , T. G., 2015. Application of Response Surface Methodology in Effective Recovery of Settling Pond Coal Fines by Froth Flotation. *International Journal of Coal Preparation and Utilization,* Volume 35, pp. 206 - 215.

Chikerema, P. and Moys, M., 2012. Effects of Particle Size, Shape and Density on the Performance of an Air Fluidized Bed in Dry Coal Beneficiation. *International Journal of Coal Preparation And Utilization,* 32(2), pp. 80 - 94.

Çicek, T., 2008. Dry cleaning of Turkish coal. *Energy Sources, Part A,* 30(7), pp. 593 - 605.

Das, A., Sarkar, B., Ari, V. and Roy, S., 2010. Effecient recovery of combustibles from coking coal fines. *Mineral Processing and Extractive Metallurgy Review,* 31(4), pp. 236 - 249.

de Korte , G. J. and Engelbrecht, J., 2014. Dense Medium cyclones. *International Journal of Coal Preparation and Utilization,* 34(1), pp. 49 - 58.

Dell, C. C., 1964. An improved release analysis procedure for determining coal washability. *Journal of Institute of Fuel,* Volume 37, pp. 149 - 150.

Dell, C. C., 1953. Release analysis - A new tool for ore dressing research; Recent Developments in Mineral Dressing. *Institute of Mining and Metallurgy,* 1968(35), pp. 50 - 54.

Department of Energy, 2001. *Energy.goverment.co.za.* [Online] Available at: http://www.energy.gov.za/files/esources/coal/coal_discards.html. [Accessed 20 February 2020].

Dey, S., 2012. Enhancement in hydrophobicity of low rank coal by surfactants - a critical review. *Fuel Process Technology,* 94(15), pp. 1 - 8.

Dey, S., Paul, G. M. and Pani, S., 2013. Flotation behaviour of weathered coal in mechanical and column flotation cell. *Powder Technology,* Volume 246, pp.689 - 694.

Dickinson, J. E., Jiang, K. and Galvin, K. P., 2015. Fast flotation of coal at low pulp density using the Reflux Flotation Cell. *Chemical Engineering Research and Design,* Volume 101, pp. 74 - 84.

Dwari , R. K. and Rao, K. H., 2007. Dry beneficiation of coal - a review. *Mineral Processing and Extractive Metallurgy Review,* 28(3), pp. 177 - 234.

Eskom, n.d. *Eskom Holdings SOC Ltd - Lethabo Power Station.* [Online] Available at:https://www.eskom.co.za/Whatweredoing/ElectricityGeneration/PowerStations/Pages/Lethabo_Power_Station.aspx [Accessed 23 September 2021].

Falcon , R. and Ham, A. J., 1988. The characteristics of Southern African coals. *Journal of Institute of Mining and Metallurgy,* 88(5), pp. 145 -161.

FLSmith, n.d. *Essa Pulverising mills*. [Online] Available at: https://www.flsmidth.com/en-gb/products/sampling-preparation-and-analysis/essa-pulverising-mill-bowls. [Accessed 14 January 2022].

Galvin, K. P., Pratten, S. J., Shankar, N. G., Evans, G. M., Biggs, S. R., Tunaley, D., 2001. Production of high internal phase emulsions using rising air bubbles. *Chemical Engineering Science*, 56(21 - 22), pp. 6285 - 6293.

Galvin, K. P. and van Netten, K., 2017. A new method for ultra-fast concentration of hydrophobic particles. *Chemical Engineering Science,* Volume 158, pp. 439 - 444.

Garcia, A. B., Vega, J. M. G. and Martinez-Tarazona, M. R., 1995. Effects of oil concentration and particle size on the cleaning of Spanish high-rank coals by agglomeration with n-heptane. *Fuel*, 74(11), pp. 1692 -1697.

Guan, W., Sha, J., Liu, P., Peng, Y. and Xie, G., 2018. Effect of stirring time on oil agglomeration of fine coal. *The Journal of the Southern African Institute of Mining and Metallurgy,* Volume 118, pp. 89 - 94.

Hayes, P. C., 2003. *Process Principles in Minerals and Materials Production.* 3 ed. Brisbane, Queensland: Hayes Publishing co.

Hembrom, A. and Suresh, N., 2018. Evaluation of the perfomance of water-only cyclone fro finr coal beneficiation using optimization process. *Energy Sources, Part A: Recovery, Utilization and Envonmental Effects,* 40(23), pp. 2842 - 2852.

Honaker , R. Q., Jain, M., Parekh, B. K. and Saracoglu, M., 2007. Ultrafine coal cleaning using spiral concentrators. *Mineral Engineering,* Volume 20, p. 1315 – 1319.

Hornsby , D. T., Watson , S. J. and Clarkson C, C. J., 1993. Fine coal cleaning by spiral and water washing. *Coal Preparation,* 2(1 - 4), pp. 133 - 161.

Horsfall, D. W., Zitron, Z. and De Kortes, G. J., 1986. The treatment of ultrafine, especially by froth flotation. *The Journal of South African Mining and Metallurgy,* 86(10), pp. 401 - 407.

Hou, P., Cannon, F. S., Nieto-Delgado, C., Brown, N. R. and Gu, X., 2013. Effect of preparation protocol on anchoring quaternary ammonium/ wpoxide-forming compound into granular activated carbon for perchlorate adsorption: Enhancement by Response Surface Methodology. *Chemical Engineering Journal,* Volume 223, pp. 309 - 317.

Hu, W. B., 1975. Separation effeciency. *Journal of Non-Ferrous Metals,* Volume 6, pp. 40 - 60.

Isaac, K., (2019). *The Co-Combustion Performance of South African Coal and Refuse Derived Fuel*. Chemical Engineering. Masters. University of the Witwatersrand. Available at: https://hdl.handle.net/10539/29052. [Accessed 05 May 2021].

Jing, Z., Rodrigues, S., Strounina, E., Li, M., Wood, B., Underschultz, J. R., Esterle, J. and Steel, K., 2019. Use of FTIR, XPS, NMR to characterize oxidative effects of NaCIO on coal molecular structures. *International Journal of Geology,* Volume 209, pp. 1 - 13.

Kasomo, R. M., Ombiro, S., Rop, B. and Mutua, N. M., 2018. Investigation and comparison of emulsified diesel oil and flomin C 9202 as a collector in the beneficiation of ultra-fine coal by agglo-flotation. *International Journal of Oil, Gas and Coal Engineering*, 6(4), pp. 74 - 80.

Kumar, S. and Venugopal, R., 2017. Performance analysis of jig for coal cleaning using 3D response surface methodology. *International Journal of Mining Science and Technology*, 27(2), pp. 333 - 337.

Laskowski, J. S. and Yu, Z., 2000. Oil agglomeration and its effect on beneficiation and filtration of low-rank/oxidised coals. *International Journal of Mineral Processing,* Volume 58, pp. 237 - 252.

LECO, n.d. *AC500 Isoperibol Calorimeter.* [Online] Available at: https://www.leco.com-/product/ac500. [Accessed 14 January 2022].

Li, E., Lu, Y., Cheng, F., Wang, X. and Miller, J. D., 2018. Effect of oxidation on the wetting of coal surfaces by water: experimental and molecular dynamics silumation studies. *Physiochemical Problems Mineral Processing*, 54(4), pp. 1039 - 1051.

Liao, Y., Cao, Y., Liu, C. and Zhu, G., 2016. A study of kinetics on oily-bubble flotation for a low-rank coal. *International Journal of Coal Preparation and Ultilization* , 36(3), pp. 151 - 162.

Liao, Y., Cao, Y., Liu, C., Zhao, Y. and Zhu, G., 2017. Comparison of the effect of particle size on the flotation kinetics of a low-rank coal using air bubbles and oily bubbles. *The Journal of the Southern African Institute of Mining and Metallurgy*, Volume 117, pp. 561 - 566.

Lu, Y., Li, E., Cheng, H., Wang, X., Du, Z., Cheng, F. and Miller, J., D., 2018. Effect of oxygen functional groups on the surface properties and flotation response of fine coal, comparison of rank with oxidation. *International Journal of Coal Preparation and Utilization*, 41(4), pp. 1 - 17.

Lu, Y., Wang, X., Liu, W., Li, E., Cheng, F. and Miller, J. D., 2019. Dispersion behaviour and attachment of high internal phase water-in-oil emulsion droplets during fine coal flotation. *Fuel,* Volume 253, pp. 273- 282.

Luo, Z., Fan, M., Zhao, Y., Tao, X., Chen, Q., Chen, Z. 2008. Density Dependent Separation of Dry Fine Coal in A vibrated Fluidized Bed. *Powder Technology,* 187(2), pp. 119 - 123.

Ma, G., Bu, X., Xie, G., Pen, Y., Sha, J., Xia , W. and Wu, E., 2018. Comparison study of separation performance of a spiral and dense-medium cyclone on cleaning coal. *International Journal of Coal Preparation and Utilization,* pp. 1 - 9.

Maharana , B. S. and Suresh, N., 2020. Separation characteristics of 100-mm dual-cone water-only cyclone to wash high NGM coal. *International Journal of Coal Preparation and Utilization,* 40(1), pp. 37 - 50.

Majumder, A. K. and Barnwal, J. P., 2011. Processing of coal fines in a water-only cyclone. *Fuel,* Volume 90, pp. 834 - 837.

Maledi, N, B., (2017). *Characterisation of Mineral Matter in South African Coals using Micro-Roman Spectroscopy and other techniques*. Doctor of Philosophy. University of the Witwatersrand, Johannesburg, South Africa. [Online] Available at: https://scholar.google.co.za/citations?user=y80UdJ8AAAAJ&hl=en. [Accessed 23 January 2022].

Malvern Mastersizer, n.d. *Laxmi Analytical Laboratories*. [Online] Available at :http://www.laxmilab.com/particle-size-testing-by-malvern-mastersizer-2815639.html. [Accessed 15 January 2022].

Manser, R. J., Barley, R. W. and Wills, B. A., 1991. The shaking table concentrator - the influence of operating conditions and table parameters on mineral separation - the development of a mathematical model for normal operating conditions. *Minerals Engineering,* 4(3 - 4), pp. 369 - 381.

MARC, n.d. *MARC Technologies.* [Online] Available at: https://www.marctech.com.au-/contact-us/. [Accessed 14 January 2022].

Marmur, A., Volpe, C. D., Siboni, S., Amirfazli, A. and Drelich, W. J., 2017. Contact angles and wettability:towards common and accurate terminology. *Surface Innovations,* 5(1), pp. 3 - 8.

Mashaba, P.M. and Bada, S.O., (2021). Coaltech Annual Report. [Online] Available at:https://coaltech.co.za/about-us/annual-reports. [Accessed 30 January 2022].

Mehrotra, V. P., Sastry, K. V. and Morey, B. W., 1983. Review of oil agglomeration techniques for processing of fine coals. *International Journal of Mineral Processing,* Volume 11, pp. 175 - 201.

Meshram, P., Purohit, B. K., Sinha, M. K., Sahu, S. K. and Pandey, B. D., 2015. Demineralization of low grade coal - a review. *Renewable and Sustainable Energy Reviews,* Volume 41, pp. 745 - 761 .

Michael, L., Turek and Mark , S. and Klima, 2003. Dense-medium cycloning of fine coal refuse. *Coal Preparation,* 23(5 - 6), pp. 267 - 284.

Mohanta, S., Chakraborty, S. and Meikap, B. C., 2013. Optimization Process of an Air Dense Medium Fluidized Bed Separator for Treating High-Ash Non-coking Indian Coal. *Mineral Processing and Ectractive Metallurgy Review,* 34(4), pp. 240 - 248.

Mohanty , M., Zhang, B., Wang , H., Mahajan , A., Akbari , H., Bashir , Z., Ramamoorthy , S. and Hi, J., 2014. Development and demonstration of an automation and control system for coal spirals. *International Journal of Coal Preparation and Utilization,* 34(3 - 4), pp. 157 - 1713.

Mohanty, M. K., Honaker, R. Q., Patwardhan, A. and Ho, K., 1998. Coal flotation washability: An evaluation of the traditional procedures. *Coal Preparation,* 19(1 - 2), pp. 33 -49.

Netten, K., Moreno-Antanasio, R. and Galvin K, P., 2014. Fine particle beneficiation through selective agglomeration with an emulsion binder. *Industrial and Engineering Chemistry Research,* Volume 53, pp. 15747 - 15754.

Netten , K., Moreno-Antanasio, R. and Galvin, K. P., 2015. A kinetic study of a modified fine coal agglomeration process. *Procedia Engineering,* Volume 102, pp. 508 - 516.

Netten, K., Moreno-Atanasio, R. and Galvin, K. P., 2016. Selective agglomeration of fine coal using a water-in-oil emulsion. *Chemical Engineering Research and Design,* Volume 110. pp. 54-61.

Netten, K., Ernst, T., Moreno-Atanasio, R. and Galvin, K. P., 2017a. Fast and selective fine coal agglomeration using an economic binder. *Centre for Advanced Particle Processing and Transport,* 17 March, pp. 1 - 12. Available at: https://www.acps.com.au/shop/publications/conference-proceedings/2016-sixteenth-conference-proceedings/. [Accessed 20 March 2020].

Netten, K., Borrow, D, J. and Galvin, K. P., 2017b. Fast agglomeration of ultra-fine hydrophobic particles using a high-internal-phase emulsion binder comprising permeable hydrophobic films. *Centre for Advanced Particle Processing and Transport,* Newcastle Institute for Energy and Resources 30 March, pp. 10658 - 10666. Available at:https://pubs.acs.org/doi/abs/10.1021/acs.iecr.7b02215?casa_token=dCET0Iwg3T0AAAAA:fXGJ0F86s8BYQxwsXJIOelVpYdRp_TxRQ8qD2O1_XYUoB2e5zttZvzGx87sFIr_e_NBKtnnR4IK_Cg. [Accessed 20 March 2020].

Netten, K. and Galvin, K. P., 2018. Rapid beneficiation of fine coal tailings using a novel agglomeration. *Fuel Processing Technology,* Volume 176, pp. 205 - 210.

Nicol, S. K., Smitham, J. B. and Hinkley, J. T., 1994. *Measurement of coal flotation efficiency using the tree flotation technique.* Cracow, Poland, Energy Technology.

Nienaber, E. C. and Auret, L., 2019. Experimental modelling and plant simulation of spiral concentrators:Comparing response surface methodology and extended Holland-Batt models. *Minerals Engineering,* Volume 141, pp. 1 - 19.

Ozer, M., Basha, O. M. and Morsi, B., 2017. Coal-Agglomeration Process: A review. *International Journal of Coal Preparation and Utilization,* 37(3), pp. 131 - 167.

Ozgen, S., 2013. *Studies of a hydrocyclone to produce clean coal from Tuncbilek/Turkey fine lignite tailings.* Philadelphia, Department of Research and Development, General Directorate of Turkish Coal Enterprise (TKI). Available at: https://www.researchgate.net/publication/273948755_Studies_of_a_Hydrocyclone_to_Produce_Clean_Coal_from_TuncbilekTurkey_Fine_Lignite_Tailings. [Accessed 14 January 2022].

Ozonoh, M., Aniokete, T. C., Oboirien, B. O. and Daramola, M. O., 2018. Techno-economic analysis of electricity and heat production by co-gasification of coal, biomass and waste tyre in South Africa. *Journal of Cleaner Production,* Volume 201, pp. 192 - 206.

Patil, D. P., Bhaskar, K. U., Jakhu, M. R. and Rao, T. C., 1997. Removal of graphite from lead rougher concentrate. *International Journal of Mineral Process,* Volume 49, pp. 87 - 96.

Peng, Y., Liang, L., Tan, J., Sha, J. and Xie, G., 2015. Effect of flotation reagent adsorption by different ultra-fine coal particles on coal flotation. *International Journal of Mineral Processing,* Volume 142, pp. 17 - 21.

Perry, D. L. and Grint, A., 1983. Application of XPS to coal characterization. *Fuel,* Volume 62, pp. 1024 - 1033.

Pichot, R., (2012). *Stability and characterisation of emulsions in the presence of colloidal particles and surfactants.* Chemical Engineering. Ph.D. University of Birmingham. Available at: http://etheses.bham.ac.uk/id/eprint/3271. [Accessed 05 June 2020].

Pisupati, S. V. and Scaroni, A. W., 1993. Natural weathering and laboratory oxidation of bituminous coals: organic and inorganic structural changes. *Fuel,* 72(4), pp. 531 - 542.

Qu, J. Tao, X., He, H., Zhang, X., Xu, N. and Zhang., B., 2015. Synergistic effect of surfactants and a collector on the flotation of a law-rank coal. *International Journal of Coal Preparation and Utilization,* 35(1), pp. 14 - 24.

Ramsaywok, P., Vermaak, M. K. and Viljoen, R., 2010. Case study: high capacity spiral concentrators. *The Journal of the Southern African Institute of Mining and Metallurgy,* Volume 110, pp. 637 - 642.

Ramsaywok, P. and Mathumbu, P., 2017. *A straight up single pass comparison of a low-cut spiral and a conventional spiral in the South African coal industry,* s.l.: Exxaro Resources Ltd.

Ramudzwagi, M., Tshiongo - Makgwe, N. and Nheta, W., 2020. Recent developments in beneficiation of fine and ultra-fine coal -review paper. *Journal of cleaner production,* Volume 276, pp. 1 - 11.

Road Map, 2011. Overview of the South African Coal value chain. [Online] Available at: http://www.fossilfuel.co.za/initiatives/2013/SACRM-Value-Chain-Overview.pdf. [Accessed 20 April 2021].

Ruhman, M. and Gupta, R., 2017. Review on chemical upgrading of coal: production process, potential application and recent developments. *Fuel Process Technology,* Volume 158, pp. 35 - 36.

Sahinoglu, E. and Uslu, T., 2015. Role of recovery sieve size in upgrading of fine coal via oil agglomeration technique. *Fuel Processing Technology,* Volume 138, pp. 21 - 29.

Sahu, L., Bhattacharya, S. and Dey, S., 2019. Release analysis of coal fines: Evolution of the methodology and critical issues involved. *The Journal of Southern African Institute of Mining and Metallurgy,* Volume 119, pp. 595 - 606.

Sampaio, C H; Aliaga, W; Pacheco, E T; Petter, E; Wotruba, H., 2008. Coal beneficiation of Candiota mine by dry jigging. *Fuel Processing Technology* , Volume 89, pp. 198 - 202.

Sampaio , C. H., Ambrós, W. M., Cazacliu, B., Moncunill, J. O., José, D S., Miltzarek, G L., de Brum, I. A. S., Petter, C. O., Fernandes, E. Z. and Oliveira, L F., 2020. Destoning the Moatize coal seam, Mozambique,. *Minerals,* 10(771), pp. 1 - 13.

Sarikaya, M. and Ozbayoglu, G., 1990. Electrokinetics of oxidised coal. *Fuel Processing Technology,* Volume 24, pp. 459 - 466.

Sen, R. and Swaminathan, T., 2004. Response surface modeling and optimization to elucidate and analyze the effects of inoculum age and sizeon surfactin production. *Biochemical Engineering Journal* , Volume 21, pp. 141 - 148.

Sen, R., Srivastava, S. K. and Singh, M. M., 2009. Aerial oxidation of coal analytical methods instrimental techniques and test methods: a survey. *Indian Journal Chemical Technology,* 16(10), pp. 3 - 35.

Setsepu, R. L., Abdulsalam, J., Weiersbye, I. M. and Bada, S. O., 2021. Hydrothermal Carbonization of Searsia lancea Trees Grown on Mine Drainage: Processing Variables and Product Composition. *ACS Omega,* Volume 6, pp. 20292 - 20302.

Shariati, S., Ramadi, A. and Salsani, A., 2015. Beneficiation of low-grade phosphate deposits by a combination of calcination and shaking tables: Southwest Iran. *Minerals,* Volume 5, pp. 367 - 379.

Sharma, K. K., Kalyani, V. K., Charan, T. G. and Sinha, A., 2012. Application of a Central Composite Design with Response Surface Methodology in Beneficiation Studies of Coal Fines Using an Oleo-Flotation Process. *International Journal of Coal Preparation and Utilization,* 32(5), pp. 225 - 237.

Sivrikaya, O., 2014. Cleaning study of a low-rank lignite with DMS, Reichert spiral and flotation. *Fuel,* Volume 119, pp. 252 - 258.

Stat-Ease, (n.d). General Sequence of Analysis » Fit Summary (RSM/MIX Model Selection). [Online]. Available at: https://www.statease.com/docs/v11/contents/analysis/fit-summary/. [Accessed 02 May 2021].

Steyn, M. and Minnitt, R. C. A., 2010. Thermal coal products in South Africa. *The Journal of the Southern African Institute of Mining and Metallurgy,* Volume 110, pp. 593 - 599.

Tao, D., Luttrell, G. H. and Yoon, R. H., 2000. A parametric study of froth stability and its effect. *International Journal of Mineral Processing,* Volume 59, pp. 25 - 43.

Teimouri, S., (2020). *Feasibility study on the use of imidazolium-based ionic liquids in the extraction of gold.* Masters of Science in Engineering. University of the Witwatersrand. Available at:https://wiredspace.wits.ac.za/handle/10539/31360. [Accessed 05 August 2021].

Wagner, N., Malumbazo, N. and Falcon, R., 2018. *Southern African Coals and Carbons.* Cape Town: Struik Nature.

Wang, Q., Niida, H., Apar, P., Chen, Q., Gui, L., Qian, Q., Mitsumura, N., Kurokawa, H., Sekiguchi, K. and Sugiyama, K., 2012. Influential factors on the oil agglomeration process for recovery from different grade coals. In: H. Itoh, C. A. Brebbia and V. Popov, eds. *Waste Management and the Environment VI.* Southampton: WIT Press, pp. 1 - 448.

Wang, G; Bai, X; Wu, C; Li, W; Liu, K; Kiani., 2018. Recent advances in the beneficiation of ultrafine coal particles. *Fuel Processing Technology,* Volume 178, pp. 104 -125.

Wills, B. A. and Napier-Munn, T., 2006. *An introduction to the practical aspects of ore treatment and mineral recovery.* Seventh ed. s.l.:Elsevier Science and Technology Books.

Xia, W., Yang, J. and Liang, C., 2013. A short review of improvement in flotation of low rank/oxidised coals by pretreatments. *Powder Technology,* Volume 237, pp. 1 - 8.

Xing, Y., Gui, X., Cao, Y., Wang, Y., Xu, M., Wang, D. and Li, C., 2017. Effect of compound collector and blending frother on froth stability and flotation perfomance of oxidised coal. *Powder Technology*, Volume 305, pp. 166 - 173.

Xu, M., Xing, Y., Gui, X., Cao, Y. and Wang, L., 2017. Effect of ultrasonic pretreatment on oxidised coal flotation. *Energy Fuels,* 31(12), pp. 14367 - 14373.

Yadav, A. M., Chaurasia, R. C., Suresh, N. and Gajbhiye, P., 2018. Application of artificial neural networks and response surface methodology approaches for the prediction of oil agglomeration process. *Fuel,* Volume 220, pp. 826 - 836.

Yang, X., Zhao, Y., Luo, Z., Song, S., Duan, C., Dong, L. 2013. Fine Coal Dry Cleaning Using a Vibrated Gas-Fluidized Bed. *Fuel Processing Technology,* Volume 106, pp. 338 - 343.

Zeng, H., Shi, C., Huang, J. and Li, L., 2015. Recent experimental advances on hydrophobic interactions at solid/water and fluid or water interfaces. *Journal of Biomaterials and Biological Interfaces,* Volume 11, pp.1 - 11.

Zhang, B., (2008). *Performance optimization of a compound spiral for fine and ultra-fine coal cleaning.* Mineral Processing Engineering. MSc. University of China. Available at: https://search.proquest.com/openview/5c23507760d2b5b2925bd0582388e5f6/1?cbl=18750&diss=y&pq-origsite=gscholar. [Accessed 09 September 2020].

Zhang, R., Xia, Y., Guo, F., Sun, W., Cheng, H., Xing, Y. and Gui, X., 2020. Effect of microemulsion on low-rank coal flotation by mixing DTAB and diesel oil. *Fuel,* Volume 260, pp. 1 - 6.

Zhao, W., Fierro, V., Zlotea, C., Aylon, E., Izquierdo, M. T., Lareoche, M. and Celzard, A., 2011. Optimization of activated carbons for hydrogen storage. *International Journal of Hydrogen Energy,* Volume 36, pp. 11746 - 11751.

Zhao, Y., Fu, Z., Yang, X., Luo, Z., Duan, C., Song, S., Cai, L. 2015. Fine Coal Dry Cleaning using an Air Dense Medium Fluidized Bed with Improved Magnetite Medium. *Procedia Engineering*, Volume 102, pp. 1133 - 1141.

APPENDICES

Appendix A: Washability data for the beneficiation tests

Table A-1: Washability results for discard coal 1 beneficiation using HIP W/O emulsion

HIP W/O emulsion binder								
5 kg/ton								
Time (sec)	Coal sample	Yield (g)	Fractional yield, %	Ash content, %	Cumulative yield, %	Cumulative ash content, %	Combustible recovery, %	Ash rejection %
30	Conc 1	30	12.50	11.76	12.50	11.76	15.61	94.99
30	Conc 2	9	3.75	13.31	16.25	12.12	20.21	93.29
30	Conc 3	5	2.08	14.85	18.33	12.43	22.72	92.23
30	Tail 2	47	19.58	27.64	37.92	20.28	42.77	73.78
30	Tail 3	5	2.08	27.80	40.00	20.68	44.90	71.81
30	Tail 1	144	60.00	35.11	100.00	**29.34**	100.00	0.00
	FEED	240	100.00	**29.34**				
7 kg/ton								
Time (sec)	Coal sample	Yield (g)	Fractional yield, %	Ash content, %	Cumulative yield, %	Cumulative ash content, %	Combustible recovery, %	Ash rejection %
30	Conc 1	80	34.33	13.71	34.33	13.71	41.93	83.96
30	Conc 2	24	10.30	15.35	44.64	14.09	54.27	78.57
30	Conc 3	9	3.86	18.70	48.50	14.45	58.71	76.11
30	Tail 2	34	14.59	37.33	63.09	19.74	71.66	57.54
30	Tail 3	4	1.72	31.76	64.81	21.06	73.31	55.68
30	Tail 1	82	35.19	46.42	100	**29.34**	100	0
	FEED	233	100.00	**29.34**				
9 kg/ton								
Time (sec)	Coal sample	Yield (g)	Fractional yield, %	Ash content, %	Cumulative yield, %	Cumulative ash content, %	Combustible recovery, %	Ash rejection %
30	Conc 1	109	46.39	18.46	46.39	18.46	53.53	70.81
30	Conc 2	47	20.00	20.58	66.39	19.10	76.01	56.78
30	Conc 3	11	4.68	26.36	71.07	19.58	80.89	52.57
30	Tail 2	32	13.62	40.22	84.69	22.90	92.41	33.90
30	Tail 3	6,0	2.54	48.78	87.23	23.65	94.25	29.68
30	Tail 1	30	12.77	68.20	100	**29.34**	100	0
	FEED	235	100.00	**29.34**				

Sec = seconds; Conc = concentrate; Tail = tailing

Table A-2: Washability results for discard coal 1 beneficiation using kerosene

kerosene								
5 kg/ton								
Time (sec)	Coal sample	Yield (g)	Fractional yield, %	Ash content, %	Cumulative yield, %	Cumulative ash content, %	Combustible recovery, %	Ash rejection %
30	Conc 1	46	18.47	17.42	18.47	17.42	21.59	89.03
30	Conc 2	16	6.43	17.83	24.90	17.53	29.06	85.13
30	Conc 3	6	2.41	18.02	27.31	17.57	31.86	83.65
30	Tail 2	64	25.70	24.20	53.01	20.78	59.43	62.45
30	Tail 3	6	2.41	29.03	55.42	21.14	61.85	60.06
30	Tail 1	111	44.58	39.53	100	**29.34**	100	0
	FEED	**249**	100	**29.34**				
7 kg/ton								
Time (sec)	Coal sample	Yield (g)	Fractional yield, %	Ash content, %	Cumulative yield, %	Cumulative ash content, %	Combustible recovery, %	Ash rejection %
30	Conc 1	123	53.25	17.73	53.25	17.73	61.99	67.82
30	Conc 2	18	7.79	19.27	61.04	17.93	70.89	62.70
30	Conc 3	5	2.16	22.35	63.20	18.08	73.27	61.05
30	Tail 2	34	14.72	39.53	77.92	22.13	85.87	39.89
30	Tail 3	2	0.87	44.94	78.79	22.38	86.54	43.83
30	Tail 1	49	21.21	55.17	100	29.34	100	0
	FEED	**231**	100	**29.34**				
9 kg/ton								
Time (sec)	Coal sample	Yield (g)	Fractional yield, %	Ash content, %	Cumulative yield, %	Cumulative ash content, %	Combustible recovery, %	Ash rejection %
30	Conc 1	140	54.05	25.22	54.05	25.06	57.20	53.53
30	Conc 2	35	13.51	24.42	67.57	25.22	71.66	42.29
30	Conc 3	25	9.65	28.21	77.22	25.45	81.47	30.32
30	Tail 2	35	13.51	38.8	90.73	27.44	93.17	15.13
30	Tail 3	9	3.47	45.07	94.21	28.09	95,87	9.80
30	Tail 1	15	5.79	49.62	100	**29.34**	100.00	0
	FEED	**259**	100	**29.34**				

Sec = seconds; Conc = concentrate; Tail = tailing

Table A-3: Washability results for discard coal 2 beneficiation using 5 kg/ton of HIP W/O emulsion

Discard coal 2, (5 kg/ton)							
Time (sec)	Coal sample	Yield (g)	Fractional yield, %	Ash content, %	Cumulative yield, %	Cumulative ash content, %	Combustible recovery, %
30	Conc 1	3	1.3	31.16	1.30	31.16	2.48
30	Conc 2	3	1.3	31.87	2.61	31.52	4.17
30	Conc 3	3	1.3	31.69	3.91	31.57	5.87
30	Tail 2	52	22.6	37.03	26.52	36.22	32.95
30	Tail 3	14	6.1	43.3	32.61	37.55	39.51
30	Tail 1	155	67.4	52.21	100	48.71	100
FEED		**230**	100	**48.71**			

Sec = seconds; Conc = concentrate; Tail = tailing

Table A-4: Washability results for discard coal 3 beneficiation using 5 kg/ton of HIP W/O emulsion

Discard coal 3, (5 kg/ton)							
Time (sec)	**Coal sample**	**Yield (g)**	Fractional yield, %	Ash content, %	Cumulative yield, %	Cumulative ash content, %	Combustible recovery, %
30	Conc 1	10	4.41	17.23	3.96	17.40	6.14
30	Conc 2	2	0.88	17.57	4.85	17.46	7.36
30	Conc 3	3	1.32	17.97	6.17	17.59	9.19
30	Tail 2	41	18.06	33.22	24.23	29.16	29.49
30	Tail 3	13	5.73	42.73	29.96	31.75	35.02
30	Tail 1	159	70.04	44.28	100	41.71	100
FEED		**227**	100	**41.71**			

Sec = seconds; Conc = concentrate; Tail = tailing

Table A-5: Washability results for discard coal 4 beneficiation using 5 kg/ton of HIP W/O emulsion

Discard Coal 4, (5 kg/ton)							
Time (sec)	Coal sample	Yield (g)	Fractional yield, %	Ash content, %	Cumulative yield, %	Cumulative ash content, %	Combustible recovery, %
30	Conc 1	6	3	12.12	3	12.12	3.08
30	Conc 2	8	3	12.7	6	12.45	7.16
30	Conc 3	5	2	13.33	8	12.68	9.68
30	Tail 2	31	13	29.39	21	23.04	22.46
30	Tail 3	10	4	22.08	25	22.88	27.01
30	Tail 1	180	75	30.54	100	28.63	100
FEED		**240**	100	**28.63**			

Sec = seconds; Conc = concentrate; Tail = tailing

Table A-6: Washability results for discard coal 5 beneficiation using 5 kg/ton of HIP W/O emulsion

Discard coal 5, (5 kg/ton)							
Time (sec)	Coal sample	Yield (g)	Fractional yield, %	Ash content, %	Cumulative yield, %	Cumulative ash content, %	Combustible recovery, %
30	Conc 1	7	3.07	12.7	3.07	12.70	4.02
30	Conc 2	8	3.51	13.11	6.58	12.92	8.59
30	Conc 3	8	3.51	13.81	10.09	13.23	13.13
30	Tail 2	29	12.72	39.59	22.81	27.93	24.65
30	Tail 3	10	4.39	26.16	27.19	27.64	29.51
30	Tail 1	166	72.81	35.44	100	33.32	100
FEED		**228**	100	**33.32**			

Sec = seconds; Conc = concentrate; Tail = tailing

Appendix B: Plagiarism report

With the cover and declaration page attached.